Mechanisms and systemic relevance of immune cell specific virus replication

Inaugural-Dissertation

zur

Erlangung des Doktorgrades

Dr. rer. nat.

der Fakultät für

Biologie

an der

Universität Duisburg-Essen

vorgelegt von

Sarah-Kim Friedrich-Becker

aus Gladbeck

Juni 2021

Die der vorliegenden Arbeit zugrunde liegenden Experimente wurden am Institut für Immunologie des Universitätsklinikums Essen durchgeführt.

1. Gutachter: Prof. Dr. Karl Sebastian Lang
2. Gutachter: Prof. Dr. Matthias Gunzer

Vorsitzender des Prüfungsausschusses: Prof. Dr. Sven Brandau

Tag der mündlichen Prüfung: 31.01.2022

Danksagung

An erster Stelle möchte ich Professor Karl Lang danken. Lieber Karl, vielen Dank, dass du mir in der Zeit in deinem Labor den Weg zu selbständiger, wissenschaftlicher Arbeit gezeigt hast. Du hast mir immer genug Freiraum geschaffen, um mich entfalten zu können aber gleichzeitig genug Anleitung gegeben, damit ich mich nicht verliere. Auch bei Problemen hattest du immer ein offenes Ohr und konntest mich stets durch deine große Erfahrung leiten.

To the members of Karl's lab, even if most of you will not read this, since you are now located all over the globe, I really wanted to thank you from my heart for your help and the great teamwork. Dear Vikas, Thamer, Vishal, Judith, Rosa and not the least Michael and all the rest, it was an honor for me to work with you in Karl's lab!

Ein weiterer großer Dank gebührt meinen Eltern. Nur durch eure große Unterstützung konnte ich diesen Weg gehen. Meiner Mutter danke ich dafür, dass sie immer für mich da ist. Auch in schweren Zeiten haben wir alles zusammen gemeistert. Du hast mich zu dem Menschen gemacht, der ich heute bin.

Lieber Papa, ich danke dir für alles was du jemals für mich getan hast. Ich weiß, dass du da, wo auch immer du gerade bist, immer ein Auge auf mich hast.

Nicht zuletzt geht mein letzter Dank an meinen Ehemann, Marcel Becker. Danke, für die zahllosen Male, in denen du mich unterstützt hast. Du hast ich immer zum Weitermachen ermutigt und warst immer an meiner Seite.

Table of Contents

1. Introduction

1.1. The immune system

The immune system is composed of various factors and cells, which protect the body from harm by distinguishing between self and foreign structures. This defense system can be divided into four general arms: A) the general physical barriers of the body are composed of epithelial cell layers and mucus layers which overlay the respiratory and gastrointestinal tract and epithelial cilia, B) the complement system and other antimicrobial proteins, C) the innate immune system, and C) the adaptive immune system.

Cells of the immune system prevent harm from disease-causing pathogens like viruses, bacteria or parasites by different mechanisms: avoidance, resistance, or tolerance. These immune cells are mainly leukocytes, which development begins in the bone marrow with a multipotent hematopoietic stem cell (HSC). HSCs give rise to cells of a more limited developmental potential which are divided into two branches (Figure 1): myeloid and lymphoid progenitors.

Myeloid progenitor cells give rise to a great variety of different immune cells, like erythrocytes, megakaryocytes, mast cells and myeloblasts. Myeloblasts can generate granulocytes and monocytes. Granulocytes are essential players of the innate immune system and are named after their characteristic presence of granules in the cytoplasm. Neutrophile granulocytes or neutrophils phagocyte and destroy pathogens with the help of degradative enzymes, which are stored in intracellular vesicles. Eosinophils and basophils provide a variety of toxic proteins and enzymes to fight against invading pathogens. In contrast, monocytes give rise to macrophages (MΦ), which engulf and eliminate microorganisms, and dendritic cells (DCs) which ingest large amounts of fluids via macropinocytosis.

Lymphoid progenitors give rise to T and B lymphocytes, natural killer (NK) cells and DCs. T and B lymphocytes express highly diverse antigen receptors and form the center of the adaptive immune system.

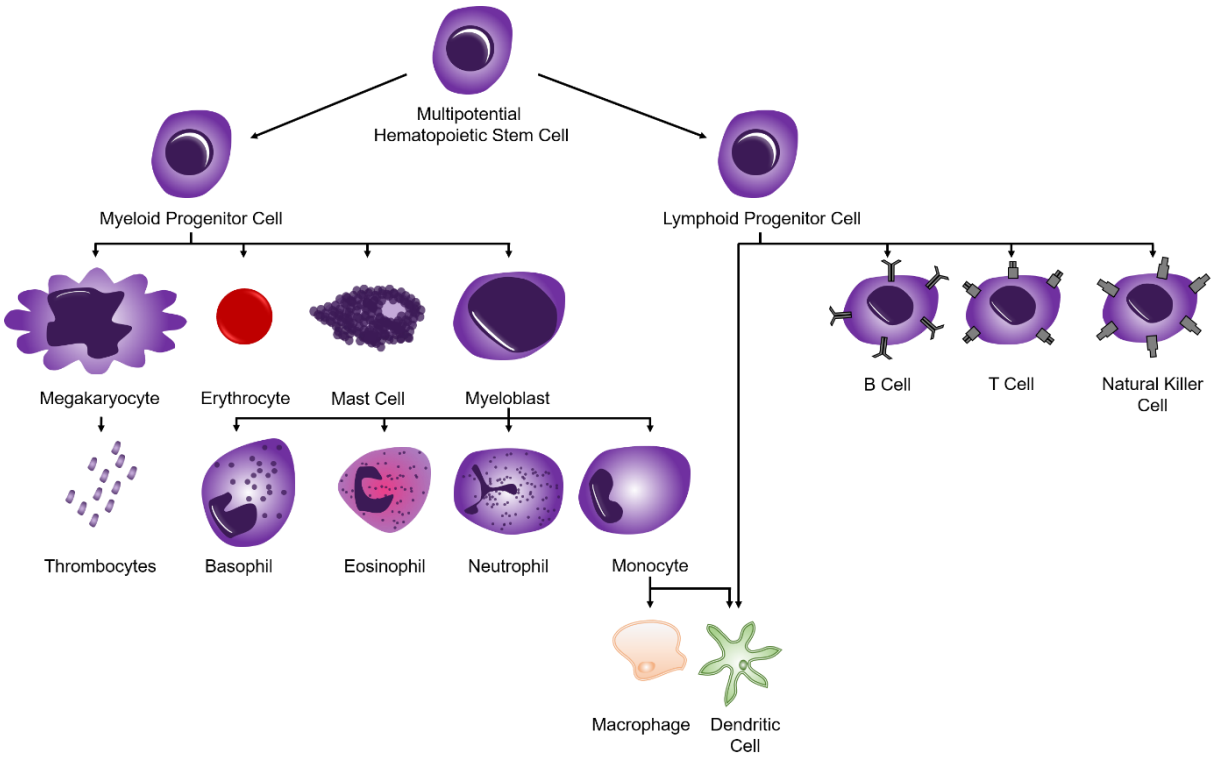

Figure 1: Development of immune cells from hematopoietic stem cells

Immune cells develop from a multipotent hematopoietic stem cell. The main two lineages myeloid and lymphoid progenitor cells give rise to innate and adaptive immune cells. Myeloid progenitor cells can develop into megakaryocytes, erythrocytes, mast cells and myeloblasts. Myeloblasts represent progenitor cells of granulocytes and monocytes. Granulocytes can be differentiated into basophils, eosinophils, and neutrophils. Monocytes however can further develop into MΦs and DCs. Lymphoid progenitor cells give rise to B and T lymphocytes, NK cells and DCs (Image adapted from:(Wang, Huang, and Chen 2017)).

1.1.1. The innate immune system

Innate immune recognition is provided by cells which are of hematopoietic and non-hematopoietic origin. The innate immune system provides the first line of defense against invading pathogens. Sensor cells detect conserved patterns of pathogens or damaged cells. By detection of inflammatory inducers via innate recognition receptors, sensor cells can initiate the production of inflammatory mediators as cytokines and chemokines. Cytokines are generally secreted molecules by immune cells, which can affect cells with the appropriate receptor. Chemokines do not only affect cells with the appropriate receptor, they also act as chemoattractants, meaning their expression can drive cells like neutrophils and macrophages from the bloodstream into the infected tissue.

1.1.1.1. Pattern recognition receptors

Recognition of foreign structure relies on sensing of highly conserved patterns by receptors. Foreign molecules are be sensed via PRRs (pattern recognition receptors), which can be distinguished in pathogen-associated molecular pattern (PAMPs) or damage-associated molecular patterns (DAMPs). DAMPs are molecules released by damaged cells, and PRRs like TLR2 or RIG-1 can be found in the cell membrane, in subcellular compartments such as endosomes or as secreted forms in the bloodstream (Medzhitov and Janeway 1997). PRR expression can be found in professional immune cells, such as dendritic cells and macrophages as well as in non-professional immune cells. Generally, PRRs can be divided into four groups: TLRs (Toll-like receptors), NLRs (NOD-like receptors (nucleotide-binding oligomerization domain-like receptors)), CLRs (C-type lectin receptors) and RLRs (retinoic acid-inducible gene 1 (RIG-1) like receptors). Activation of PRRs is not only essential for activation of innate immunity, but also induces co-stimulatory signals for activation of adaptive immune cells, such as T cells (Medzhitov, Preston-Hurlburt, and Janeway 1997). Another essential function of PRRs is the induction of anti-microbial and pro-inflammatory responses. PRR activation engages transcription of genes encoding for type I interferons, chemokines, pro-inflammatory cytokines, antimicrobial proteins, and various other proteins.

1.1.1.1.1. Toll-like receptors

TLRs, the best characterized family of PRRs, sense invading pathogens on the cell membrane, in endosomes or lysosomal compartments. Various TLRs have been identified in mice (13 different TLRs) and human (10 different TLRs) (Akira, Uematsu, and Takeuchi 2006). TLRs can recognize different components of invading pathogens, including viruses, bacteria, or fungi. TLR1 and TLR5 are specialized to sense bacterial components. Whereas TLR1 senses triacyl lipoproteins, TLR5 senses flagellin. Both TLRs are located at the plasma membrane. TLR1 usually forms dimers with TLR2, which recognizes lipoproteins of bacteria, viruses, parasites and from the host itself. TLR2 also forms heterodimers with TLR6, which senses diacyl lipoproteins of viruses or bacteria. Via the formation of these heterodimers, recognition of distinct lipoproteins can be assured. Depending on the cell type and source of the lipoprotein, stimulation of TLR2 heterodimers can result in the production of various pro-inflammatory cytokines including interferon type I (IFN type I) or can induce an IFN type I dependent response (Jin et al. 2007). TLR4 mainly senses LPS (lipopolysaccharides) from the cell membrane of gram-negative bacteria. In contrast, nucleic acids can be sensed by a greater variety of TLRs. TLR3 recognizes double-stranded RNA (dsRNA) on the cell surface or in the endosomal compartment. Single-stranded RNA (ssRNA) from viruses is sensed by TLR7 in mice and TLR7 and TLR8 in human. TLR9 senses so-called CpG-motifs of unmethylated DNA from viruses and bacteria. Activation of nucleic acid sensing TLRs results in the production of proinflammatory cytokines as well as type I IFNs (Figure 2).

Activation of TLRs by binding of their respective ligand leads to the transcriptional upregulation of various cytokines. Depending on the adapter molecules linked to the TLRs, different signaling cascades are induced. One essential downstream adaptor of TLRs is MyD88 (myeloid differentiation primary response 88), which is present for all TLRs besides TLR3. Interaction of MyD88 with IRAK-4 (IL-1R-associated kinase 4) activates other IRAK family kinases (Kawagoe et al. 2008). The complete kinase signaling results in NF-κB (nuclear factor 'kappa-light-chain-enhancer' of activated B-cells) migration into the nucleus and transcriptional activation of proinflammatory cytokines. In addition, activation of TLR7 and TLR9 leads to the induction of type I IFNs via IRF7 (interferon regulatory factor 7), in a MyD88 dependent manner. Activation of TLR3 and TLR4 leads to signaling via the TRIF (TIR-domain-containing adapter-inducing interferon-β) pathway, resulting in IRF3-dependent cytokine induction (Akira, Uematsu, and Takeuchi 2006).

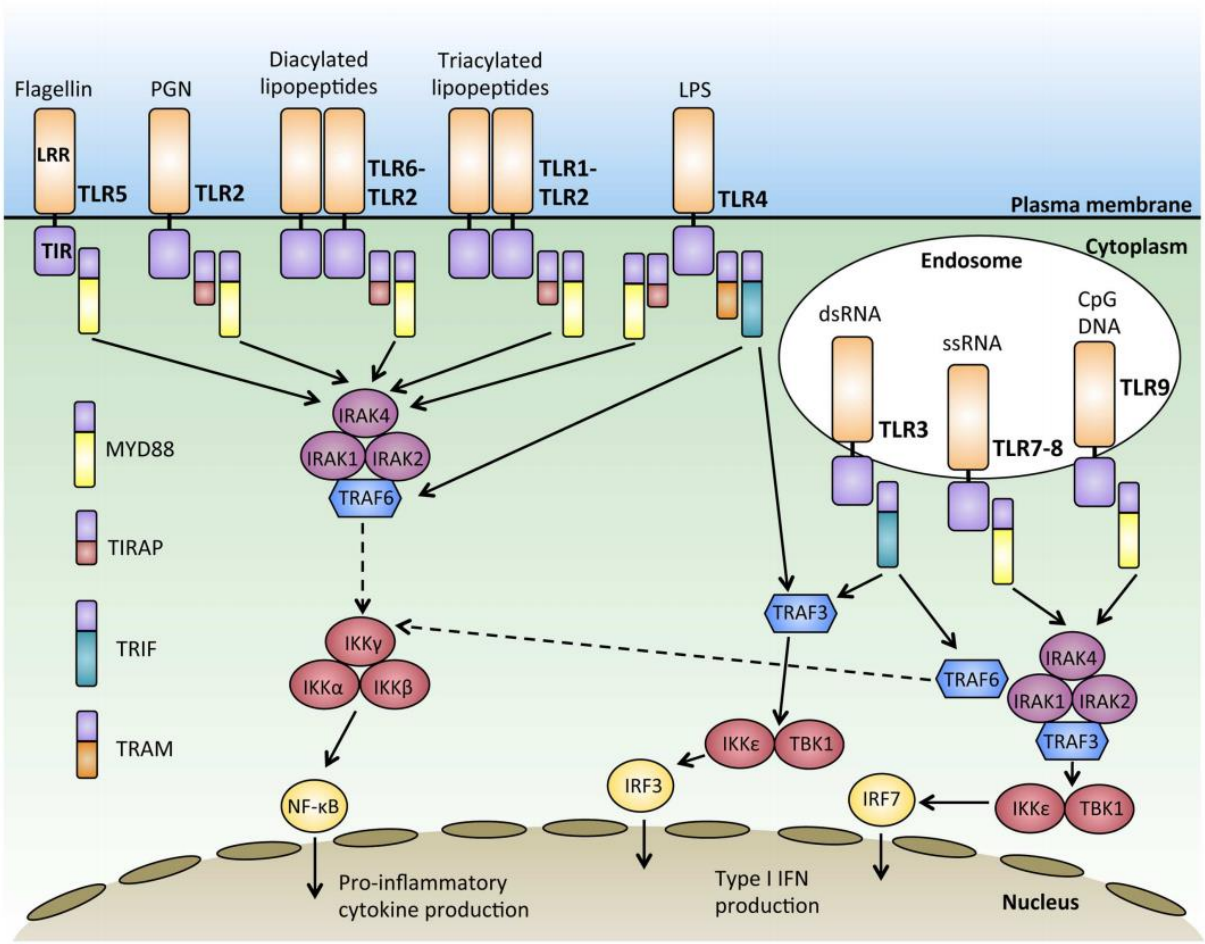

Figure 2: Recognition of conserved molecular patterns by TLRs

TLRs are the best investigated form of PRRs. Activation of TLRs by their respective ligands leads to activation of transcriptional activators such as NF-κB, IRFs or MAPK (mitogen-activated protein kinase). TLRs located in different compartments of cells can detect distinct structures. For example, TLR1, TLR2, TLR6, TLR4, TLR5 and TLR11 are located on the cell membrane detecting components like LPS (TLR4) or flagellin (TLR5). TLR3, TLR7 and TLR9 are located in intracellular endosomes and bind to RNA (TLR3, TLR7) or DNA (TLR9) structures. Finally, translocation of transcriptional factors into the nucleus results in the induction of cytokines and chemokines (Image source: (Wang et al. 2014)).

1.1.1.1.2. Other PAMP-sensors

Other family members of PAMP-sensors are NOD-like receptors (NLRs) and C-type lectin receptors (CLRs). The family of NLRs senses nucleotides via a binding domain and C-terminal leucine-rich repeats (Inohara et al. 2005). NLRs can be found in the cytosolic compartment of cells. NLRs, which are composed of a pyrin domain, are components of the inflammasome and activate caspase 1. NOD1 and NOD2, which harbor a CARD domain (caspase activation and recruitment domain), activate transcriptional upregulation of cytokines via NF-κB. Together with TLRs, NLRs binding of foreign pathogens activate the production of proinflammatory cytokines.

CLRs are located on the transmembrane region of cells and sense carbohydrates of pathogens. Activation of CLRs can either induce TLR dependent immune responses or mediate the production of proinflammatory cytokines (Geijtenbeek and Gringhuis 2009).

Recognition of intracellular virus in cells is mainly achieved by the group of RIG-I-like receptors (RLRs). RLRs consist of the cytoplasmic receptors RIG-I, MDA5 (melanoma differentiation-associated gene 5) and LGP2 (laboratory of genetics and physiology 2), which recognize dsRNA of viruses (Takeuchi and Akira 2009). RIG-I detects short dsRNA fragment of around 1 kb harboring a triphosphate, whereas MDA5 senses longer dsRNA fragments from 2 kb size. Especially RIG-I was shown to be essential for sensing of various viruses, including VSV (vesicular stomatitis virus). Lack of RIG-I resulted in a defective induction of inflammatory cytokines and type I IFNs upon VSV infection, whereas MDA5 deficiency did not alter cytokine production (Kato et al. 2006). LPG2, which is lacking the CARD of the RLRs, is essential to regulate RIG-I and MDA5 responses (Rothenfusser et al. 2005; Saito et al. 2007). Activation of RLRs result in CARD IPS-1 (IFN-β-promoter stimulator 1 (alternative names: CARDIF , MAVS)) interaction (Kawai and Akira 2006). The downstream signaling cascade leads to the expression of type I IFNs via various signaling factors such as IRF3 and IRF7.

1.1.1.2. Interferon system

Sensing of foreign structures by PRRs such as TLRs and RLRs upon virus infection results in the transcription and production of anti-viral type I IFNs. Type I IFNs are polypeptides, which are produced and secreted by most cells and fulfill cardinal functions in the control of infections. They induce an anti-viral status in infected and adjacent cells and, therefore, can limit the spread of viral particles. Furthermore, type I IFNs are essential to modulate the innate and activate the adaptive immune response (Ivashkiv and Donlin 2014). Activation of the type I IFN signaling

pathway is initiated by binding of IFNα and IFNβ to the heterodimeric interferon-α/β receptor (IFNAR) (Figure 3). This receptor consists of one IFNAR1 and one IFNAR2 subunit. Binding of type I IFNs to the IFNAR results in JAK1 (Janus kinase 1) and TYK2 (tyrosine kinase 2) dependent phosphorylation of the cytoplasmatic transcription factors STAT1 (signal transducer and activator of transcription 1) and STAT2 (Levy and Darnell 2002; Stark and Darnell 2012). Upon their dimerization and translocation into the nucleus, STAT1 and STAT2 form a complex with the IFN-regulatory factor 9 (IRF9). By binding to their consensus sequence on the genomic DNA, this complex activates the transcription of interferon stimulated genes (ISGs) such as OAS1 (2′-5′-oligoadenylate synthase1) or MX1 (IFN-induced GTP-binding protein Mx1) (Ivashkiv and Donlin 2014).

STAT1 or STAT3 homodimers activate gamma-activated sequences (GAS), which induce transcription of pro-inflammatory cytokines (van Boxel-Dezaire, Rani, and Stark 2006). The IFN type I response is enhanced by an intrinsic feedback loop: STAT1 and IRF9 are ISGs, which are highly upregulated already by low amounts of type I IFNs (Hu et al. 2002; Hu et al. 2005; Tassiulas et al. 2004; Venkatesh et al. 2013). This mechanism is especially essential in early innate immune cells such as macrophages (Venkatesh et al. 2013).

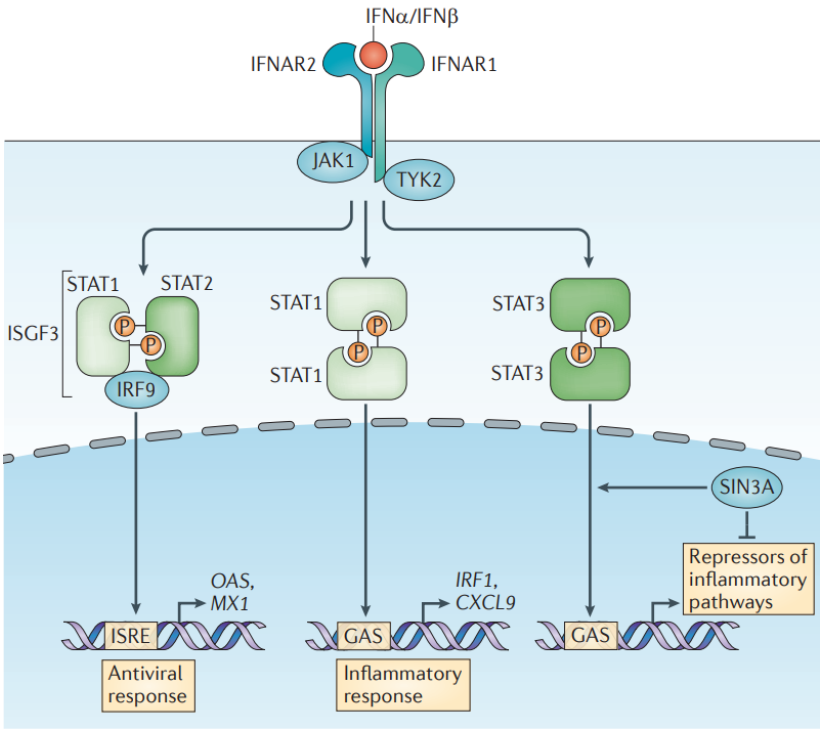

Figure 3: Interferon type I signaling

Binding of IFNα or IFNβ to their respective receptor, IFNAR, activates JAK1 and TYK2, which results in recruitment and phosphorylation of STAT1 and STAT2. Migration of ISGF3 (STAT1, STAT2 and IRF9 complex) into the nucleus initiates binding to ISRE (interferon-sensitive response element) and upregulation of anti-viral

genes. Homodimers formed by STAT1 or STAT2 bind GAS elements and result in expression of inflammatory response genes or transcription of repressors of inflammatory pathways (Image source: (Ivashkiv and Donlin 2014)).

1.1.1.3. Ubiquitin specific protease 18

Deubiquitinating enzymes are essential for several biological processes such as transcriptional silencing, growth control, or immune regulation. The ubiquitin-specific protease 18 (*Usp18*, Protein: USP18, also known as UBP43) functionality is branched into two arms: cleavage of the ubiquitin like modifier ISG15 (interferon-stimulated gene 15) and interaction with the IFNAR (Basters, Knobeloch, and Fritz 2018). ISG15 expression is highly induced by interferon (Der et al. 1998). Modification of ISG15 is performed by a three-step enzymatically process, which induction includes E1, E2 and various E3 enzymes. The conjugation of ISG15 is reversible by the deISGylation function of the isopeptidase site of USP18.

The second arm of USP18 function influences interferon signaling: USP18 specifically binds to the IFNAR2 subunit and prevents the interaction of JAK1 with the IFNAR (Malakhova et al. 2006). Absence of USP18 results in prolonged phosphorylation of STAT1 and STAT2 and initiates expression of anti-viral genes (Zou et al. 2007).

1.1.1.3.1. Role of USP18 in cell development and maintenance

USP18 is involved in the development and maintenance of several cell types and organs. It impacts progression of the cell cycle e.g., in the case of HeLa cells by interacting with S-phase kinase associated protein 2 (Vuillier et al. 2019). Moreover, generation of conventional $CD11b^+$ DCs is impaired in *Usp18*-deficient mice (Cong et al. 2012). The decreased number of $CD11b^+$ DCs is attributed to the interferon dependency of their development. Further, Th17 cells, which display a crucial subpopulation of $CD4^+$ T cells, show altered appearance in USP18 deficient mice (Liu et al. 2013). Not only for the development of several cell types USP18 represents an important factor. It also shows high anti-inflammatory capacity for various organs. In mice brain, absence of USP18 was associated with a strong interferon type I dependent brain destruction. USP18 expression in white matter microglial cells was essential to preserve their quiescent state.(Goldmann et al. 2015; Schwabenland et al. 2019). In line with this, absence of USP18 also results in interferon-driven beta cell apoptosis in pancreas, which was linked to type 1 diabetes (Santin et al. 2012). In addition, in humans *USP18*-deficiency has a major

impact on the physiological development and leads to a severe pseudo-TORCH ((T)oxoplasmosis, (O)ther Agents, (R)ubella, (C)ytomegalovirus, and (H)erpes Simplex) syndrome. Symptoms of this malady are neurodegeneration and congenital infection in the absence of a pathogen (Meuwissen et al. 2016).

1.1.1.3.2. USP18 and infections

USP18 influences the outcome of viral infections on different levels. It can directly interact with ISG15ylated viruses, like Influenza B, and hereby alter viral protein synthesis and replication (Zhao et al. 2016). USP18 can also influence the outcome of an infection in an indirect manner by influencing the IFN type I response. In an HIV infection, enhanced expression of USP18 in human memory $CD4^+$ T cells results in a reduced viability by type I IFN signaling (Dagenais-Lussier et al. 2019). Another essential mechanism, which is influenced by the intracellular expression of USP18 in special subsets of macrophages and dendritic cells is enforced virus replication (EVR), which here will be later examined in more detail.

1.1.1.4. Macrophages

Macrophages display an important subset of innate immune cells. They differ in their localization, ontogeny, and phenotype. Macrophages were the first cell type identified to be specialized in phagocytosis. Regarding their ontogenesis, macrophages derive from three different sources: fetal liver, yolk sac and hematopoietic stem cells (Geissmann et al. 2010; Gautier et al. 2012). Macrophages are involved in various processes like body development, repair, homeostasis und immune responses (Wynn, Chawla, and Pollard 2013).

1.1.1.4.1. CD169 macrophages

Spleen and lymph node resident $CD169^+$ macrophages are a minor but crucial subpopulation of macrophages (den Haan and Martinez-Pomares 2013). Unlike other macrophages, $CD169^+$ macrophages are characterized by their constitutive high surface expression of the sialoadhesin, CD169 or Siglec-1. $CD169^+$ macrophages differ from other macrophages not only by their expression of CD169, which was first discovered as a receptor for un-opsonized sheep

erythrocytes (Crocker and Gordon 1986). CD169 further functions as a receptor for sialyated pathogens (Macauley, Crocker, and Paulson 2014), different viruses (Gummuluru, Pina Ramirez, and Akiyama 2014; Sewald et al. 2015; Perez-Zsolt et al. 2019), exosomes (Saunderson et al. 2014) and is a cross-priming partner for DCs (van Dinther et al. 2018). These macrophages are strategically positioned at the end of small blood conduits, bordering the marginal zone of the subcapsular sinus lymph nodes.

Proper development and function of spleen and lymph node $CD169^+$ macrophages rely on the intact structure of splenic tissue. Therefore, several factors balance $CD169^+$ macrophage maintenance. Due to their location above the B cell follicle, B cells display a crucial factor for $CD169^+$ macrophage development. The entire lack of B cells or B cell derived TNFα (Tumor necrosis factor alpha) and LT (Lymphotoxin) as well as factors which directly influence B cell development directly affect $CD169^+$ macrophage development (Junt et al. 2006; Khairnar et al. 2015; Xu et al. 2015; Koroleva, Fu, and Tumanov 2018).

Due to their strategic physiological positioning, these macrophages are essential to protect against fatal virus infections (Moseman et al. 2012). As $CD169^+$ macrophages build the first line of defense against blood borne pathogens, they form crucial gatekeepers to prevent e.g., neurotropic viruses such as VSV from CNS (central nervous system) invasion during subcutaneous infections (Eloranta and Alm 1999; Junt et al. 2007; Iannacone et al. 2010; Chavez-Galan et al. 2015). Capture of viruses and promotion of local virus replication, known as enforced virus replication, is essential for activate immunity and to enhance virus control in case of a VSV infection (Honke et al. 2011). Accelerated viral replication in $CD169^+$ MΦs is promoted by the cell intrinsic expression of the interferon signaling inhibitor USP18 (Honke et al. 2011).

1.1.1.5. Dendritic cells

Dendritic cells are a class of phagocytes of the immune system which can be divided into two main functional types: conventional dendritic cells (cDCs) and plasmacytoid dendritic cells (pDCs). DCs display professional antigen presenting cells (APCs) in a very heterogenous class of cells which express a variety of cell surface markers. Hematopoietic precursor cells give rise to immature DCs (iDCs) which can reside in blood, peripheral or lymphoid tissues and organs. iDCs have a high phagocytic capacity but express rather low levels of MHC II (major histocompatibility complex II) and costimulatory molecules (Sato and Fujita 2007). Upon

engulfment of pathogens and activation of PRRs, DCs highly upregulate MHC II, as well as costimulatory molecules like CD40, CD80 and CD86. The so matured DCs (mDCs) can now travel via afferent lymphatics towards dLNs (draining lymph nodes) to activate antigen specific T cells.

Mouse conventional DCs display a very heterogenic population which can be distinguished by their expression of cell surface markers i.e. CD8, CD4 and CD11b. $CD8^{+}CD4^{-}$DCs make up to 20 %, $CD4^{+}$ $CD8^{-}$ DCs make up to 40 % and $CD4^{-}CD8\alpha^{-}$ DCs make up to 15 % of spleen resident dendritic cells (Vremec et al. 2000). $CD8^{+}CD4^{-}$ DCs which are usually $CD11c^{high}CD11b^{-}$ can be found in the T cell area of the spleen. Therefore, it is not surprising that they highly contribute to T cell activation (den Haan, Lehar, and Bevan 2000; Shortman and Heath 2010). Moreover, $CD8^{+}CD4^{-}$ DCs were identified as the major producers of type I IFN similar to pDCs (plasmacytoid dendritic cells) (Hochrein et al. 2001). $CD4^{+}CD8^{-}$ and $CD4^{-}CD8^{-}$ DCs are located in the marginal zone of the spleen and can migrate into the T cell zone upon activation (Ingulli et al. 2002). In contrast to cDCs, pDCs display only little capacity to activate and stimulate T lymphocytes. Upon activation, pDCs initiate the production of large amounts of type I IFNs. Thereby, pDCs are very efficient in sensing intracellular viral RNA and induce a rapid pathogen response (Swiecki and Colonna 2015).

1.1.1.6. Macrophages and Dendritic cells in the context of enforced virus replication

Enforced virus replication (EVR) is an essential immune mechanism to enhance local virus replication in specialized immune cells and depends on the expression of USP18. It has been shown that $CD169^{+}$ macrophages and cDCs expression high amounts of USP18, already in naïve states (Honke et al. 2011; Honke et al. 2013). Beyond the strong immune activation after viral infections via the above-mentioned activation mechanism of PRRs, the more recent found mechanism of EVR also plays an essential role in pathogen infection. Virus amplification in these cells caused by the suppression of interferon signaling provides sufficient amounts of antigen to on the one hand amplify the innate immune response in other succumbing infected immune cells, and on the other hand thereof ensure appropriate activation of adaptive immune cells.

1.2. The adaptive immune system

Unlike the innate immune system, the adaptive immune system is composed of specialized cells, which induce immunity against specific pathogens. It provides long-lived protection, memory formation and forms the foundation for vaccination. Majorly, T and B lymphocytes, a subset of leukocytes, mediate adaptive immunity. In contrast to germline encoded PRRs of the innate immune system which detect highly conserved molecular patterns, antigen receptors of lymphocytes detect versatile numbers of antigenic epitopes. Their receptor diversity builds the essential cornerstone of the specificity of the adaptive immune response.

1.2.1. Somatic recombination

Somatic or VDJ recombination is a capital process in the development of lymphocytes, which assures immunological diversity by formation of a distinct repertoire of T cell receptors (TCR) and immunoglobulins, which form the B cell receptor (BCR) (Schatz and Swanson 2011). By randomly arranging the gene segments of the variable (V), joining (J) and diversity (D) regions, the immunoglobulin and TCR antigen binding regions are formed.

VDJ recombination is initiated by a nick formation at the recombination signal sequence (RSS) of the segment coding region. The RSS is composed of a heptamer formed by the base pairs CACAGTG, a spacer, which consists of either 12 or 23 base pairs and a subsequent nonamer. The 12 bp or 23 bp spacer refers to one or two turns of the DNA helix, respectively. A 12 base pair spacer coding segment is always joined to a 23 base pair spacer coding segment, which assures that the coding segments are correctly ligated (Ramsden, Baetz, and Wu 1994). The enzymes which are majorly involved in VDJ-recombination are RAG-1(recombination activating gene 1) and RAG-2 (Fugmann et al. 2000; Mundy et al. 2002). These enzymes allow the chromosome to form a loop and bring the coding segments for recombination in close proximity. Mechanistically, RAG-1 incises into one chromosomal strand behind the segment coding region and forms a nick between coding segment and heptameric spacer. The formed 3-prime hydroxyl residue forms a hairpin structure with the other strand. This leads subsequently to a double strand break and release of the heptameric spacer region and discard of the loop strand fragment (Curry, Geier, and Schlissel 2005). Next, breaking the formed hairpin structure at the end of the coding segment via the enzyme Artemis occurs. The enzyme cleaves at the side of the hairpin randomly, by which an overlap of one strand is created (Ma et al. 2002). A DNA-polymerase fills in the gaps of one strand by adding so called P nucleotides. The terminal deoxynucleotidyl transferase (TdT) then fills the gaps between the two blunt ends and joins the

coding segments via so called N nucleotides. This mechanism creates increased diversity. The classical nonhomologous end joining of the DNA repair pathway involves several proteins, such as XRCC1 (X-ray repair cross-complementing protein 1) and DNA Ligase-IV (Lieber 2008).

1.2.2. T cells

1.2.2.1. T cell development

T lymphocytes develop in the thymus from bone marrow-derived progenitor cells. Within the thymus, T cell progenitors undergo several steps of maturation, which can be followed up by their expression of cell surface markers. Development of T cells in the thymus is spatially separated and takes place in several thymic regions. The first state in the T cell development is characterized by the absence of the surface markers CD4 and CD8. The double negative (DN) T cells can further develop either in γδ or αβ expressing T cells. αβ TCR expressing T cells primary express the α-pre-TCR, which does not undergo rearrangement (von Boehmer and Fehling 1997). It pairs with the β-chain of the TCR. The locus of the β-chain undergoes somatic rearrangement. The αβ-pre-TCR is associated at the cell surface with several proteins, which form the CD3/ζ-complex. Active signaling via the pre-TCR is essential for further development and absence results in cell arrest at this state. After successful signaling via the pre-TCR, immature T cells undergo expansion, which is followed by somatic recombination of the α-locus of the TCR, leading to the expression of the mature αβ TCR. At this point, the developing T cells start to express the surface molecules CD4 and CD8. The double positive (DP) T cells undergo selection to further develop into single positive T cells. Most of the DP T cells are neglected during this point of selection, when their TCR binds to the self-antigens presented on MHC molecules of cortical thymus epithelial cells with too low affinity. On the other hand, strong binding of the TCR to the presented self-ligand induces apoptosis in a small fraction of T cells. This negative selection ensures elimination of autoreactive T cells (Robey and Fowlkes 1994). Immature T cells, which bind to self-antigens and generate medium intense signaling undergo positive selection and develop into single positive (SP) T cells in the thymic medulla. Interaction of CD8 or CD4 of DP T cells with MHC I or MHC II, respectively, designates the development of SP $CD8^+$ or $CD4^+$ T cells. The predominant interaction of either CD4 or CD8 with the MHC molecule on the thymic epithelial cell is influenced by its proximity to the TCR.

Naïve, mature T cells migrate to the peripheral lymphoid organs via blood vessels (Germain 2002).

1.2.2.2. T cell activation

Peripheral T cell differentiation is divided into three phases: a) clonal expansion, b) contraction and c) memory phase (Figure 4).

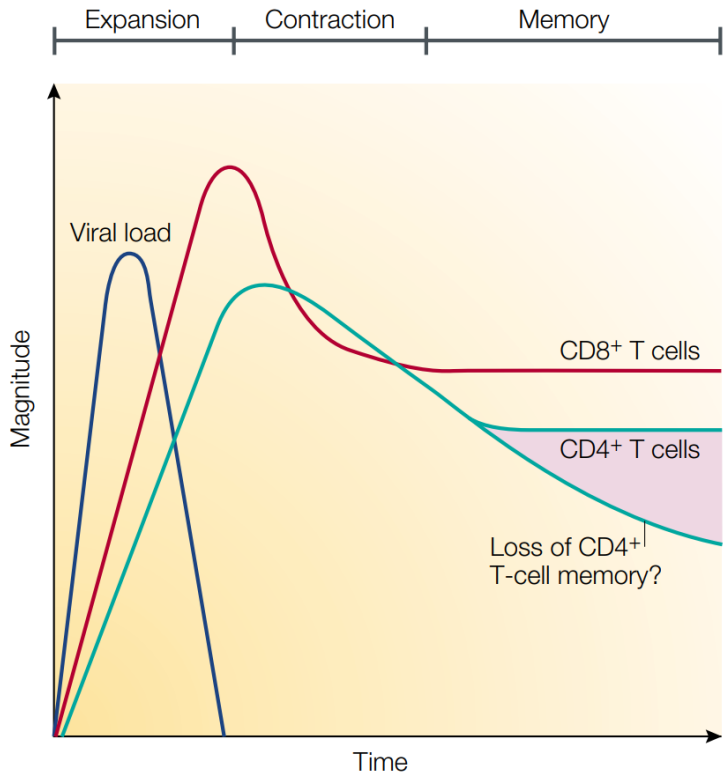

Figure 4: T cell activation

The three steps of T cell activation are: expansion, contraction, and memory formation. During a viral infection, T cells encounter DCs presenting viral antigens via MHC molecules. They provide signals for T cell proliferation. T cells expand and clear viral infections by e.g. direct killing of virus infected cells. Without signals for survival, most of the T cells undergo apoptosis. The T cell population contracts. Some of the effector T cells survive and develop into memory T cells. Those memory T cells can last for years and proliferate faster during a second infection (Image source: (Kaech, Wherry, and Ahmed 2002)).

Naïve T cells circulate through SLOs (secondary lymphoid organs) and migrate to the T cell zone. Activation of cDCs by pathogen binding to TLRs enhances the processing of peptides and their presentation on MHC molecules. Further, enhanced expression of CCR7 (C-C chemokine receptor type 7) guides DCs towards the T cell zone. Here, DCs encounter naïve T

cells, which leads to their activation, also called T cell priming. Binding of T cells to DCs is performed via several cell surface molecule interactions, such as CD2 CD58 interactions and LFA-1 (lymphocyte function-associated antigen 1) to ICAM1 (intercellular adhesion molecule 1) or ICAM2 interactions. The TCR complexed to CD3 on the T cell surface binds to the molecule presented on the MHC molecule on the APC. The TCR is further associated to either CD4 or CD8, which bind to MHC class II or I respectively, enhancing the cell-to-cell interaction. LFA-1 interactions increase the binding between T cell and DC, which can last for several days. During this time, the activated T cells proliferate, which is called clonal expansion. Clonal expansion calls for three different signals to ensure proper multiplication: MHC binding to the TCR to promote T cell activation, B7 immunoglobin binding to CD28 for survival, and cytokine mediated differentiation by e.g., IL-6, IL-12 or IL-4. Once T cells are differentiated into effector T cells, they do not need co-stimulation when they encounter posterior their specific antigen.

Effector cytotoxic CD8 T cells are hereby able to kill virus infected cells, without need of co-stimulatory signals. Also, CD4 effector cells play a major role, when it comes to the clearance of viral infections. CD4 effector cells provide help by additional activation of APCs, which in turn help to activate naïve T cells.

At the resolution of viral infection, the majority of the effector T cells die due to the lack of survival signals by absence of pro-survival cytokines or downregulation of the respective receptor. The clonal contraction of T cells is mediated either by intracellular BIM (B cell lymphoma 2–interacting mediator) mediated or extracellular Fas mediated apoptosis (Hand and Kaech 2009).

T cells which did not lose their sensitivity to pro-survival cytokines, mainly IL-7 and IL-15, and display an enhanced expression of the cell survival promoting molecule BCL2 (B-cell lymphoma 2) develop into memory T cells (Pulle, Vidric, and Watts 2006). Their restimulation upon a recurrent antigen encounter during a second infection happens faster and memory T cells are more sensitive to restimulation. Upon restimulation, memory T cells produce IFNγ and TNFα.

1.2.3. B cells

1.2.3.1. Development of B Cells

B cell development begins in the bone marrow or fetal liver from multipotent progenitor cells. Initially VCAM1(vascular cell adhesion protein 1) on bone marrow stromal cells (BMSC) binds to VLA-4 (very late antigen-4) of multipotent progenitor cells. At this point, D-J rearrangement of the heavy chain is initiated (D-J_H). Binding of SCF (stem cell factor) on BMSC to cKIT on early Pro-B cells induces expression of the IL-7 receptor (IL-7R). Besides IL-7, Fms-like tyrosine kinase 3 ligand (Flt3-L) as well as various transcription factors such as IKAROS (IKAROS family zinc finger 1), EBF (early B cell factor 1) and IRF8 (interferon regulatory factor 8) play a crucial role (Tobon, Izquierdo, and Canas 2013; Melchers 2015). IL7 released from BMSCs drives further maturation of early Pre-B cells into Pro-B cells. Down-regulation of VLA-4 and cKIT as well as transcription of the gene for the heavy chains are initiated. Joining of V_H segment to the D-J_H segment completes V_HDJ_H recombination at late Pro-B cell state. The Pro-B cell is released from the BMSC and the translated heavy chains are presented of the cell surface. Association of the heavy chain and surrogate light chain protein complex, forms the large Pre-B cell receptor (Pre-BCR). Signaling though the Pre-BCR is crucial for further development and leads to down-regulation of RAG expression (Kitamura et al. 1992). Pre-B cells then undergo massive expansion. Subsequently, light chain rearrangement occurs. Light chain and heavy chain form the immunoglobulin complex at the immature B cell surface which is known as B cell receptor (BCR). The immature B cells undergo a process called receptor editing, which is one essential process in formation of central tolerance. Receptor editing is based on one step light chain rearrangement, by which autoreactive light chains are replaced by downstream located light chains. Depending on their developmental origin, B cells are divided into B-1 cells or B-2 cells, originating from fetal liver or bone marrow, respectively.

1.2.3.2. B cell activation

Activation of naïve B cells is initiated by binding of the surface receptor to specific antigens. B cells develop into antibody producing plasma cells or memory B cells. Two possible ways lead to B cell activation: T cell independent activation or T cell dependent activation (Figure 5).

In the T cell independent (TI) activation of B cells, TI antigens stimulate the antibody production. TI type I antigens like LPS, CpG or poly I:C activate B cells via TLRs and induce

B cell proliferation (Mond, Lees, and Snapper 1995; Obukhanych and Nussenzweig 2006). Despite their inability of isotype switching by activation of type I antigens, B1 and marginal zone (MZ) B cells rapidly produce IgM for around one to three days after antigen exposure. IgM antibodies are pentameric molecules conjoined by disulfide bonds (B., A., and J. 2002). TI type II antigens such as polysaccharides activate the BCR and induce an antigen specific B cell response, which can only activate mature B cells. The plasma cells have a life span of two to three weeks and migrate to extrafollicular regions of the spleen. Generally, the IgM antibodies produced by TI B cell activation display low affinity to antigens, compared to antibodies produced by T cell dependent B cell activation.

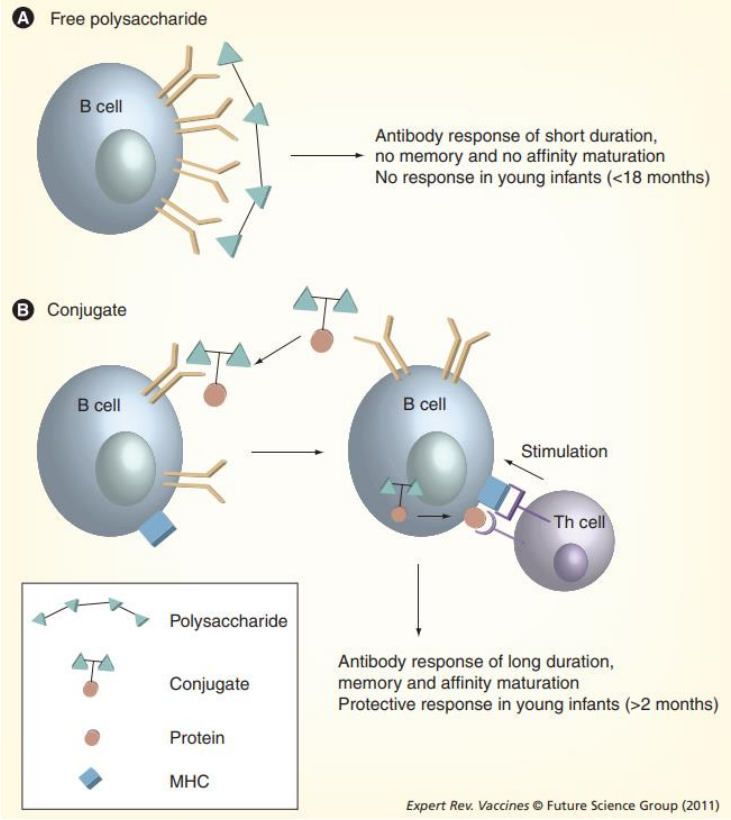

Figure 5: T cell dependent and independent activation of B cells

B cell activation independent from T cells in the presence of for example polysaccharides results in a short life IgM antibody response and no memory formation (A). T cell dependent activation of B cells leads to the production of a long-term antibody response, memory formation and a protective antibody response (B). (Image source: (Poolman and Borrow 2011))

The T cell dependent (TD) B cell activation is divided into two spatially distinct phases. In the early phase after antigen exposure, naïve CD4 T cells become antigen activated by professional APCs. B cells binding to antigen become activated and migrate to the T cell area. Interaction

of activated CD4 T cells and B cells occurs at the interface of the T cell area and follicles. Enhanced expression of costimulatory molecules and presentation of peptide fragments from antigens via MHC II on activated antigen specific B cells results in T cell activation through B cell T cell interaction. The activated T cell upregulate CD40L expression which induces cytokine mediated isotype switching of B cells by CD40-CD40L interactions. Isotype switching is an activation-initiated recombination event with the help of the cytidine deaminase AID (activation-induced cytidine deaminase) (Stavnezer, Guikema, and Schrader 2008).

1.2.4. Pathogens

Invading microorganisms can be divided into two general groups: commensal and pathogenic organisms. Pathogens are disease causing agents, such as bacteria, prions, fungi, parasites, and viruses, whereas commensal organism do not harm their host under physiological conditions.

1.2.4.1. Viruses

Viruses display the most abundant pathogens on earth. Despite their great heterogeneity viruses share one common feature: their replication cycle depends on the host. Upon viral entry into their targeted host cell by one specific or several entry receptors, such as phosphatidylserine or sialic acid (SA) residues, the viral genome is released into the cell. The replication of the viral genome relies on the host's replication machinery. Newly synthesized viral genome and proteins are finally assembled into novel virus particles and released from their host cells.

1.2.4.1.1. VSV

Vesicular stomatitis virus (VSV) is a negative-stranded, non-segmented RNA virus belonging to the family of *Rhabdoviridae*. The genome encodes for five proteins: glycoprotein (G), Matrix protein (M), nucleoprotein (NP), large protein (LP) and the phosphoprotein.

Entry of VSV into host cells is performed via binding of the VSV-G to its receptor. The receptor, phosphatidylserine, is an ubiquity expressed molecule on cell membranes (Lichty et al. 2004). Subsequent to endocytic cell entry, viral and cell membranes fuse, which is the initial step in the VSV replication cycle. Due the broad expression of the VSV receptor, it can infect

a great variety of animals, like cattle, swine, and rodents. Also in humans a VSV infection can lead to a symptomatic, influenza-like illness (Whelan 2008).

VSV infection results in a strong cytokine and cellular response. Viral sensing of VSV is performed mainly by TLR7 and RIG-I (Lund et al. 2004; Yoneyama et al. 2004; Fink et al. 2006). Hereby, VSV is sensed in DCs and $CD169^{+}$ macrophages (Solmaz et al. 2019). Activation of TLR7 results in MyD88 orchestrated induction of an interferon type I response, which is inevitable for the control of the viral infection and the prevention of neuroinvasive replication. Further, VSV replication elicits a strong T cell response. Independent from T cells, an initial VSV infection results in a fast and strong Th-independent IgM induction, followed by a Th-dependent IgG response (Zinkernagel 1997). There is strong evidence, that each of these mechanisms on its own is inevitable to provide protection against fatal VSV infection (Bachmann et al. 1996). Especially early immune events have been shown to be essential to prevent CNS-related fatality caused by VSV. Mainly EVR, rapid antigen provision and strong immune activation were shown to be essential for the control of the cytopathic VSV infection (Honke et al. 2011).

Easy genetic modification, small size and fast replication cycle make VSV suitable as backbone for several therapeutic, recombinant approaches. On the one hand, VSV based oncolytic viruses have risen over the last years. On the other hand, VSV based vaccines against different viruses display a capital new tool. Moreover, thus sometimes described, human VSV infections are relatively rare, so that pre-existing immunity to VSV is a negligible problem for the development of VSV based vaccines (Rauch et al. 2018). Due to its natural neurovirulence, attenuation of VSV based approaches is essential to ensure safety when administered. Attenuation is commonly achieved by introduction of non-viral proteins or reassortments into the VSV genome or modification of the VSV Matrix protein (Ahmed et al. 2008; Clarke et al. 2016).

1.2.4.1.2. Influenza Virus

Influenza virus type A, B, C and D belong to the family of *Orthomyxoviridae* viruses. Classification of Influenza viruses is based on their expression of the surface antigens neuraminidase (NA) and hemagglutinin (HA). 16 HA (H1-16) and 9 NA subtypes have been described to date, among all possible combinations, the subtype H1N1 shows high persistence in human species (McAuley et al. 2019).

The viral HA protein is integrated in the viral envelope and facilitates viral attachment and uptake into the host cell by binding to sialic acid (SA) residues on host cells, which majorly influences IAV (Influenza A virus) tropism (Imai and Kawaoka 2012). Human influenza viruses show higher affinity towards α2,6-linked sialic acids, whereas avian IAVs prefer α2,3-linked sialic acids (Glaser et al. 2005; Chutinimitkul et al. 2010). Upon SA binding of HA subunit HA1 endocytosis is facilitated, and viral particles are trafficking towards the endosome (Matlin et al. 1981; Lakadamyali, Rust, and Zhuang 2004). Upon endosomal fusion, vRNPs (viral ribonucleoprotein) traffic towards the cell's nucleus and initiate viral mRNA transcription, followed by virus assembly (Matsuoka et al. 2013). Proteolytic activation of newly synthesized HA by host proteases in endosomes is inevitable for production of infectious IAV particles (Horimoto and Kawaoka 1994). Newly formed virus particles bud at the cell membrane and are released from the cell highly dependent on NA activity. NA removes local SA and prevents HA binding to the cell surface, thereby releasing newly formed virus from the cells (Palese et al. 1974; McAuley et al. 2019).

Host recognition of invading IAV particles is sensed by all three classes of PRRs. The respective TLRs sense viral RNA, whereby dsRNA is recognized by TLR3, and ssRNA is recognized by TLR7 and TLR8 (Figure 6). The RIG-I and NOD-like receptors sense virus present in the cytosolic fraction of infected cells, whereas TLR3 detects IAV infected cells and TLR7 (murine) and TLR8 (human) recognize viral RNA in endosomes of sentinel cells (Iwasaki and Pillai 2014). TLR3 and TLR7 induce NF-κB translocation into the nucleus and transcription of IFN type I and related genes (Diebold et al. 2004; Guillot et al. 2005).

The humoral response against IAV provides protection through specific neutralizing antibodies to the HA [20], and cell-mediated immunity (CMI) also plays a role in augmenting the B cell response. Despite the induced B cell response, T cells play an essential role in clearing IAV infection. In detail, IAV specific CD8 T cells eradicate infected cells presenting IAV-peptides on MHC class I. This process was shown to be inevitable to induce fast clearance of an IAV infection in mice (Bender et al. 1992). T cell dependent clearance of IAV infected cells was shown to be dependent on dendritic cells (McGill, Heusel, and Legge 2009; McGill and Legge 2009).

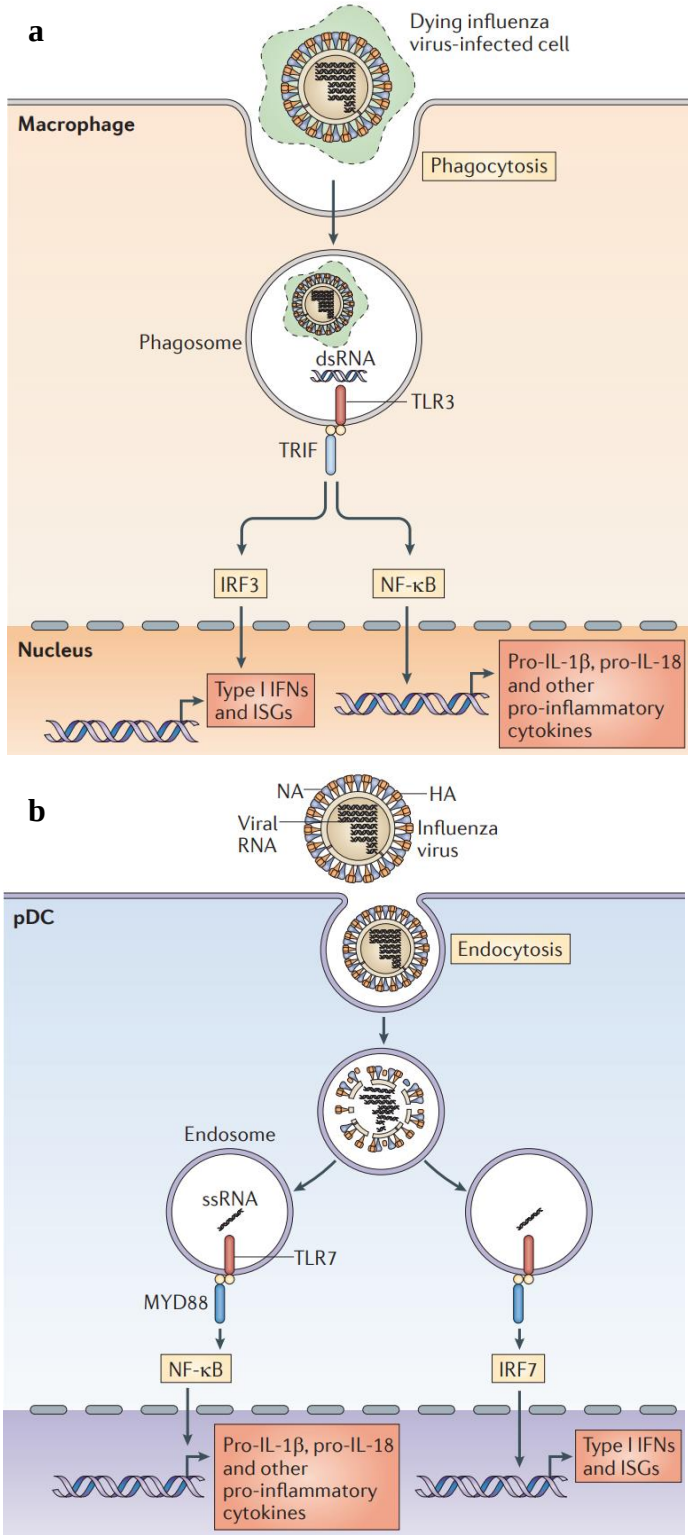

Figure 6: Innate sensing of IAV

a Dying IAV infected cells are phagocytized by macrophages. TLR3 senses dsRNA, which leads to the induction of type I IFNs and ISGs dependent on IRF3, as well as pro-inflammatory cytokines dependent on NF-κB activation. **b** IAV uptake into DCs and release of viral ssRNA into the endosome activates TLR7 dependent MYD88 activation of NF-κB or activation of IRF7, which induce pro-inflammatory cytokines or type I IFNs, respectively. (Image adapted from: (Iwasaki and Pillai 2014))

1.2.5. Vaccination

Vaccines state a powerful tool to protect the body against disease causing pathogens like bacteria or viruses with the aid of the immune system. Vaccine development began in the late 18th century, with the first trial of Edward Jenner to find a strategy to prevent severe Smallpox virus infection ('The Vaccination History of Small-Pox Cases' 1902). In the late 19th century, Louis Pasteur followed with the development of an attenuated chicken cholera vaccine, anthrax vaccine and rabies virus vaccine. The mechanism of immunization by vaccines is to introduce disease-causing pathogens in an attenuated, killed or modified form into the patient to stimulate the immune system (Pulendran and Ahmed 2011). Throughout the centuries several approaches were developed, which can be dived into different groups: Replicating vaccines and non-replicating vaccines. The class of replicating vaccines is composed of live-attenuated vaccines and recombinant vaccines, whereas non-replicating vaccines are inactivated/killed vaccines, subunit vaccines, capsular polysaccharides, toxoids and protein- or peptide-based vaccines (Figure 7).

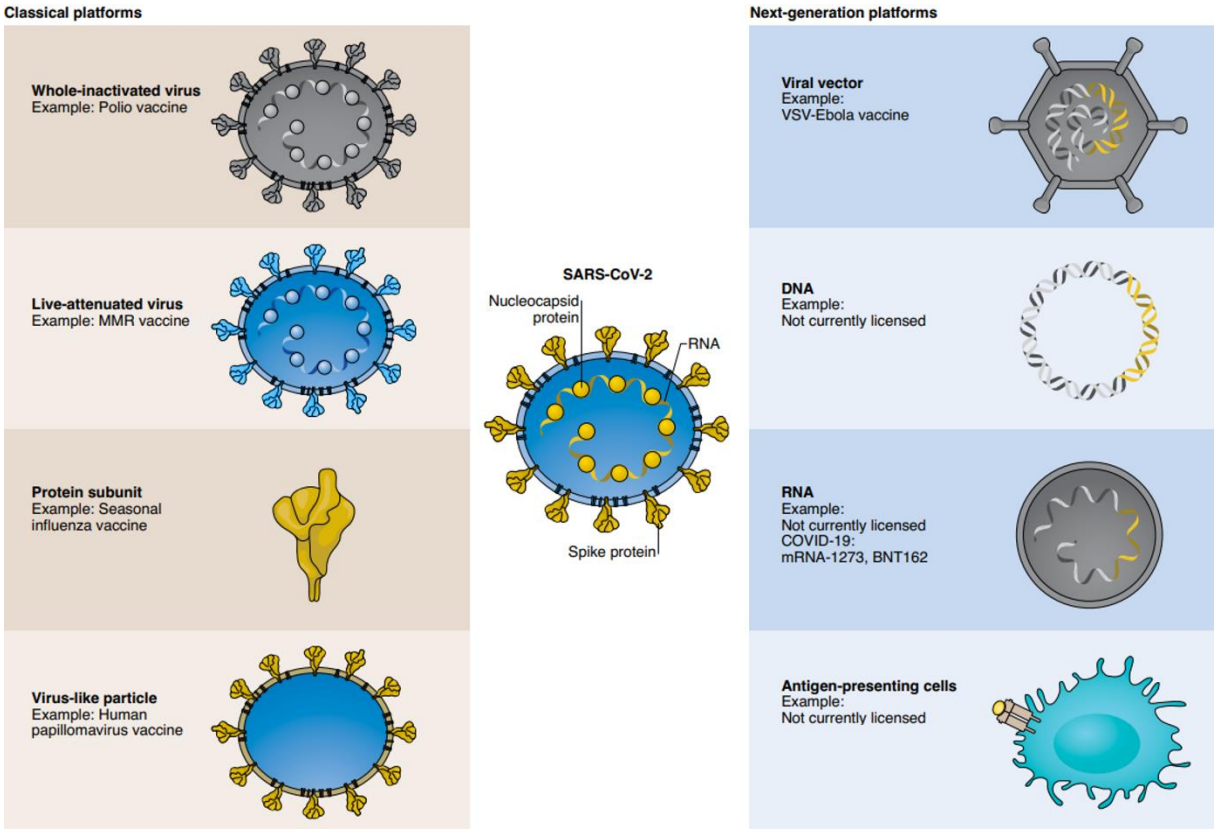

Figure 7: Overview of current technologies in vaccine development

Anti-viral vaccines use several different components of the virus. The whole inactivated virus particles are for example used in Polio virus vaccines. Small modifications of the virus for example by passaging leads to a replication competent but attenuated whole virus. This approach is used e.g., for the MMR vaccine. Further modification of the original virus is used to generate VLPs (Virus like particles) which lack the ability of

replication by the loss of genomic information. VLPs are used for example for papillomavirus vaccines. Use of only small parts of the whole virus is used in several other vaccine approaches. Protein subunits are used in the influenza vaccine, whereas genetic information can be used for three different approaches. Viral vectors, such as the VSV-EBOV vaccine use parts of the information in combination with a shuttle virus like VSV. DNA vaccines use the genetic material of DNA viruses. In contrast, the recently licensed COVID-19 RNA vaccines use the mRNA of the SARS-CoV-2. Antigen expressing cells are currently not a tool for vaccination (Image adapted from (van Riel and de Wit 2020)).

1.2.5.1. Non-live vaccines

The group of non-live vaccines is formed by inactivated vaccines, killed vaccines, and subunit vaccines. Inactivated vaccines or killed vaccines have been used for several human diseases like Polio virus (PV), Rabies virus, Influenza virus or Hepatitis A virus. Pathogens are inactivated by using radiation, heat or chemical treatment. Poor stimulation of the immune system is overcome by the use of adjuvants, which stimulate innate or adaptive immunity (Marciani 2003). Adjuvants, like IC31 (oligonucleotides, cationic peptides) or flagellin (bacterial protein linked to antigen) and CpG (CGC oligonucleotides with or without alum or emulsion) are used to induce Th1 cell relating immunity by triggering combination of targets or specific TLRs respectively.

1.2.5.2. Live vaccines

Live vaccines can be subdivided into two groups: Live attenuated vaccines (LAV) and recombinant or viral vector vaccines.

LAV belong to the class of most frequently used vaccines against viruses rather than bacteria. This technique introduces undirected genetic mutations in the pathogens, which leads to an adaption of growth in the abnormal host and is associated with decreased growth and pathogenicity in human individuals. Vaccines against Measles virus, Rubella virus, Mumps virus, Varicella virus, Influenza virus, Polio virus and Junín virus were developed by passaging and selection of clones in cell culture or non-human hosts. The disadvantage of this process is the genetic instability and potential remaining pathogenicity of the live attenuated vaccine. Even in the early origins of LAV via variolation, backmutations of the attenuated smallpox virus occurred rather often and led to a high mortality of two to three percent. Also, in later approaches, backmutations occurred and led to a rather rare case of paralysis after the administration of live attenuated Polio virus vaccine. Still, LAV display the most powerful tools

for disease control, by induction of immune responses by activating e.g., different TLRs resulting in activation or inhibition of DCs (Tsuji et al. 2000; Querec et al. 2006). Final protection against the pathogen is maintained by formation of neutralizing antibodies or virus-specific T cells (Plotkin 2008; Levin et al. 2008).

Recombinant viral vector-based vaccines are an uprising technology over the last years. This approach relies on the ability to introduce one or several antigens of pathogens in the host, administered with or without adjuvants. One additional approach is to genetically engineer antigens of the target virus into harmless vectors.

1.2.5.2.1. VSV-EBOV

VSV-EBOV represents the current approach of an Ebola virus vaccine. The Ebola virus is a ssRNA virus, which leads to hemorrhages, coagulation defects, multiorgan failure and death. From 2014 to 2016 the Ebola virus epidemic resulted in over 11,000 deaths in Afrika. The recombinant vaccine is based on a VSV vector which expresses the Ebola virus glycoprotein. Administration of the VSV-EBOV results in protection by the activation of a strong interferon signature and B cell activation (Menicucci et al. 2019).

2. Aim of the thesis

Innate immune recognition is the first essential process to protect the body against lethal harm caused by pathogens such as viruses. The mechanism of viral sensing via PRRs is well described. It is known that control of viral replication is a fragile process which must be tightly counterbalanced. Innate immune mechanisms which are essential to provide host protection by simultaneously allow restricted viral replication in specialized cells have recently been investigated after the systemic infection with the vesicular stomatitis virus. Especially EVR has been shown as crucial mechanism, which on the one hand drives USP18 dependent viral replication in subsets of macrophages and dendritic cells. On the other hand, EVR provides sufficient amounts of antigen to efficiently activate an immune response. Absence of EVR by ubiquitous deletion of USP18 from mice hereby lead to a fatal outcome after VSV infection.

Immunization with replication competent viral vector vaccines such as VSV-EBOV as well as natural occurring infections with viruses such as IAV demands strong immune responses to provide protection. To date, it is still unknown whether USP18 mediated EVR is an essential mechanism maintaining innate and adaptive immunity in both cases. Therefore, we investigated the systemic role of EVR for immune cell specific replication of the viral vector vaccines VSV-EBOV. Further utilizing the model of IAV, we specifically analyzed the role of USP18 mediated enforced replication and its influence on the activation of the immune system in the background of infections with relevant human pathogens. These two interdepending parts highlight the importance of enforced virus replication in the context of viral infections and will be evaluated in the two chapters of this thesis:

Chapter 1: Systemic relevance of immune system specific replication

Chapter 2: Mechanism of immune system specific IAV replication

3. Materials and Methods

3.1. Materials

3.1.1. Chemicals and Reagents

Table 1: List of Chemicals and Reagents

Reagent	**Supplier**
IMDM powder	Sigma-Aldrich
Laemmli Sample Buffer (2 X)	Bio-Rad
30 % Acrylamide/Bis Solution	Bio-Rad
Acetone	Honeywell
Agarose	Sigma-Aldrich
Ammonium persulfate (APS)	Sigma-Aldrich
Bovine Serum Albumin Fraction V (BSA)	PAA
Brefeldin A	Sigma-Aldrich
$CaCl_2$	Sigma-Aldrich
Chloroform	Merck
Corn oil	Sigma-Aldrich
Crystal violet	SERVA
DEPC-Treated Water	Thermo Fisher Scientific
DMEM	PAN-Biotech
DNAse	Roche
dNTPs	Promega
DPBS w/o Mg^{2+}, Ca^{2+}	PAN-Biotech
Ethanol	Sigma-Aldrich
Ethidium bromide	Carl Roth
Ethylenediaminetetraacetic acid (EDTA)	Roth
FastRuler Middle Range DNA Ladder	Thermo Fisher Scientific
Fetal Calf Serum (FCS)	Gibco
Dako Fluorescent Mounting medium	Agilent
Formaldehyde-Solution (37 %) (Formalin)	AppliChem
Glycerol	Sigma-Aldrich
Glycine	Sigma-Aldrich

IMDM powder	Sigma-Aldrich
Isoflurane	AbbVie
Isopropanol	Sigma-Aldrich
L-Glutamine-Penicillin-Streptomycin Solution	Sigma-Aldrich
Liberase	Roche
Methanol	J.T. Baker
Methylcellulose	Sigma-Aldrich
$MgCl_2$	Merck
Na_2HPO_4	Honeywell
NaCl	Biochrom
NaN_3	Sigma-Aldrich
Oseltamivir Phosphate	Sigma-Aldrich
Saponin	Sigma-Aldrich
Sialidase	Roche
Skim Milk powder	AppliChem
Sodium Bicarbonate	Sigma-Aldrich
SuperSignal West Femto Chemiluminescence-Substrate	Thermo Fisher Scientific
SYBR Green PCR Master Mix	Thermo Fisher Scientific
Tamoxifen	Sigma-Aldrich
Taq Polymerase	Promega
Tetramethylethylendiamin (TEMED)	Carl Roth
Tissue-Tek O.C.T. Compound	Sakura Finetek
TPCK Trypsin	Sigma-Aldrich
Tris(hydroxymethyl)aminomethane (Tris base)	Sigma-Aldrich
TrisHCl	Sigma-Aldrich
TRIzol Reagent	Thermo Fisher Scientific
Trypsin/EDTA	PAN-Biotech
Tween 20	Sigma-Aldrich

Table 2: Media, Buffer and Solutions

Name	**Company**
IMDM solution (2 X)	100 g IMDM, 3,024g sodium bicarbonate, 900 ml A. dest, pH 7.6
Methylcellulose (2 X)	10 g methylcellulose, 500 ml A. dest
Agarose solution (4 %)	100 ml DMEM, 4 g Agarose
CaMg (100 X)	1g $CaCl_2$, 1g $MgCl_2$, 100 ml A. dest
Crystal violet solution	5 g crystal violet, 200 ml methanol, 110 ml formalin (36.5 %), 640 ml A. dest
FACS buffer (10 X)	25 mM EDTA, 100 ml FCS, 95,55 g PBS, 10 g NaN_3, 850 ml A. dest
FACS buffer (1 X)	100 ml FACS buffer (10 X), 900 ml A. dest
Infection medium	500 ml DMEM, 3 ml 30 % BSA, 5 ml L-Glutamine-Penicillin-Streptomycin solution
Infection PBS	500 ml DPBS, 3 ml 30 % BSA, 5 ml CaMg (100 X)
MACS buffer	500 ml DPBS, 2 mM EDTA, 0,5 % BSA
Methylcellulose overlay	1 volume IMDM (2 X), 1 volume methylcellulose (2 X)
PBST	1000 ml of PBS, 1 ml of Tween 20
SDS lysis buffer	5 ml 10 % SDS, 4 ml 1 M tris(hydroxymethyl)aminomethan pH 6,8, 5 ml glycerol, 31 ml A. dest
SDS running buffer (10 X)	144 g glycine, 30 g Tris base, 10 g SDS, 1000 ml A. dest
SDS running buffer (1 X)	100 ml SDS running buffer (1 X), 900 ml A. dest
Tissue digestion solution	0,5 % SDS, 5 mM EDTA, 200 mM NaCl, 5 mM TrisHCl
Transfer buffer (10 X)	144 g glycine, 30 g Tris base, 1000 ml A. dest
Transfer buffer (1 X)	100 ml transfer buffer (10 X), 700 ml A. dest, 200 ml methanol
TSM buffer	20 mM tris(hydroxymethyl)aminomethan (pH 7.4), 150 mM NaCl, 1 mM $CaCl_2$, 2 mM $MgCl_2$, 0.5 % BSA

Table 3: List of Kits

Name	Company
GoTaq G2 DNA Polymerase	Promega
IFNα mouse ELISA Kit	Thermo Fisher Scientific
QuantiTect Reverse Transcription Kit	Qiagen
Pan DC MicroBeads, mouse	Miltenyi Biotec

Table 4: List of Antibodies and Lectins

Name	Company
Anti-Ebola surface glycoprotein (clone KZ52)	absolute antibody
Anti-Rabbit, fluorescently marked	Thermo Fisher Scientific
Anti-VSV-G tag	Abcam
CD11c (clone N418)	eBioscience
CD169 (clone MOMA-1)	Bio-Rad.
CD4 (clone L3T4)	eBioscience
CD8a (clone 53-6.7)	eBioscience
F4/80	eBioscience
F4/80 (clone BM8)	eBioscience
Fixable viability Dye	eBioscience
GAPDH	eBioscience
IFNγ (clone XMG1.2)	eBioscience
Influenza A H1N1 (A/Puerto Rico/8/34) hemagglutinin	Sino Biological
Influenza A H1N1 (A/Puerto Rico/8/34) Matrix protein	Sino Biological
MAL II lectin, biotinylated	Vector Laboratories
Streptavidin, fluorescently marked	eBioscience
α-mouse HRP	Jackson ImmnoResearch
α-rabbit HRP	Jackson ImmnoResearch

Table 5: List of Peptides

Virus	Sequence	Company
IAV	ASNENMETM	Anaspec
VSV	YTDIEMNRLGK	Anaspec

3.1.2. Primer

Table 6: Genotyping primer

Name	Target	Sequence
CAG-Cre	Cre recombinase und CAG promotor	Cre1: GTA GGT GGA AAT TCT AGC ATC ATC C Cre2: CTA GGC CAC AGA ATT GAA AGA TCT Cre3: GTG AAA CAG CAT TGC TGT CAC TT Cre4: GCG GTC TGG CAG TAA AAA CTA TC
*CD169*iCre	Cre recombinase under CD169 promotor	CD169-F2: GCT TAC GGT GCT TGC TGG AT CD169-R: CAT AGT CTA GGC TTC TGT GC Cre-R8: AGG GAC ACA GCA TTG GAG TC
Usp18 floxed	P-Lox sides *Usp18*	FW: CAC CTC CAT TTG GTT TCA GG RV: AAC TCC TTC CTC TGG CTT CC

Table 7: qRT-PCR Primer

Name	Catalogue-Nr.	Company
Ifna2	QT00253092	Qiagen
Ifna4	QT01774353	Qiagen
Ifna5	QT00327656	Qiagen
Ifnß1	QT00249662	Qiagen
GAPDH	QT01658692	Qiagen

Table 8: Virus specific primer

Name	Sequence	Company
Influenza strain A/Puerto Rico/8/34 segment 7 Matrix protein 2	5‘CTTCTAACCGAGGTCGAAACG3‘ 5‘GGGCATTTTGGACAAAG/TCGTCTA3‘	Biomers
VSV NP Primer	5’TAAATGAPGATGAKACPATGCAATC3’ 5′-ACKCAIGTPACPCGPGACCATCT-3′	Biomers

3.1.3. Lab supplies

Table 9: List of supplies

Name	Company
1.5 ml tubes	Eppendorf
1000 µl pipette tips	Starlab
15 ml conical tubes	Corning
2 ml tubes	Eppendorf
20 µl pipette tips	Starlab
200 µl pipette tips	Starlab
24-well plate	TPP
50 ml conical tubes	Corning
70 µm cell strainer	Corning
96-well plates (F) flat-bottom	TPP
96-well plates round (U) bottom	TPP
Blotting paper	Thermo Fisher Scientific
Cover glasses	Thermo Fisher Scientific
Cryotubes	Thermo Fisher Scientific
HistoBond+ microscope slides	Paul Marienfeld
MicroAmp 384-well Plate	Applied Biosystems
Nitrocellulose membrane	Thermo Fisher Scientific
Optical sealing foil	Roche
Staining chamber	Simport
Staining dish	DWK Life Sciences

Stainless steel beads	Qiagen
T175 cell culture flasks	Thermo Fisher Scientific

3.1.4. Software

Table 10: List of software

Name	**Company**
PubMed	http://www.ncbi.nlm.nih.gov
BZ-II Analyzer software	Keyence
PowerPoint	Microsoft
Word	Microsoft
Excel	Microsoft
ImageLab	BioRad
Prism 8.3.0	GraphPad
FlowJo 7.6.1	FlowJo

3.1.5. Hardware

Table 11: List of hardware

Name	**Company**
Centrifuge 5810R	Eppendorf
Centrifuge Mirco 220R	Hettich
ChemiDoc MP System	BioRad
Cryotome CM3050S	Leica
FACS LSR Fortessa	Becton Dickinson
FLUOstar Omega	BMG Labtech
GeneAmp PCR System 9700	Applied Biosystems
Light Cycler 480	Roche
Microscope BZ-900	Keyence
Mini-PROTEAN Tetra Handcast Systems	BioRad
Nanodrop 2000c Spectrophotometer	Peqlab
TissueLyser II	Qiagen
QuadroMACS Separator	Miltenyi Biotec

PCR cycler	Thermo Fisher Scientific

3.1.6. Biologicals

3.1.6.1. Cell lines

All cell lines which were used for this study were obtained from ATCC or gifted by collaborators. Cell maintenance was performed in humidified atmosphere in the presence of 5 % CO_2 and 37 °C.

Table 12: Cell lines

Cell line	Entity	Company/ collaboration
BHK cells	Baby Hamster Kidney	ATCC
Vero cells	African Green Monkey Kidney	ATCC
Vero E6 cells	African Green Monkey Kidney	ATCC
MDCK II cells	Canine Kidney	Prof. Dr. Tenbusch, RUB

3.1.6.2. Mice

All mice used for this study were housed in single ventilated cages under controlled standard conditions. All animal experiments were performed with the authorization of Veterinäramt Nordrhein-Westfalen (LANUV, Düsseldorf, Germany) and in accordance with the German law for animal protection.

C57BL/6J

Wildtype C57BL/6J mice were purchased at Taconic Bioscience and used for infection experiments or as naïve controls. This mouse line depicts the standard inbred mouse model.

***Usp18*$^{fl/fl}$**

The *Usp18* gene of these mice in flanked by LoxP sites (short term “floxed”). LoxP sites display the recognition sequences for the Cre recombinase.

B6N.Cg-Tg(CAG-cre/Esr1*)5Amc/CjDswJ (Cag^{CRE})

Mice expressing the Cre-recombinase under the CAG-Promotor. The Cre recombinase is a recombinase derived from the bacteriophage P1 and joined to the ligand-binding domain of the estrogen receptor. Ubiquitous expression of the CAG-promotor allows high expression of the Cre recombinase after administration of the estrogen receptor ligand Tamoxifen.

***Usp18*$^{fl/fl}$ x Cag^{CRE}**

Mouse line generated by crossing *Usp18*$^{fl/fl}$ with B6N.Cg-Tg(CAG-cre/Esr1*)5Amc/CjDswJ (CAG^{cre}). After administration of Tamoxifen, the Cre recombinase specifically cuts out floxed alleles of *Usp18*. This results in an inducible *Usp18* gene knockout model, which does not bury the disadvantages of a constitutive knockout model. This mouse line does not display cell development malfunctions as visible in constitutive *Usp18* gene knockout models.

CD169-Cre

Mouse line with Cre recombinase expression under the CD169 promotor.

***Usp18*$^{fl/fl}$ x *CD169*-Cre**

Mouse line generated by crossing *CD169*-cre with *Usp18*$^{fl/fl}$ mice. In this mouse line, *Usp18* is constitutively knocked out in all cells, which express CD169. This model can be used to investigate the influence of USP18 in CD169^{+} macrophages. It allows specific analysis of cell targeted gene deletion without side effects on the development or function of other cell types.

***Ifnar*$^{-/-}$**

Mouse line with constitutive knockout of the interferon-α/β receptor (IFNAR).

3.1.6.3. Viruses

Table 13: Viruses

Virus	**Company/ collaborator**
Influenza virus strain A/Puerto Rico/8/1934 H1N1 (IAV)	Prof. Dr. Tenbusch
Vesicular stomatitis Virus (VSV)	D. Kolakofsky
Vesicular stomatitis Virus expressing the Ebola virus Glycoprotein (VSV-EBOV)	Prof. Dr. Addo

3.2. Methods

3.2.1. Cell culture

All cells used were cultured in DMEM medium in the presence of L-Glutamine-Penicillin-Streptomycin (PSG) solution. MDCK II and Vero E6 cells were cultured in the presence of 10 % FCS, Vero cells and BHK cells in the presence of 5 % FCS. Cells were passaged twice a week or upon 80-90 % confluency. Cell culture medium was removed from the cell culture flasks by aspiration. The cell layers were washed once with DPBS and five milliliters of Trypsin/EDTA solution was added to a T175 culture flask. After incubation for three to five minutes at 37 °C, Trypsin/EDTA solution was inactivated by adding DMEM culturing medium containing FCS. Cell suspensions were collected and centrifuged for five minutes at 1400 rpm, 4 °C. Supernatant was discarded by aspiration, cell pellets were resuspended in fresh culturing medium and seeded into new cell culture flasks. Culturing of cells was proceeded at 37 °C, 5 % CO_2 in a humidified incubator.

3.2.2. Virus propagation

3.2.2.1. VSV and VSV-EBOV propagation

The cell culture medium of BHK cells with a confluence of 90 % was removed by aspiration. BHK cells were infected with $1x10^4$ PFU/ml VSV or VSV-EBOV in five milliliters of 2 % FCS, 1 % PSG containing DMEM. After 30 minutes of infection, 45 ml of fresh cell culture medium (DMEM, 2 % FCS, 1 % PSG) was added and BHK cells were incubated for 48 hours at 37 °C, 5 % CO_2. Virus containing supernatant was collected and centrifuged for 20 minutes, 4000 rpm, 4 °C. Supernatant was transferred to cryotubes and stored at -80 °C afterwards. Virus titers were determined via VSV or VSV-EBOV plaque assay.

3.2.2.2. IAV propagation

MDCK II cells with a confluence of 80 % were washed with PBS once. IAV was added at a MOI of 0.001 to the cells in infection PBS and incubated at 37 °C, 5 % CO_2 for 30 minutes. Infection PBS was removed by aspiration and infection medium was added. Cells were observed until cytopathic effect was visible. Virus containing supernatant was harvested and centrifuged at 4000 rpm, 4 °C for 20 minutes. The supernatant was transferred into cryotubes,

and long-term storage of virus was performed at -80 °C. Virus titers were determined via IAV plaque assay.

3.2.3. Virus titer determination

3.2.3.1. VSV and VSV-EBOV plaque assay

For determination of VSV or VSV-EBOV titers, plaque assay was performed. One day in prior Vero cells (VSV plaque assay) or Vero E6 cells (VSV-EBOV plaque assay) were seeded out. The respective cells were harvested as mentioned in cell culture protocol (Chapter 3.2.1) and cell concentration was adjusted to $7x10^5$ cells/ml in cell culture medium. Then 400 µl of the cell suspension was added to each well of a 24-well plate and incubated for 24 hours at 37 °C and 5 % CO_2 in a humidified incubator. For virus titers analysis of organs, samples were collected in a 2 ml tube with a stainless-steel bead in 1 ml of DMEM with 2 % FCS and 1 % PSG. Samples were either snap-frozen in liquid nitrogen and stored at -80 °C until analysis or immediately analyzed after harvest. For further analysis, organs were homogenized with the Qiagen Tissue Lyser II for ten minutes and 25 Hz. Afterwards, samples were centrifuged for five minutes at 6000 rpm at 4 °C. Non-organ samples were harvested and stored at -80 °C or immediately analyzed. Eleven serial 1:3-dilutions of samples in DMEM (2 % FCS, 1 % PSG) were performed in a 96-well round bottom plate. The supernatant of pre-seeded cells on 24-well plated was removed. Every second dilution (row 2, 4, 6, 8, 10, 12) was transferred to a 24-well plate (row 1, 2, 3, 4, 5, 6, respectively) with the pre-seeded, confluent cells. After one hour of incubation at 37 °C, 5 % CO_2, 200 µl of methylcellulose overlay was added per well to the cells. Visualization of plaques was performed after 24 h (VSV) or 48 h (VSV-EBOV) of incubation via crystal violet staining. Therefore, supernatant was removed from the 24-well plate and 400 µl crystal violet staining solution was added to each well. After 30 minutes of incubation, the solution was removed and plates were washed with water, dried and plaques were counted. Virus titer were calculated as following:

Calculation of virus titers

$$\text{Virus titer } \left(\frac{\text{PFU}}{\text{ml of sample}}\right) = \text{a} * 3 * 10^{\text{b}-1} * 5 * c$$

a= plaques counted in one well

b= row, in which plaques were counted

c=dilution factor organs

3.2.3.2. IAV plaque assay

Twenty-four hours prior to IAV plaque assay, MDCK II cells were seeded out in 24-well plates with a density of $7x10^5$ cells/ml in 400 µl of culturing medium per well and incubated at 37 °C, 5 % CO_2 in a humidified incubator. For analysis of IAV titers, organs were harvested in a 2 ml tube with 1 ml of PBS with a stainless-steel bead. Organs were either frozen in liquid nitrogen and stored at -80 °C or immediately used for analysis. Samples, which were not derived from organs, were harvested and either used directly in the assay or stored at –80 °C until analysis. For IAV plaque assay, organs were homogenized with Qiagen Tissue Lyser II according to above mentioned procedure (Chapter 3.2.3.1). Eleven serial 1:3-dilutions of samples in PBS were performed in a 96-well plate. Supernatant of pre-seeded MDCK II cells was removed and every second dilution (row 2, 4, 6, 8,1 0, 12) was transferred to pre-seeded confluent MDCK II cells (row 1, 2, 3, 4, 5, 6, respectively). After incubation for two hours, media was entirely removed and cells were overlaid with DMEM containing 1 % BSA, 1 mg/ml TPCK-Trypsin and 0.11 volume of 4 % agarose solution. Therefore, 4 % agarose solution was melted completely and cooled for two minutes at room temperature. Then the melted agarose solution was added to 37 °C tempered DMEM containing 1 % BSA. TPCK-Trypsin was added at last. Solution was shaken vigorously and quickly transferred to MDCK II cells using a 12-channel pipette. The 24-well plates were incubated for 72 h at 37 °C and 5 % CO_2 in a humidified incubator. Plaques were visualized via crystal violet staining. Therefore, 400 µl of crystal violet solution was added to each well and incubated for one hour at room temperature. Afterwards, plates were washed and dried. Plaques were counted and virus titer were calculated as described in Chapter 3.2.2.1.

3.2.4. Treatments

3.2.4.1. Tamoxifen treatment

Mice expressing the CAG-promotor and control mice were injected intraperitoneally with 4 mg of Tamoxifen in 100 µl of corn oil at eight-, six- and four-days prior infection. Therefore, 4 g of Tamoxifen was added to 100 ml of corn oil at heated at 37 °C, shaking until Tamoxifen was dissolved. Tamoxifen solution was aliquoted and stored at -20 °C. Prior to injection Tamoxifen aliquots were heated at 37 °C for 20 min in the dark, until Tamoxifen was complete dissolved. Habitus of Tamoxifen treated mice was carefully observed during this procedure. After a three-day reconstitution period, mice were infected a d0.

3.2.4.2. Sialidase treatment

To remove sialic acid residues from cells, mice were treated with 0.012 U Sialidase in PBS i.p.. Treatment was performed twice a day, starting one day in prior to infection. Treatment was adjusted from published protocol (Schneider et al. 2015).

3.2.4.3. Oseltamivir treatment

Oseltamivir dissolved in H_2O was administered orally at the dose of 0.1 mg/kg two times a day starting one day prior to infection (Bird et al. 2015).

3.2.5. Immunohistochemistry

Organs were removed from fresh sacrificed mice and snap frozen in Tissue-Tek O.C.T. Compound. Samples were stored at -80 °C. Seven micrometer sections were cut with help of a cryotome and transferred to HistoBond+ microscope slides. For immunostaining of tissues, microscope slides were incubated in acetone for ten minutes in staining dishes at room temperature. Microscope slides were removed from acetone and air dried until acetone was completely evaporated. Samples were surrounded with a hydrophobic barrier with help of ImmEdge pen and dried for two minutes at RT. Non-specific binding sides were blocked with 2 % FCS in PBS for 15 minutes at room temperature. Samples were incubated with antibodies diluted in 2 % FCS/PBS for 30 to 60 minutes at room temperature in dark staining chambers. Antibodies were diluted 1:100-1:200, depending on manufacturer's recommendation. Hereinafter, samples were washed with 2 % FCS in PBS and, if necessary, incubated with a secondary or tertiary antibody according to the above-mentioned procedure. After a final washing step with 2 % FCS in PBS, slides were mounted with Dako Fluorescent Mounting medium and cover glasses were added. Samples were dried for 30 minutes at RT protected from light and analyzed. Processing of images was performed with Keyence BZ-9000 microscope.

3.2.6. DNA isolation and genotyping

Ear punches of mice were incubated in 250 µl of tissue digestion buffer in the presence of 12.5 µl Proteinase K (30 mg/ml) overnight at 56 °C. One volume of isopropanol was added to the samples, mixed, and incubated at -80 °C for ten minutes. Samples were centrifuged for ten minutes at 15000 rpm, 4 °C and DNA pellets were washed twice with 70 % ethanol. DNA pellets were airdried and 50 µl of DEPC-treated water was added. One microliter of prepared DNA was added to 24 µl of PCR master mix (s. Table 14).

Table 14: PCR master mix

Reagent	Volume (µl)
DEPC H_2O	17.96
Taq buffer (5 X)	5
dNTPs (10 mM)	0.5
Primer	0.1 (each)
Taq Polymerase	0.25

PCR was performed and samples were analyzed by gel electrophoresis. Briefly, 15 µl of sample were added to one lane on the agarose gel, beginning at lane two. To the first lane, five microliters of FastRuler Middle Range DNA Ladder were added. The agarose gel was run at ~130 V in a gel electrophoresis chamber, until the running front headed to 1 cm of the lower end of the gel. Analysis of the agarose gel was performed using a UV-light chamber. DNA was visualized using ethidium bromide as staining reagent.

3.2.7. RNA isolation

RNA isolation was performed with TRIzol reagent according to manufacturer's protocol. Briefly, organs of mice were harvested in a RNase-free 2 ml tube containing 1 ml of TRIzol reagent and a stainless-steel bead and immediately frozen in liquid nitrogen. Samples were stored at -80 °C or directly processed afterwards. Frozen samples were smashed in TRIzol reagent using Qiagen TissueLyser II according to mentioned procedure (Chapter 3.2.3.1) at room temperature. Afterwards, 200 µl of chloroform were added to 1 ml of TRIzol reagent to each sample, mixed thoroughly for 15 seconds and incubated for three minutes at room temperature. Samples were centrifuged for 15 minutes at 15000 rpm, 4 °C. The aquatic upper

phase was transferred into a fresh, RNase-free 1.5 ml tube and 500 µl of isopropanol were added. The samples were incubated for 15 minutes on ice and centrifuged for ten minutes at 15000 rpm, 4 °C. The RNA pellets were washed twice with 70 % ethanol and the supernatant was removed using a vacuum pump. DEPC-treated water was added to the completely dried RNA pellet. Samples were stored at –20 °C for 7 days. Long-term storage was performed at -80 °C.

3.2.8. cDNA synthesis

The RNA concentration was determined using a Nanodrop 2000c Spectrophotometer and adjusted to 100 to 400 ng/µl with DEPC-treated water. For cDNA synthesis QuantiTect Reverse Transcriptase Kit was used according to Table 15. A total amount of 500 ng of RNA were adjusted to a total volume of 6 µl with of RNase-free water. To all samples, 1 µl of Genomic DNA Wipeout buffer was added. Samples were mixed and incubated for three minutes at 42 °C. Then 2 µl of Reverse Transcription buffer, 0.5 µl of each, Primer Mix and Reverse Transcriptase, were added per sample. Samples were incubated for 30 minutes at 42 °C. Reverse Transcription was inactivated for three minutes at 95 °C. Finally, 40 µl of RNase-free water were added and cDNA samples were stored at -20 °C to -80 °C.

Table 15: cDNA synthesis

Reagent	**Volume or Concentration**
RNA	500 ng
Genomic DNA Wipeout buffer	1 µl
3 min at 42 °C	
Reverse Transcription buffer	2 µl
Primer Mix	0.5 µl
Reverse Transcriptase	0.5 µl
30 min at 42 °C	
3 min at 95 °C	
RNase-free water	40 µl

3.2.9. qRT-PCR

Quantitative reverse transcription polymerase chain reaction (qRT-PCR) was performed to analyze gene expression. For qRT-PCR analysis, cDNA samples were mixed with Sybr Green mastermix and specific primers to a total volume of 10 µl.

Table 16: qRT-PCR mastermix

Reagent	Volume (µl)
qRT-PCR primer	1.5
Sybr Green fast mastermix	1.5
DEPC-treated H2O	5

Briefly, all reagents for the qRT-PCR mastermix (Table 16) were mixed in a RNase-free 1.5 ml tube for each primer used. Eight microliters of the mastermix were added to one well of a 384-well plate. To this, 2 µl of cDNA were added to each well. For a reference control, two naïve cDNA samples were used. Samples were analyzed with the Light Cycler 480 using either Sybr Green qRT-PCR Program (Table 17) for standard primers or PR8 qRT-PCR Program (Table 18) for IAV PR8 primers.

Table 17: Sybr Green qRT-PCR Program

<table>
<tr><th colspan="2">Step</th><th>Temperature (°C)</th><th>Time</th></tr>
<tr><td colspan="2">Reverse Transcription</td><td>50</td><td>10 min</td></tr>
<tr><td colspan="2">Inactivation RT</td><td rowspan="2">95</td><td rowspan="2">10 min</td></tr>
<tr><td colspan="2">Activation Polymerase</td></tr>
<tr><td rowspan="2">40 cycles</td><td>Denaturation</td><td>95</td><td>15 sec</td></tr>
<tr><td>Annealing/ Elongation/ Fluorescence measurement</td><td>60</td><td>60 sec</td></tr>
<tr><td colspan="2">Melting curve</td><td>50-95</td><td></td></tr>
</table>

Table 18: PR8 qRT-PCR Program

Step		Temperature (°C)	Time
Reverse Transcription		50	20 min
Inactivation RT		95	15 min
Activation Polymerase			
48 cycles	Denaturation	95	10 sec
	Annealing/ Elongation	61	60 sec
	Fluorescence measurement 1	72	30 sec
	Fluorescence measurement 2	81	15 sec
Melting curve		50-99	

3.2.10. Interferon α ELISA

Interferon alpha ELISA from serum of infected mice was performed according to manufacturer's protocol.

3.2.11. FACS staining

3.2.11.1. Influenza staining

Mice in prior infected with IAV or control mice were sacrificed, spleens were immediately removed and digested with Liberase/DNAse I. Five microliters of each Liberase (20 mg/ml) and DNAse (16,7 mg/ml) were added to 500 µl of DMEM (digesting solution). Organs were manually crushed using a syringe needle and 500 µl of digesting solution was added. Samples were incubated for 25 minutes at 37 °C. Afterwards, organs were brought to single cell suspension by vigorously mixing the solution with a pipette. Samples were centrifuged and washed one time with FACS buffer and centrifuged for five minutes at 1400 rpm and 4 °C. Antibodies for surface molecule detection were diluted in FACS buffer and 50 µl of antibody solution was added per sample. Samples were incubated for 30 minutes at 4 °C protected from light. Samples were washed with 1 ml of FACS buffer and centrifuged as described before.

Supernatant was removed and cells were fixed with 2 % formalin in PBS for ten minutes protected from light and centrifuged one time for five minutes at 1400 rpm, 4 °C. Cells were permeabilized with 2 % saponin in FACS buffer for 15 minutes protected from light and washed one time as described before. Then, samples were incubated with Influenza A H1N1 (A/Puerto Rico/8/34) Hemagglutinin antibody in 2 % saponin containing FACS buffer followed by washing and incubation with secondary fluorescently marked antibody. Samples were analyzed using the FACS LSR Fortessa II. Briefly, four million cells were recorded. Results were analyzed using FlowJo program according to described gating strategy (Figure 8, Figure 9).

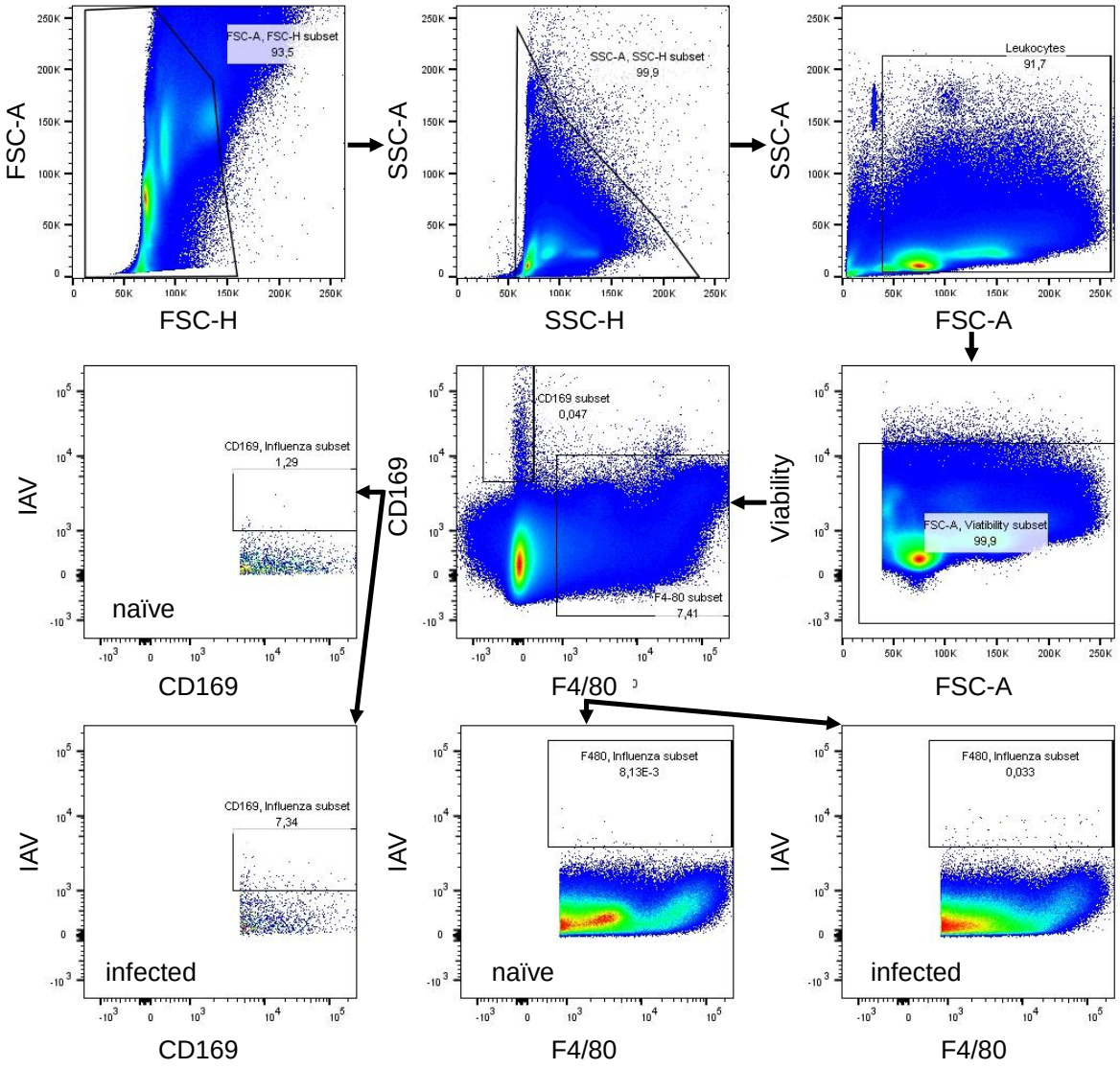

Figure 8: Gating strategy for IAV infected macrophages

Analysis of IAV infected macrophages via Flow cytometry. Briefly, viable cells were distinguished into $CD169^+$ and $F4/80^+$ cells. IAV HA expression was analyzed in cell subpopulations.

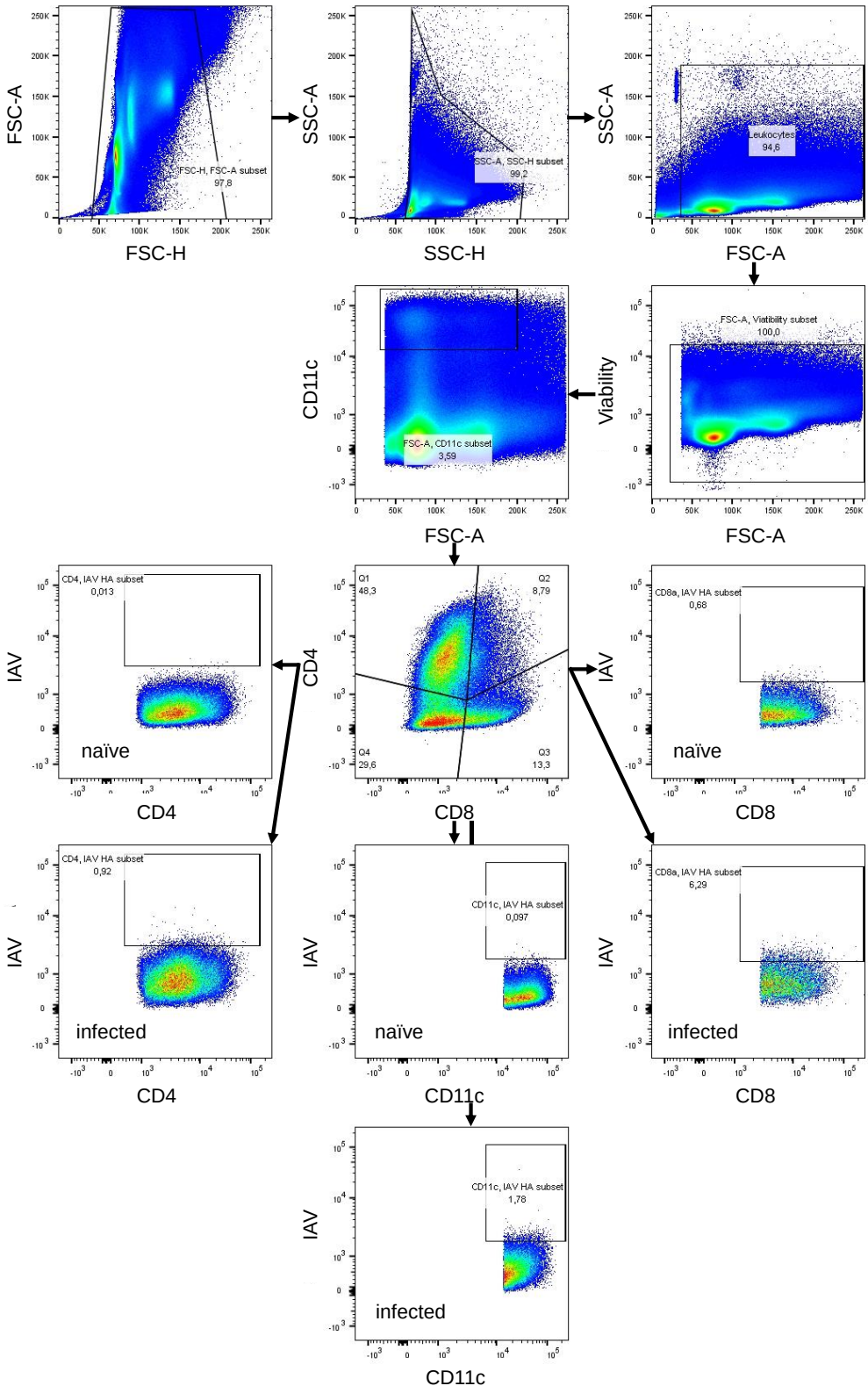

Figure 9: Gating for IAV infected DCs

Analysis of IAV infected dendritic cells via Flow cytometry. Briefly, $CD11c^+$, viable cells were distinguished by their expression of CD4 or CD8. $CD4^+$, $CD8^+$ or $CD4^-CD8^-CD11c^+$ cells were analyzed for their intracellular expression of Influenzas HA protein.

3.2.11.2. T cell restimulation and intracellular cytokine staining

Organ samples of pre-infected mice were collected and brought to single cell suspension by manual disruption trough a 70 µm nylon mesh filter. Samples were washed one time with DMEM 2 % FCS, 1 % PSG by centrifugation at 1400 rpm for five minutes at 4 °C. Then, samples were incubated with 0.1 µg/ml in of adequate peptide (Table 5) in DMEM 2 % FCS, 1 % PSG for one hour at 37 °C and 5 % CO_2. Control samples were incubated without peptide under the same conditions. Retrograde transport of proteins was blocked with Brefeldin A. Therefore, 10 µg/ml of Brefeldin A in DMEM 2 % FCS, 1 % PSG was added to each sample and incubation was performed overnight at 37 °C and 5 % CO_2. Surface antigens (CD4, CD8) were stained as described in Chapter 3.2.10.1 and samples were fixed and permeabilized according to the above-mentioned conditions. Intracellular IFNγ proteins were stained with anti-IFNγ antibody in 2 % saponin in FACS buffer. Samples were washed with 1 ml of 2 % saponin in FACS buffer and centrifuged at 1400 rpm at 4 °C for five minutes. Analysis of samples was performed using the FACS LSR Fortessa. Final analysis was performed with FlowJo software according to mentioned gating strategy (Figure 10).

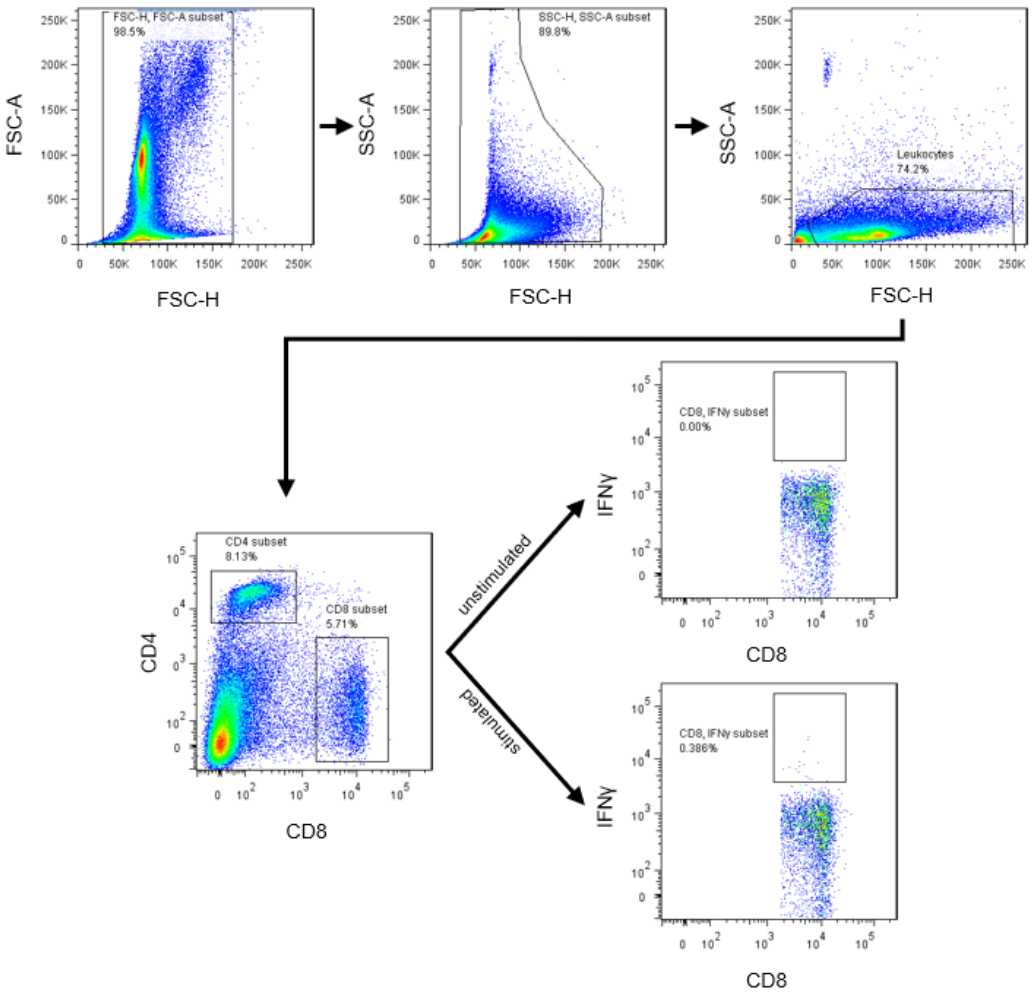

Figure 10: Gating strategy ICS

Analysis of IFNγ expression of $CD8^+$ cells via FACS LSR Fortessa II was performed in the presence (stimulated) or absence (unstimulated) of virus specific peptide. Leukocytes were distinguished into $CD4^+$ and $CD8^+$ cells. $CD8^+$ cells were investigated for IFNγ expression.

3.2.12. Sialic acid staining

Sialic acid residues on cell surfaces were stained according to published protocol (Arias et al. 2009; van Dinther et al. 2018). Briefly, mouse spleen samples were collected and digested with Liberase/DNAse according to the conditions mentioned in Chapter 3.2.10.1. Organs were brought to single cell suspension and washed one time with TSM buffer by centrifugation at 1400 rpm for five minutes at 4 °C. Biotinylated MAL II lectin was diluted in TSM buffer (1:100), added to each sample and incubated for 30 minutes at 37 °C. After one-time washing with TSM buffer and centrifugation as mentioned before, samples were incubated with antibodies for additional staining diluted in TSM buffer for 30 mins at 4 °C. Analysis of samples was performed with the FACS LSR Fortessa II. Gating strategy of immune cells was performed according to Figure 8 and Figure 9. Sialic acid expression was displayed as mean fluorescent intensity.

3.2.13. Neutralizing antibody assay (VSV and VSV-EBOV)

One day prior to performance of neutralizing antibody assay, cells were seeded out in 96-well flat-bottom plates. Briefly, $2x10^5$ Vero cells (VSV) or Vero E6 cells (VSV-EBOV) were seeded out in 200 µl of cell culture medium per well in a 96-well flat-bottom plate. VSV neutralization assay samples were diluted 1:40 in DMEM, 2 % FCS, 1 % PSG. VSV-EBOV neutralization assay samples were diluted 1:10 as described before. Complement components in serum samples were heat inactivated for 30 min at 56 °C. For analysis of VSV neutralizing IgG antibodies, samples were incubated with 0.1 M of β-mercaptoethanol for one hour at RT to remove IgM antibodies. Then, 12 serial 1:2-dilutions were performed in a 96-well plate in DMEM, 2 % FCS, 1 % PSG. After addition of $1x10^2$ PFU of VSV or VSV-EBOV per well in 100 µl of DMEM, 2 % FCS, 1 % PSG, plates were incubated for exactly 90 min at 37 °C, 5 % CO_2. Samples were transferred to the pre-seeded Vero or Vero E6 cells for VSV or VSV-EBOV neutralizing antibody assay, respectively and incubated for two hours at 37 °C, 5 % CO_2. After two hours of incubation, 100 µl of methylcellulose overlay solution were added to each well. VSV samples were incubated for 24 h at 37 °C, 5 % CO_2., VSV-EBOV samples were incubated for 48 h under the same conditions. To visualize plaques, supernatant was removed and 100 µl of crystal violet staining solution per well was added. After 30 min staining solution was removed, plates were washed, and plaques were counted. Wells were counted as neutralized, if at least a 50 % reduction in viral load was visible.

3.2.14. MACS isolation of dendritic cells

MACS isolation of pan DCs was performed according to Pan DC MicroBeads, mouse manufacturer's protocol. Briefly, spleen samples of naïve and IAV infected mice were digested according to previously mentioned protocol (3.2.10.1). After washing with MACS buffer for one time by centrifuging for five minutes at 1400 rpm at 4 °C, samples were mixed with pan DC magnetic beads. Samples were incubated for 15 minutes at 4 °C. Afterwards, samples were washed one time with MACS buffer and centrifuged for five minutes at 1400 rpm at 4 °C. MACS columns were assembled on magnetic stand and primed with 3 ml of MACS buffer and samples were loaded onto the columns. The flow through was discarded and columns were washed two times with 3 ml of MACS buffer. For elution of pan DCs from magnetic columns, 5 ml of MACS buffer was loaded to the columns and cells were detached from columns material by manual pressure.

3.2.15. Western Blot Analysis of IAV infected pan DCs

MACS isolated pan DCs were washed one time with PBS by centrifuging for five minutes at 1400 rpm, 4 °C. Supernatant was removed completely by aspiration. Equal amounts of cells were lysed in 95 °C preheated SDS-lysis buffer and boiled for two minutes. Samples were mixed with Laemmli buffer (2 X) containing 5 % of β-mercaptoethanol and boiled for two minutes at 95 °C. After centrifugation for one minute at 16000 rpm, samples were transferred to ice. Then, 30 µl of each sample and 5 µl of PAGE-ruler pre-stained were loaded to a 10 % Polyacrylamide-Gel (Table 19). Polyacrylamide gels were hand casted using Mini-PROTEAN Tetra Handcast Systems.

SDS-PAGE was performed for five minutes at 50 V, then voltage was increased to 90 V until running front was completely running out of end of the polyacrylamide gel. SDS running puffer (1 X) was used for SDS-PAGE.

Transfer of proteins to nitrocellulose membranes was performed via wet blotting. Nitrocellulose membranes were preincubated in ice cold transfer buffer (1 X) for five minutes. Blotting module was assembled in transfer buffer (1 X) using a Mini Gel Holder Cassette. Briefly, one foam pad was topped with two sheets of blotting paper, the polyacrylamide gel, one nitrocellulose membrane, two sheets of blotting paper and a foam pad. Wet blotting was performed for 90 min at 90 V in ice cold transfer buffer (1 X).

Table 19: Recipes for stacking and resolving gels

Reagent	Stacking gel (3.5 %) per 1 gel	Resolving gel per 1 gel
30 % acrylamide/bis	450 µl	3.3 ml
0.5 M tris-HCL, pH 6.8	380 µl	
1.5 M tris-HCL, pH 8.8		3.6 ml
10 % SDS in A. dest	30 µl	98 µl
A. dest	2.11 ml	2.8 ml
TEMED	5 µl	8.1 µl
10 % APS	30 µl	98 µl

Nitrocellulose membranes were blocked for 1 h at RT with 5 % Skim Milk powder in PBST. Primary antibodies were diluted 1:1000 in 5 % Skim Milk powder in PBST and incubated overnight at 4 °C. Primary antibody solution was removed, and nitrocellulose membranes were washed three times for ten minutes with PBST at RT. Secondary antibodies were diluted 1:1000 in 5 % Skim Milk powder in PBST and incubated with the membranes for 1 h at RT. Secondary antibody solution was discarded and nitrocellulose membranes were washed three times for ten minutes with PBST. Nitrocellulose membranes were incubated for five minutes with SuperSignal West Femto Chemiluminescence-Substrate at RT in the dark and analyzed with BioRad ChemiDoc MP System and ImageLab Software.

4. Results

4.1. Chapter 1: Systemic relevance of immune system specific replication

Epidemic and pandemic viral outbreaks are a threat to the human population. Especially the Ebola virus outbreak 2014 in Africa showed the urgent need for an effective vaccine against the Ebola Zaire virus. VSV-EBOV displays a powerful tool in the control of Ebola virus outbreak. Hereinafter, we investigate the underlying mechanism, which ensures effective immunization with VSV-EBOV.

4.1.1. Enforced VSV replication

Previously, we showed that replication of cytopathic VSV in the spleen is dependent of the expression USP18 and restricted to $CD169^+$ marginal zone macrophages (Honke et al. 2011). Mouse models with ubiquitous knockout of USP18 did not only show decreased virus replication and immune activation, but also impaired immune cell development and function. As USP18 modulates functionality of Th17 cells and CD11b cells it remained unknown whether exclusively lack of USP18 in $CD169^+$ cells contributed to anti-VSV immune response (Honke et al. 2016). To get insights, we used a mouse model with CD169 cell specific gene knockout of *Usp18* (*CD169*-$Cre^{+/ki}$ x *Usp18*$^{fl/fl}$) and compared key findings to control mice (*CD169*-$Cre^{+/+}$ x *Usp18*$^{fl/fl}$). We infected *CD169*-$Cre^{+/ki}$ x *Usp18*$^{fl/fl}$ and control mice systemically with VSV and analyzed virus replication 16 hours later (Figure 11). VSV replication in inguinal lymph nodes (LNs) was below detection limit in absence of USP18 in $CD169^+$ MΦs compared to control conditions (Figure 11a). In line, analysis of VSV-NP expression via qRT-PCR showed a significant reduction in spleen and inguinal LNs of *CD169*-$Cre^{+/ki}$ x *Usp18*$^{fl/fl}$ mice compared to control mice (Figure 11b). Visualization of VSV antigen in immunohistochemical analysis of spleen sections revealed a strong colocalization of VSV-G (red) and $CD169^+$ MΦs (blue) in control mice in contrast to *CD169*-$Cre^{+/ki}$ x *Usp18*$^{fl/fl}$ mice, which did not show co-staining of $CD169^+$ MΦs with VSV-G (Figure 11c).

We concluded that USP18 expression in $CD169^+$ macrophages is essential to promote cell restricted VSV replication.

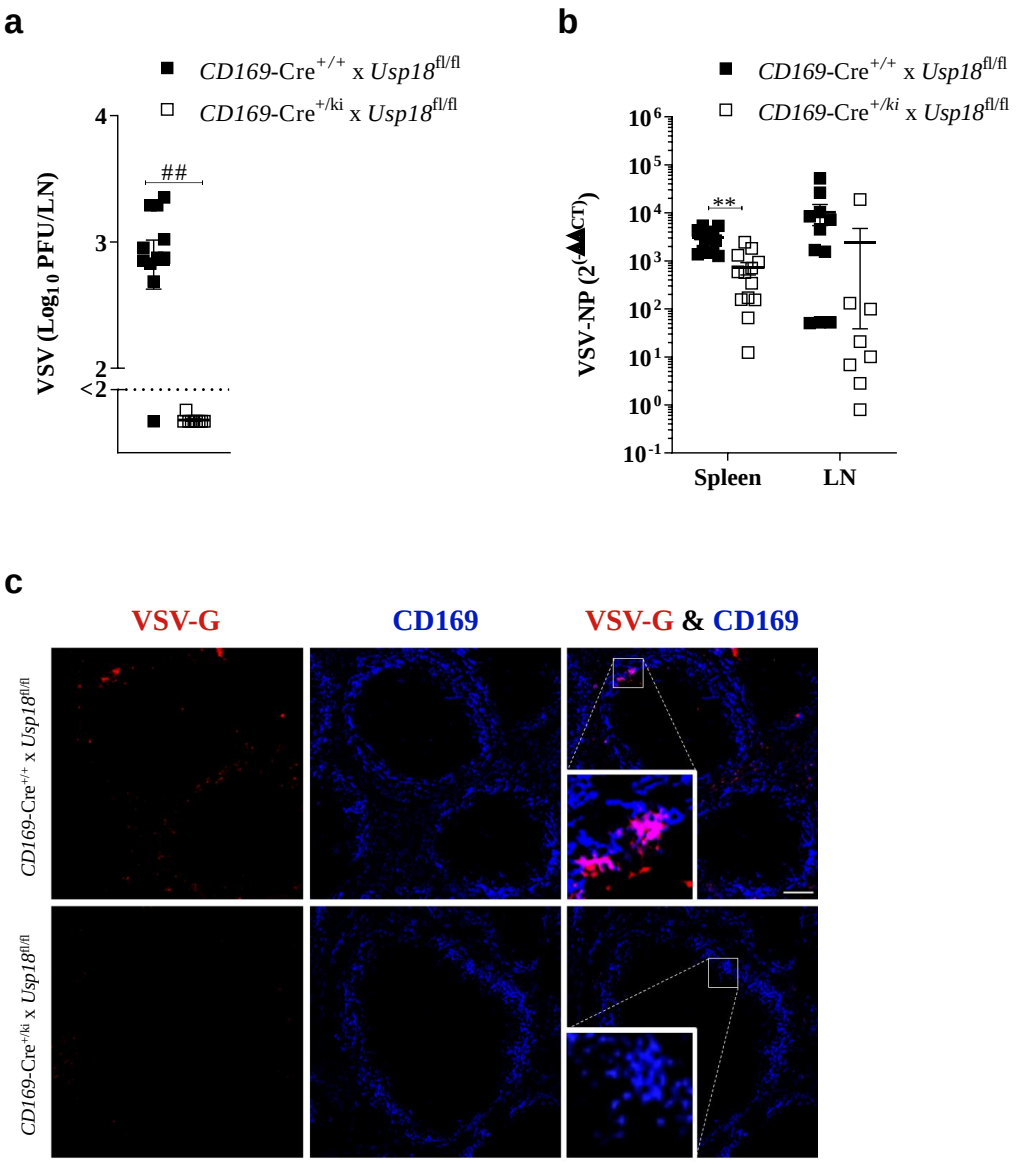

Figure 11: Enforced VSV replication in CD169$^+$ macrophages

a Viral titers in lymph nodes of *CD169*-Cre$^{+/+}$ x *Usp18*$^{fl/fl}$ (black squares) and *CD169*-Cre$^{+/ki}$ x *Usp18*$^{fl/fl}$ (white squares) mice 16 hours after i.v. infection with 2x10^6 PFU of VSV. Dotted line represents detection limit. **b** Quantitative detection of VSV-NP in spleen and inguinal lymph nodes after infection as in **a.** **c** Immunohistochemistry staining of spleen sections of mice infected as described in **a** stained for VSV-G (red) and CD169 (blue). Scale bar 100 µm. One representative picture of each group from two experiments (n=3-4) shown. **P < 0.01 and ## P < 0.0001 (Student's t-test, **a**, **b**). Data are representative of two **(a**, **b)** experiments (n=3-4 per group) (mean ± SEM (**a**, **b**)).

4.1.2. Innate immune response after systemic VSV injection

Next, we aimed to determine whether USP18 driven enforced replication of VSV in CD169^{+} macrophages is essential to enhance innate immune responses upon systemic VSV infection (Figure 12).

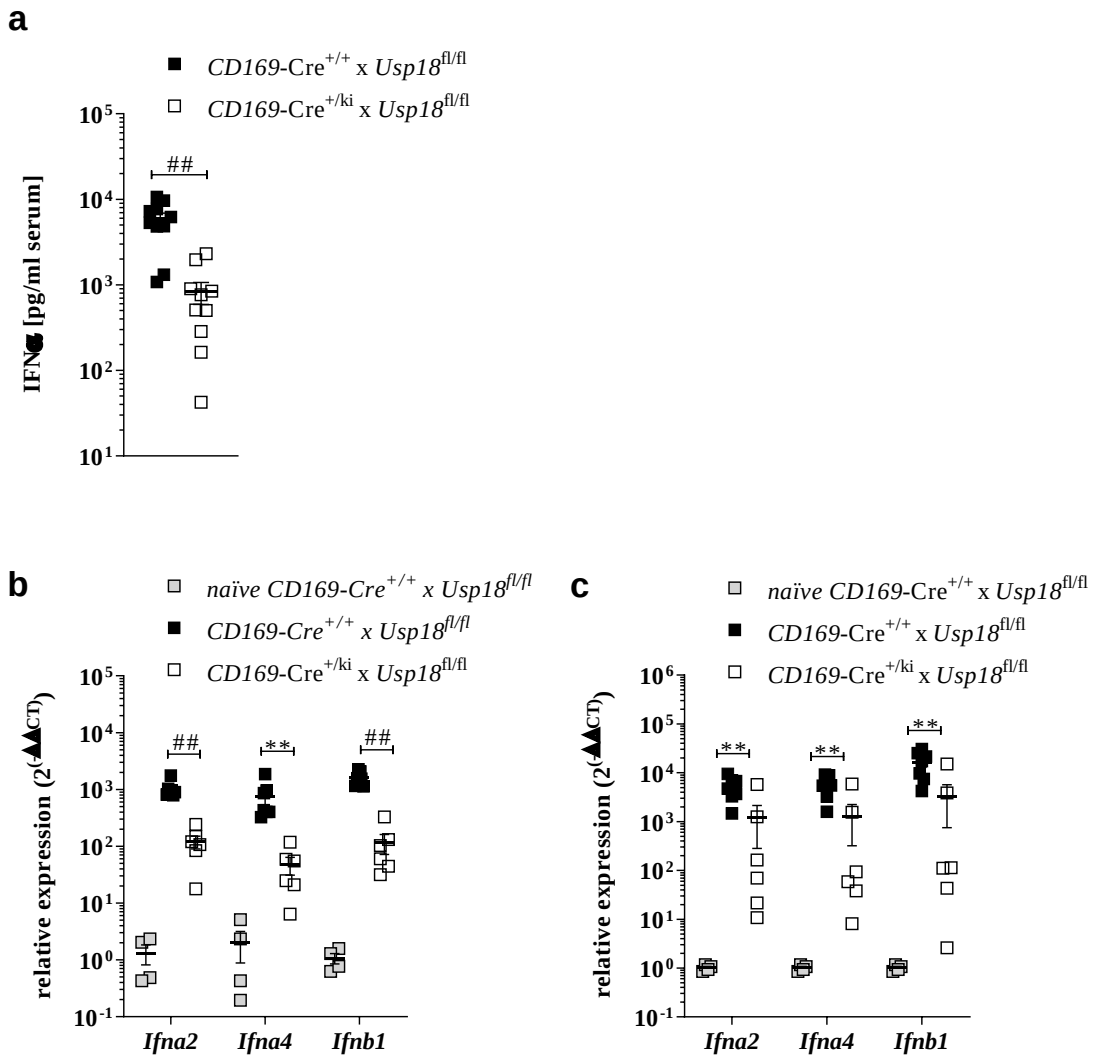

Figure 12: Systemic enforced VSV replication drives innate immunity

a IFNα serum levels 16 hours after i.v. infection with 2x10^{6} PFU of VSV of *CD169*-Cre$^{+/+}$ x *Usp18*$^{fl/fl}$ (black squares) and *CD169*-Cre$^{+/ki}$ x *Usp18*$^{fl/fl}$ (white squares) mice. **b-c** Quantitative detection of *Ifna2, Ifna4* and *Ifnb1* in spleen samples and inguinal lymph nodes after infection as described in **a**. Relative expression normalized to naïve WT samples (gray squares). **P < 0.01 and ## P < 0.0001 (Student's t-test, **a-c**). Data are representative of two **(a-c)** experiments (n=3-4 per group) (mean ± SEM (**a-c**)).

In strong contrast to control mice, *CD169*-Cre$^{+/ki}$ x *Usp18*$^{fl/fl}$ mice showed highly reduced IFNα serum levels following systemic infection with 2x10^{6} PFU of VSV (Figure 12a). Consistently, relative expression of interferon genes *Ifna2, Ifna4* and *Ifnb1* was highly decreased in spleen

(Figure 12b) and inguinal LNs (Figure 12c) 16 h post infection in *CD169*-Cre$^{+/ki}$ x *Usp18*$^{fl/fl}$ mice.

We concluded that USP18 dependent enforced replication of VSV in CD169^{+} MΦs is necessary to induce a strong, early immune response.

4.1.3. Enforced VSV replication activates adaptive immunity

As we could show that enforced replication in CD169^{+} MΦs strongly enhanced innate immune activation after systemic VSV infection, we wanted to investigate the resulting consequences for the induction of the adaptive VSV immune response (Figure 13). After intravenous injection of 2x10^{6} PFU of VSV, *CD169*-Cre$^{+/ki}$ x *Usp18*$^{fl/fl}$ mice showed a highly reduced neutralizing antibody response against VSV compared to control mice (Figure 13a+b). Serum titers of both, total neutralizing Ig and neutralizing IgG, were significantly reduced in *CD169*-Cre$^{+/ki}$ x *Usp18*$^{fl/fl}$ mice compared to control mice. To further address if the enhanced immune response in control mice is essential to protect from lethal VSV infection, we infected mice intravenously with a challenging dose of VSV. In strong contrast to control mice, *CD169*-Cre$^{+/ki}$ x *Usp18*$^{fl/fl}$ mice were highly susceptible to a fatal outcome of the VSV infection (Figure 13c). Interestingly, analysis of VSV specific CD8^{+} T cells in the spleen of mice infected intravenously with 2x10^{5} PFU of VSV did not show an alteration in IFNγ production after stimulation with the P52 peptide 12 days after infection between *CD169*-Cre$^{+/ki}$ x *Usp18*$^{fl/fl}$ and control mice (Figure 13d).

Taken together, these data indicate that USP18 dependent EVR in CD169^{+} MΦs is crucial for fast induction of a protective immune response after VSV infection by the activation of a B cell response rather than an anti-viral T cell response.

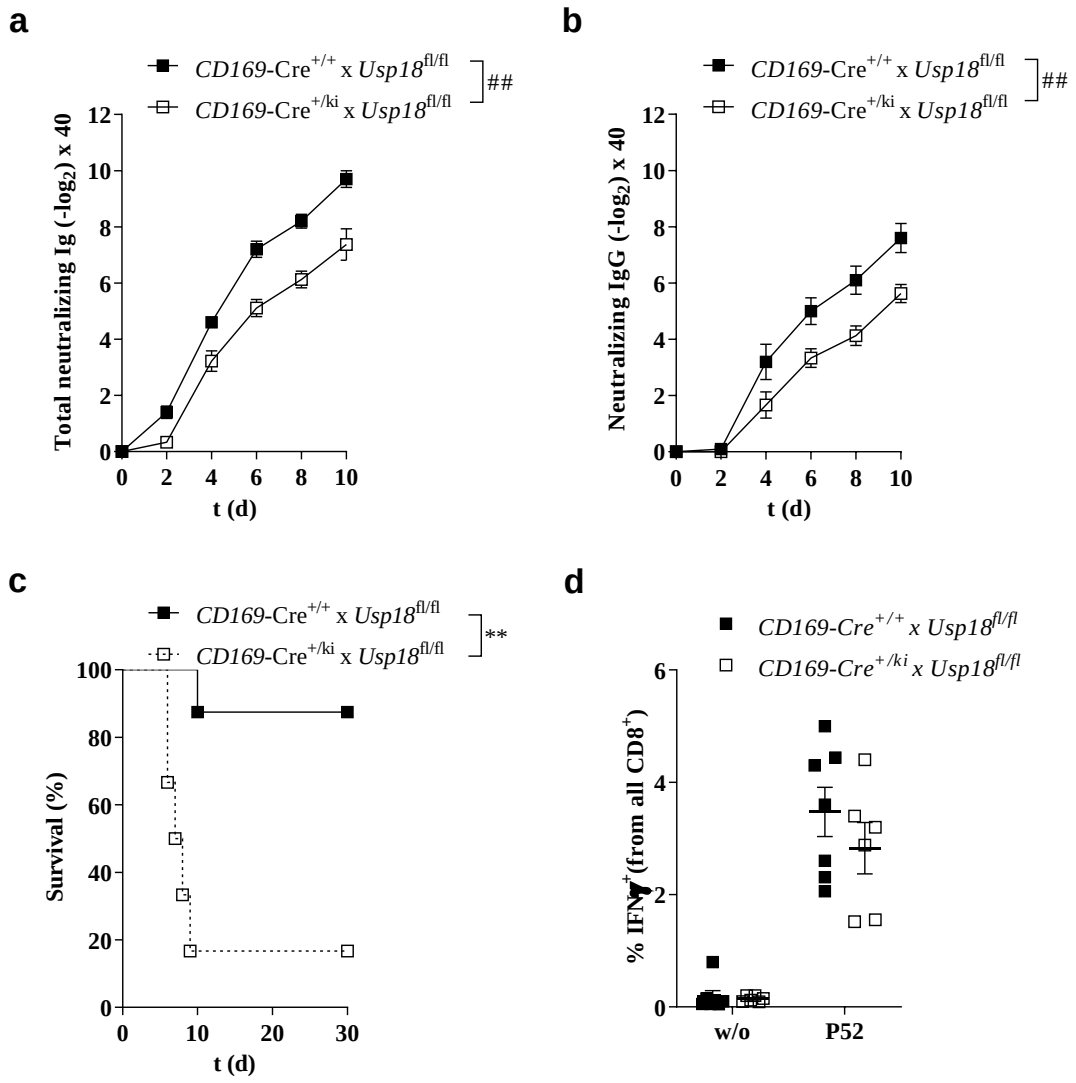

Figure 13: Influence of enforced VSV replication on the adaptive immune response

a,**b** Total neutralizing Ig (**a**) or neutralizing IgG (**b**) antibody titers in serum of *CD169*-Cre$^{+/+}$ x *Usp18*$^{fl/fl}$ (black squares) and *CD169*-Cre$^{+/ki}$ x *Usp18*$^{fl/fl}$ (white squares) mice i.v. infected with 2x10^6 PFU of VSV on indicated days after infection. **c** Survival of *CD169*-Cre$^{+/+}$ x *Usp18*$^{fl/fl}$ (black squares) and *CD169*-Cre$^{+/ki}$ x *Usp18*$^{fl/fl}$ (white squares) mice i.v. infected with 2x10^6 PFU of VSV. **d** IFNγ production of spleen CD8$^+$ cells from mice i.v. injected with 2x10^5 PFU of VSV 12 days post infection not stimulated (w/o) or stimulated with VSV peptide (P52). **P < 0.01 and ## P < 0.0001 (Two-way-Anova, **a**, **b**), (Mantel-Cox test, **c**), (Student's t-test, **d**). Data are representative of two **(a-d)** experiments (n=3-4 per group) (mean ± SEM (**a**, **b**, **d**)).

4.1.4. Enforced VSV replication after local injection

USP18 dependent enforced VSV replication in CD169^{+} MΦs is essential for the induction of a protective immune response after systemic inoculation. In contrast, administration of vaccines is often performed via intramuscular injection, directly targeting the immune response in injection site draining lymph nodes (dLNs). To investigate whether the route of injection influences EVR dependent immune activation, we infected control and *CD169*-Cre$^{+/ki}$ x *Usp18*$^{fl/fl}$ mice subcutaneously with 2x10^{4} PFU of VSV and analyzed viral replication in injection site dLNs 16 hours after injection (Figure 14). In line with our results from systemic infection, presence of USP18 in CD169 MΦs was essential to promote early VSV replication (Figure 14a). VSV titers in injection site dLNs were highly reduced concomitantly with decreased expression of VSV-NP in *CD169*-Cre$^{+/ki}$ x *Usp18*$^{fl/fl}$ mice compared to control mice (Figure 14b). Next, we investigated the localization of VSV particles in draining lymph nodes by histological analysis. dLNs of control mice showed strong colocalization of VSV-G (red) and CD169^{+} MΦs (blue), whereas expression of VSV-G was virtually absent in dLN of *CD169*-Cre$^{+/ki}$ x *Usp18*$^{fl/fl}$ mice (Figure 14c).

These data indicate that early enhanced VSV replication in CD169^{+} MΦs in injection site dLN is relying on USP18 expression, analogous to our results observed under systemic injection conditions.

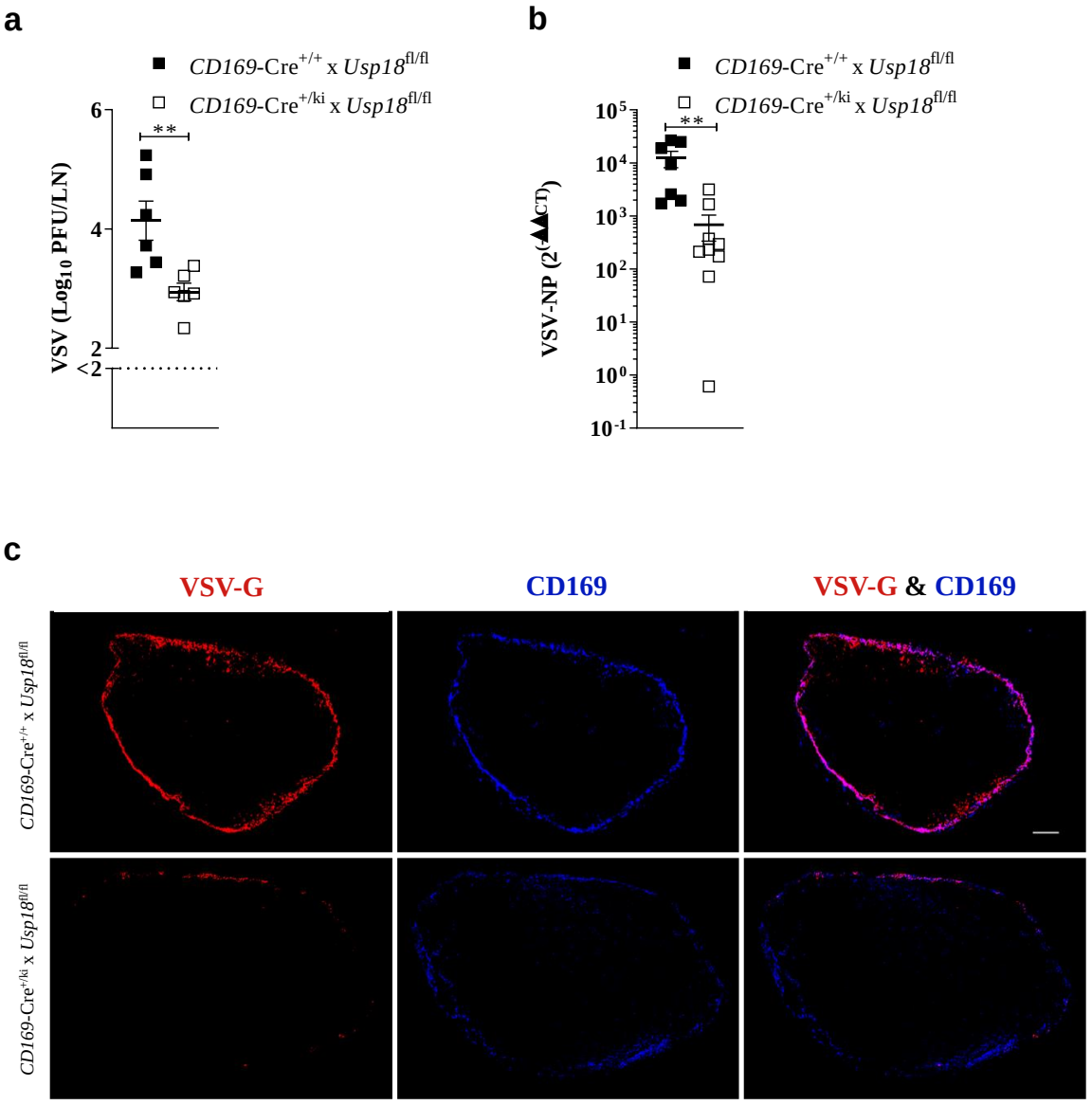

Figure 14: Enforced virus replication in dLN is essential to activate immunity

a Viral titers in dLN of *CD169*-Cre$^{+/+}$ x *Usp18*$^{fl/fl}$ (back squares) and *CD169*-Cre$^{+/ki}$ x *Usp18*$^{fl/fl}$ (white squares) mice 16 hours after s.c. infection with 2x10^4 PFU of VSV. Dotted line represents detection limit. **b** Quantitative detection of VSV-NP in injection site dLNs after infection as in **a**. **c** Immunohistochemistry staining of injection site dLN sections of mice infected as described in **a** stained for VSV-G (red) and CD169 (blue). Scale bar 100 µm. One representative picture of each group from two experiments (n=3-4) shown. **P < 0.01 and ## P < 0.0001 (Student's t-test, **a**, **b**). Data are representative of two **(a, b)** experiments (n=3-4 per group) (mean ± SEM (**a**, **b**)).

4.1.5. Local injection drives innate immunity against VSV

Furthermore, we investigated whether USP18 dependent EVR in CD169^{+} MΦs activates innate immunity in injection site dLNs after local VSV infection. We measured the relative expression of *Ifna4* and *Ifnb1* in injection site dLNs 16 hours following subcutaneous VSV infection with 2x10^{4} PFU per mouse as a marker for innate immune activation. Injection site dLNs of control mice showed a significantly increased USP18 dependent expression of type I IFNs compared to *CD169*-Cre$^{+/ki}$ x *Usp18*$^{fl/fl}$ mice (Figure 15).

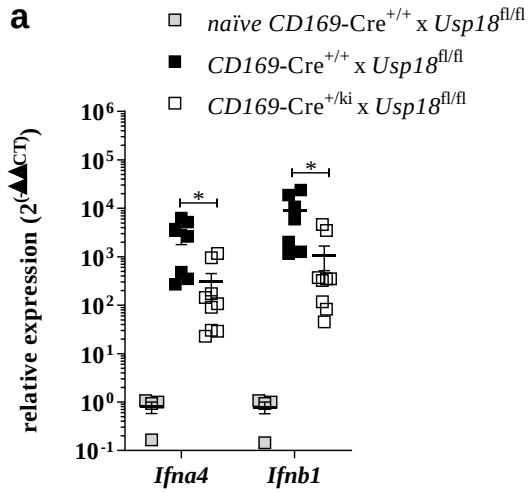

Figure 15: Innate immune response after local enforced replication

a Quantitative detection of *Ifna4* and *Ifnb1* in injection site dLNs of *CD169*-Cre$^{+/+}$ x *Usp18*$^{fl/fl}$ (back squares) and *CD169*-Cre$^{+/ki}$ x *Usp18*$^{fl/fl}$ (white squares) mice 16 h after intramuscular injection with 2x10^{4} PFU of VSV. Relative expression normalized to naïve WT samples (gray squares). * P < 0.05 (Student's t-test, **a**). Data are representative of two **(a)** experiments (n=3-4 per group) (mean ± SEM (**a**)).

We conclude, that enforced VSV replication in injection site dLNs is essential to enhance innate immune activation after local VSV infection.

4.1.6. Local VSV infection activates adaptive immunity

We demonstrated that local enforced VSV replication in CD169$^+$ MΦs activates innate immunity in an USP18 dependent fashion. Next, we analyzed the role of USP18 mediated EVR for the activation of a neutralizing antibody response after intramuscular immunization with 2x10^4 PFU of VSV. As expected, USP18 expression in CD169$^+$ MΦs enhanced neutralizing antibody response in control mice compared to *CD169*-Cre$^{+/ki}$ x *Usp18*$^{fl/fl}$ mice (Figure 16a+b).

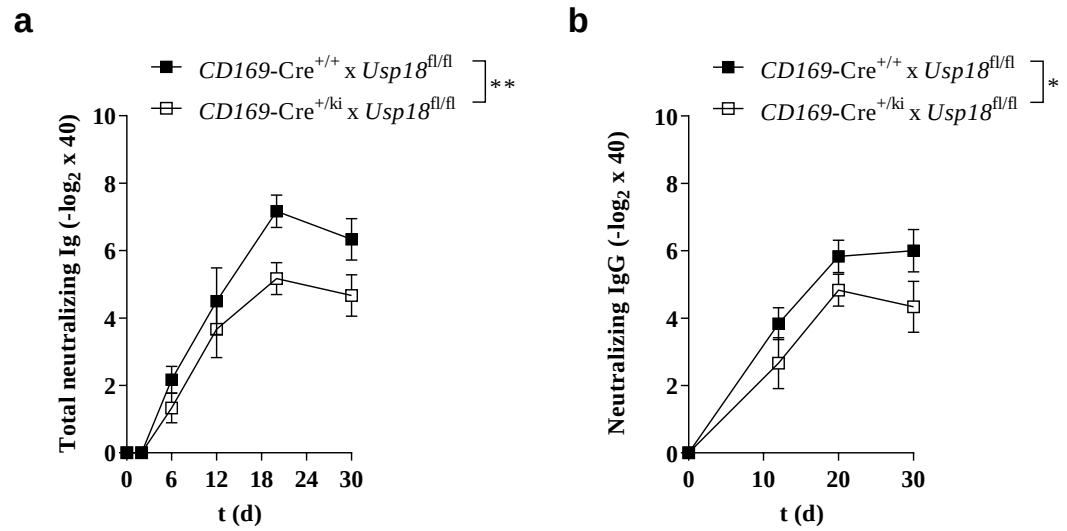

Figure 16: EVR influences adaptive immune response after intramuscular immunization with VSV

a+**b** Total neutralizing Ig (**a**) or neutralizing IgG (**b**) antibodies in serum of *CD169*-Cre$^{+/+}$ x *Usp18*$^{fl/fl}$ (black squares) and *CD169*-Cre$^{+/ki}$ x *Usp18*$^{fl/fl}$ (white squares) mice i.v. infected with 2x10^4 PFU of VSV on indicated days after infection. *P < 0.05 and ** P < 0.01 (Two-way-Anova, **a**, **b**). Data are representative of two **(a**, **b)** experiments (n=3-4 per group) (mean ± SEM (**a**, **b**)).

Taken together, these data show that after local administration of VSV, USP18 expression mediated EVR in CD169$^+$ MΦs is essential to boost adaptive immunity against a VSV infection.

4.1.7. USP18 expression in CD169^{+} MΦs enforces VSV-EBOV replication after systemic injection

VSV-EBOV is a powerful vaccine against the Ebola virus, which was engineered on the backbone of a WT VSV and the glycoprotein of the Ebola Zaire virus. Due to the genetic modification, VSV-EBOV is highly attenuated regarding its replication capacity. To get insights, if USP18 mediated EVR in CD169^{+} MΦs is essential in enhancing immunity towards an attenuated VSV vector vaccine, we infected mice systemically with VSV-EBOV (Figure 17). Seven hours after infection, control mice showed enhanced viral titers in inguinal LNs, compared to *CD169*-Cre$^{+/ki}$ x *Usp18*$^{fl/fl}$ mice (Figure 17a). As viral titers in spleen were below detection limit, we performed qRT-PCR analysis to quantify VSV-EBOV NP expression in spleen and lymph nodes. VSV-EBOV NP expression was strongly reduced in *CD169*-Cre$^{+/ki}$ x *Usp18*$^{fl/fl}$ mice compared to control mice (Figure 17b). Consistent with decreased VSV-EBOV load in the spleen of *CD169*-Cre$^{+/ki}$ x *Usp18*$^{fl/fl}$ mice, immunohistochemical analysis of spleen sections displayed strong reduction of Ebola virus GP (red) staining in *CD169*-Cre$^{+/ki}$ x *Usp18*$^{fl/fl}$ mice. Staining for Ebola virus GP was strongly restricted to CD169^{+} MΦs (blue) (Figure 17c).

These data display that USP18 in CD169^{+} MΦs is essential to promote the cell restricted replication of the highly attenuated vaccine VSV-EBOV.

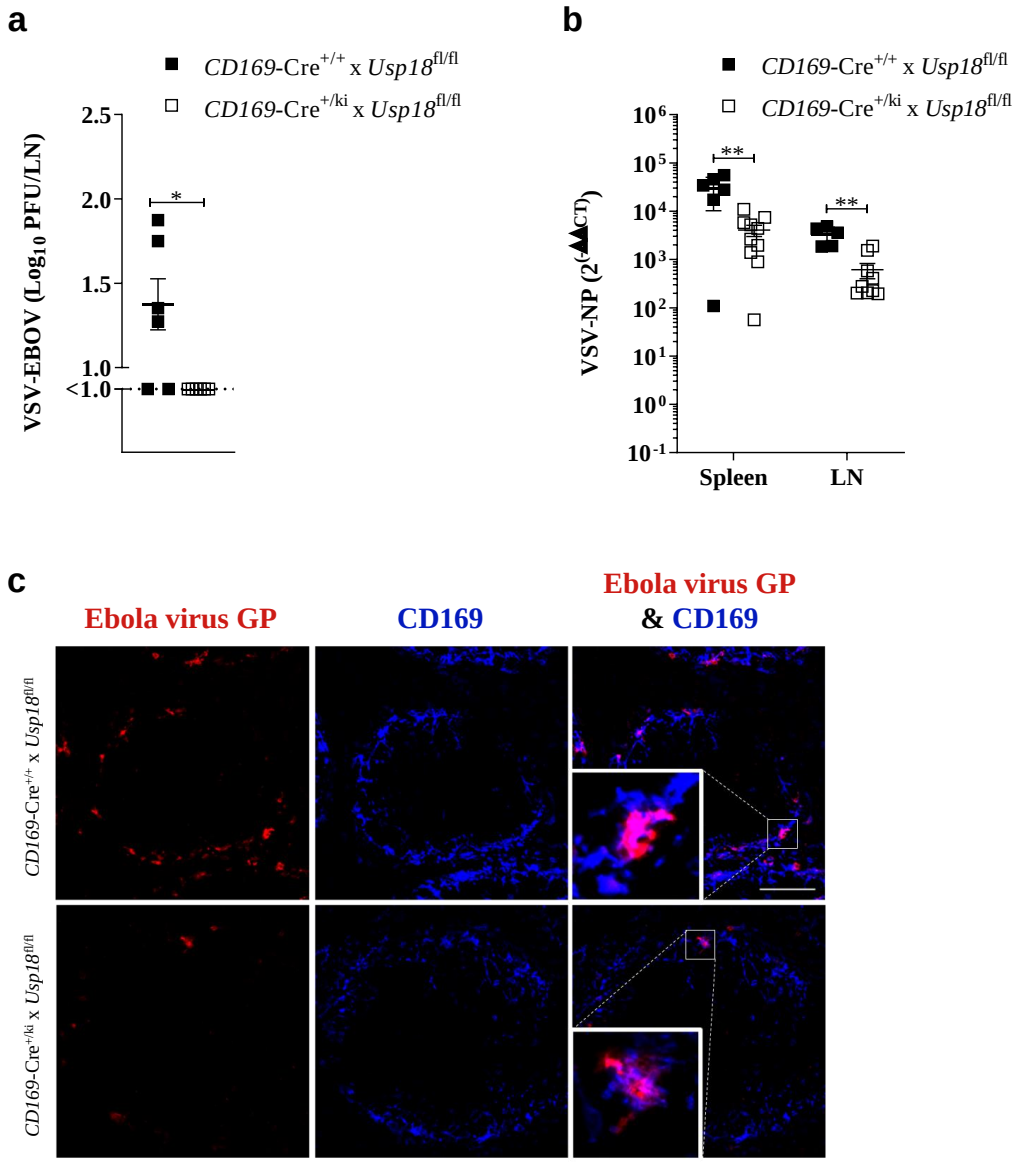

Figure 17: VSV-EBOV replication in spleen after systemic injection

a Viral titers in LNs 7 hours after i.v. infection with 3x10^6 PFU of VSV-EBOV of *CD169*-Cre$^{+/+}$ x *Usp18*$^{fl/fl}$ (back squares) and *CD169*-Cre$^{+/ki}$ x *Usp18*$^{fl/fl}$ (white squares) mice. Dotted line represents assay detection limit. **b** Quantitative detection of VSV-EBOV-NP (VSV-NP) in spleen and lymph nodes after infection as in **a**. **c** Immunohistochemistry staining of spleen sections of mice infected as described in **a** stained for Ebola virus GP (red) and CD169 (blue). Scale bar 100 µm. One representative picture shown from each group of two independent experiments (n=3-4). **P < 0.01 (Student's t-test, **a**, **b**). Data are representative of two (**a**, **b**) experiments (mean ± SEM (**a**, **b**)).

4.1.8. Enforced VSV-EBOV replication boosts innate immunity

To rule out, if USP18 expression mediated enhanced replication of VSV-EBOV in CD169^{+} MΦs is essential to promote innate immunity, we analyzed type I IFN expression as a marker for innate immune activation after 16 hours of systemic infection with 3x10^{6} PFU of VSV-EBOV (Figure 18). Control mice showed a stronger induction in serum IFNα levels (Figure 18a), as well as increased expression of *Ifna4* and *Ifnb1* in spleen (Figure 18b) and inguinal lymph nodes (Figure 18c) compared to *CD169*-Cre$^{+/ki}$ x *Usp18*$^{fl/fl}$ mice.

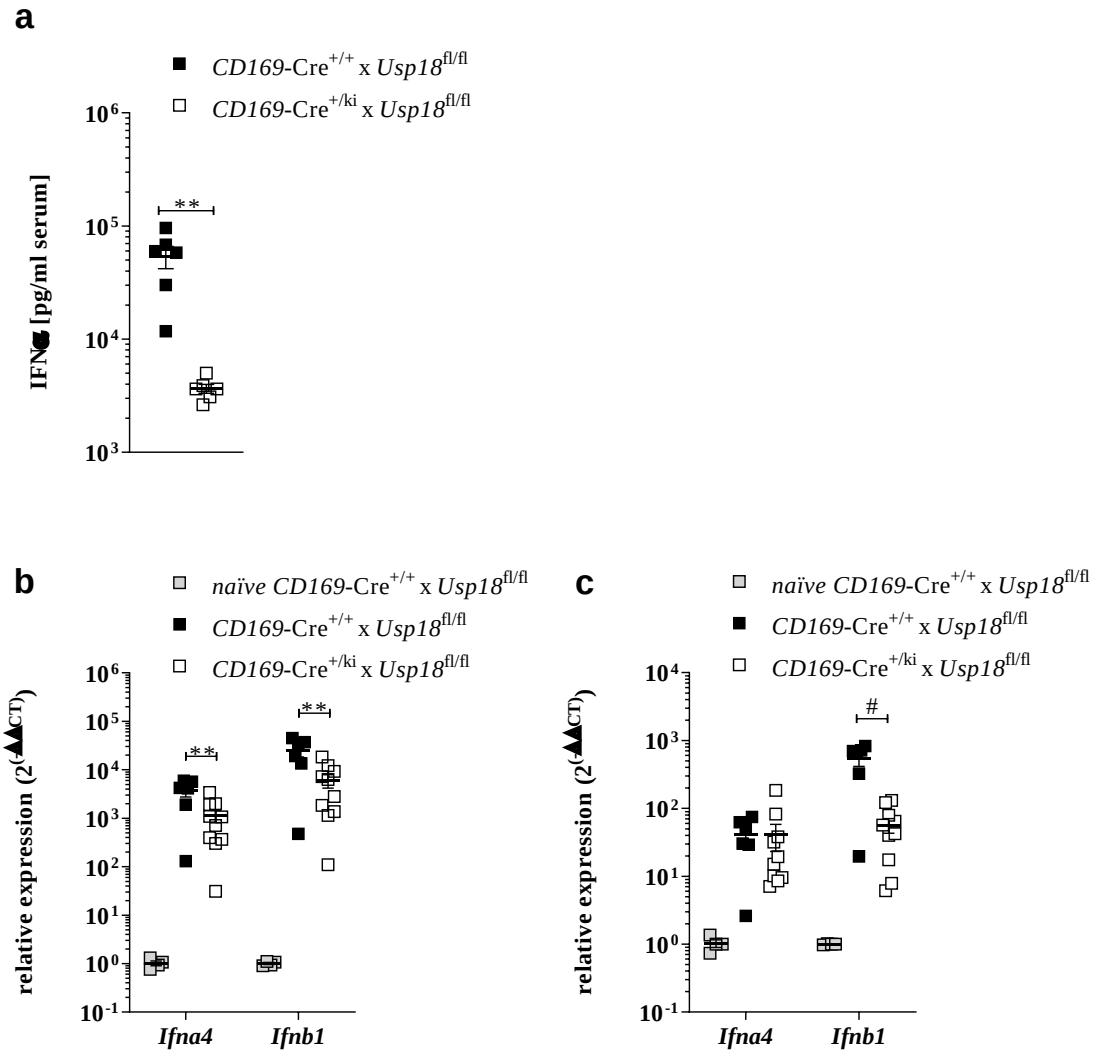

Figure 18: Enforced VSV-EBOV replication is an essential driver of innate immunity

a IFNα serum levels of *CD169*-Cre$^{+/+}$ x *Usp18*$^{fl/fl}$ (back squares) and *CD169*-Cre$^{+/ki}$ x *Usp18*$^{fl/fl}$ (white squares) mice i.v. infected with 3x10^{6} PFU of VSV-EBOV 16 h p.i. **c**. **b**+**c** Relative expression of *Ifna4* or *Ifnb1* spleen (**a**) or lymph nodes (**b**) obtained from mice infected mice as described in **a**. Relative expression normalized naïve control spleen or lymph node samples (gray squares). **P < 0.01, # P < 0.001 and ## P < 0.0001 (Student's t-test, **a**-**c**). Data are representative of two (**a**-**c**) experiments (mean ± SEM (**a**-**c**)).

These results underline that EVR of attenuated VSV-EBOV is essential to induce a strong innate immune response after systemic infection.

4.1.9. Enforced VSV-EBOV replication drives neutralizing antibody response

We demonstrated that the innate immune response is highly enhanced after VSV-EBOV administration in an USP18 expression dependent fashion, therefore, we further investigated the role of EVR in the induction of a protective adaptive immune response against VSV-EBOV. We analyzed the induction of VSV-EBOV neutralizing antibodies on displayed timepoints after systemic injection with $2x10^4$ PFU of VSV-EBOV (Figure 19). The presence of total neutralizing Ig antibodies was significantly enhanced in control mice compared to *CD169*-Cre$^{+/ki}$ x *Usp18*$^{fl/fl}$ mice (Figure 19a).

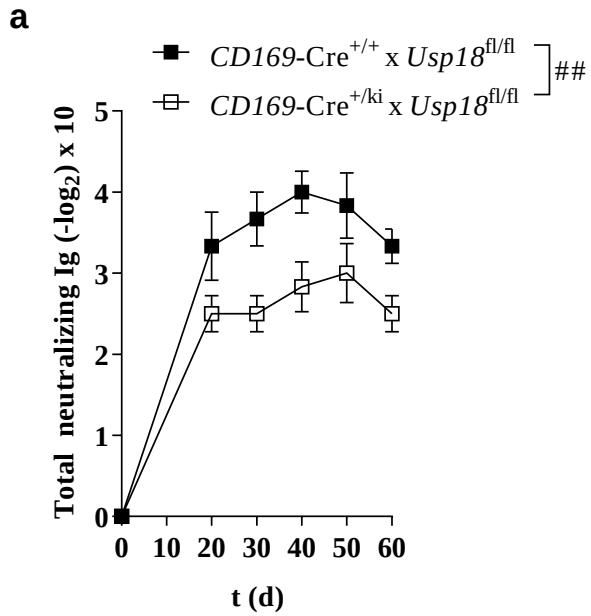

Figure 19: Systemic VSV-EBOV injection induces neutralizing antibody response

a VSV-EBOV neutralizing total Ig in serum of *CD169*-Cre$^{+/+}$ x *Usp18*$^{fl/fl}$ (black squares) and *CD169*-Cre$^{+/ki}$ x *Usp18*$^{fl/fl}$ (white squares) mice intravenously infected with $3x10^6$ PFU of VSV-EBOV on indicated timepoints. *##P* < 0.0001 (Two-way-Anova, **a**). Data are representative of two (**a**) experiments (mean ± SEM (**a**)).

We concluded, that USP18 mediated VSV-EBOV replication in CD169 MΦs is essential to boost protective adaptive immunity after systemic VSV-EBOV injection.

4.1.10. USP18 enforces VSV-EBOV replication in CD169 MΦs after local administration

Our findings highlighted the importance of USP18 mediated immune activation after systemic challenge with VSV and VSV-EBOV. We further investigated the impact of USP18 driven EVR after local immunization with the live attenuated VSV-EBOV vaccine. To analyze if the strong attenuation of VSV-EBOV impacts USP18 dependent enforced virus replication, we investigated viral replication and localization after subcutaneous vaccination with $3x10^5$ PFU of VSV-EBOV per mouse (Figure 20). In line with previous our findings, *CD169*-Cre$^{+/ki}$ x *Usp18*$^{fl/fl}$ mice showed reduced VSV-EBOV titers (Figure 20a), as well as reduced VSV-EBOV NP expression (Figure 20b) in injection site draining LNs compared to control mice. Correspondingly, immunohistochemical analysis of injection site draining lymph node sections revealed reduced Ebola virus GP (red) staining in *CD169*-Cre$^{+/ki}$ x *Usp18*$^{fl/fl}$ mice. In contrast, injection site draining lymph node sections of control mice displayed strong staining for Ebola virus GP (red) colocalizing with CD169 MΦs (blue) (Figure 20c).

These results highlight, that USP18 expression in CD169 MΦs is essential to generate detectable amounts of VSV-EBOV antigen after subcutaneous vaccination.

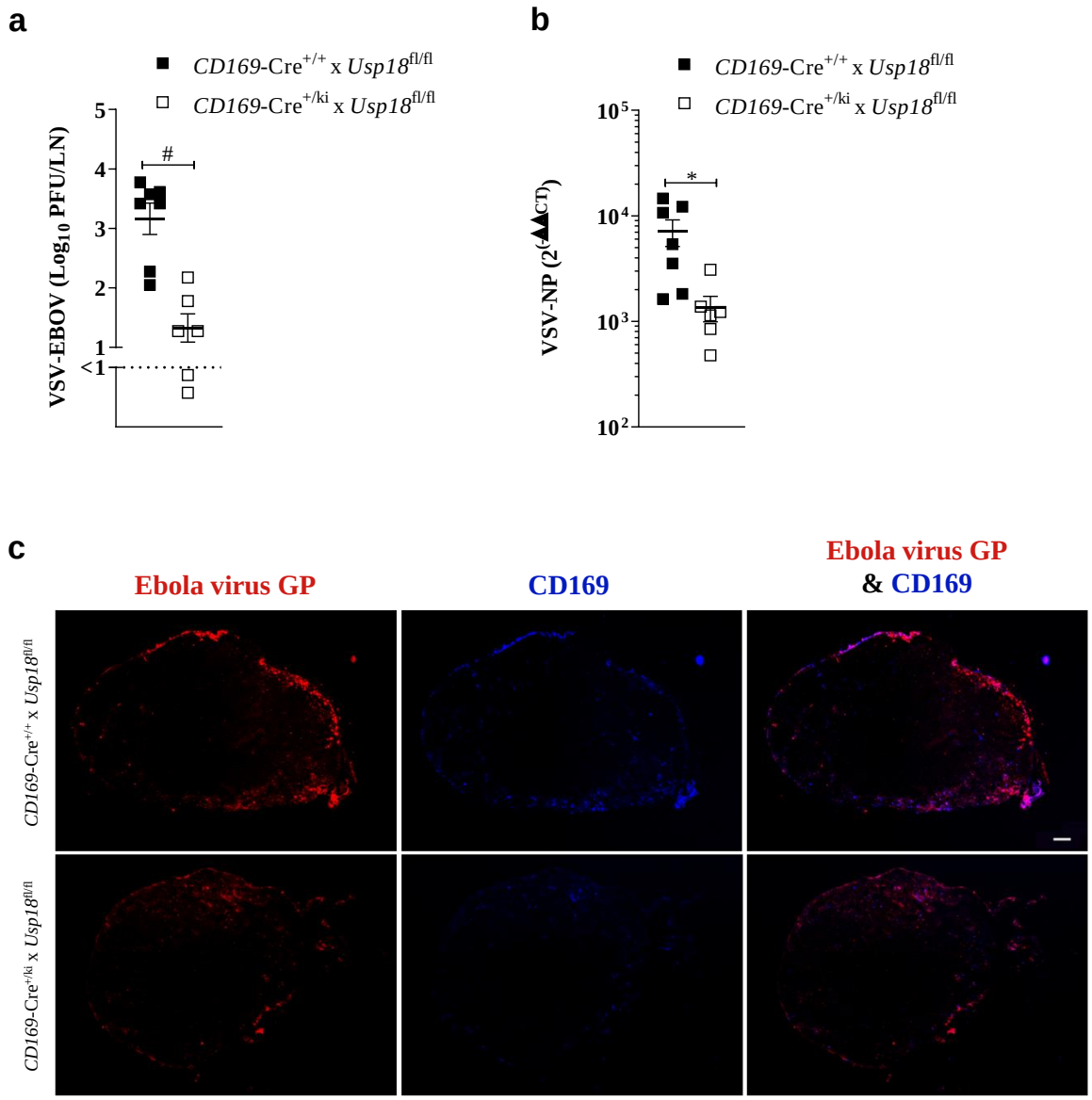

Figure 20: Subcutaneous injected VSV-EBOV replicates in dLN

a Virus titers in injection site draining lymph nodes of *CD169*-Cre$^{+/+}$ x *Usp18*$^{fl/fl}$ (black squares) and *CD169*-Cre$^{+/ki}$ x *Usp18*$^{fl/fl}$ (white squares) mice 16 hours after s.c. infection with 3x10^5 PFU of VSV-EBOV. Dotted line represents detection limit. **b** Quantitative detection of VSV-EBOV-NP (VSV-NP) with qRT-PCR in lymph nodes after infection described as in **a** normalized to naïve LNs. **c** Immunohistochemistry staining of lymph node sections of mice infected as described in **a** stained for Ebola Virus GP (red) and CD169 (blue). Scale bar 100 µm. One representative picture shown from each group of two independent experiments (n=3-4). *P < 0.05, # P < 0.001 (Student's t-test, **a**, **b**). Data are representative of two (**a**, **b**) experiments (mean ± SEM (**a**, **b)**).

4.1.11. EVR drives innate immunity after subcutaneous VSV-EBOV immunization

USP18 expression in CD169 MΦs is essential to produce detectable amounts of VSV-EBOV antigen. To examine, if enhanced antigen expression is also essential to promote innate immunity after subcutaneous immunization with $3x10^5$ PFU of VSV-EBOV, we analyzed the gene expression of type I interferons in control and *CD169*-Cre$^{+/ki}$ x *Usp18*$^{fl/fl}$ mice (Figure 21). In line with our previous data, *CD169*-Cre$^{+/ki}$ x *Usp18*$^{fl/fl}$ mice showed a highly reduced induction of *Ifna4* and *Ifnb1* expression in injection site dLNs compared to control mice (Figure 21a).

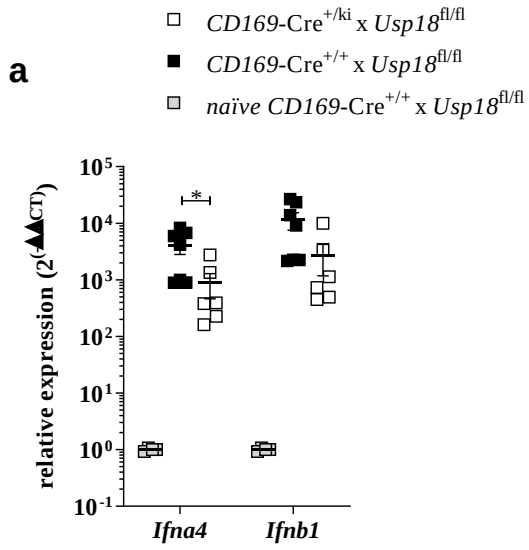

Figure 21: Enforced replication is essential for innate immune induction after VSV-EBOV

a Relative expression of *Ifna4* and *Ifnb1* in injection site draining lymph nodes of *CD169*-Cre$^{+/+}$ x *Usp18*$^{fl/fl}$ (black squares) and *CD169*-Cre$^{+/ki}$ x *Usp18*$^{fl/fl}$ (white squares) mice 16 hours after s.c. infection with $3x10^5$ PFU of VSV-EBOV. Values compared to naïve WT samples (gray squares). *P < 0.05, (Student's t-test, **a**). Data are representative of two (**a**) experiments (mean ± S.E.M (**a**)).

We concluded that local USP18 driven replication in CD169$^+$ macrophages is essential to activate innate immunity after subcutaneous immunization with the attenuated VSV-EBOV vaccine.

4.1.12. Enforced VSV-EBOV replication is essential for vaccination success

To finally prove, that USP18 expression mediated enforced replication in CD169 MΦs is essential for successful vaccination with live attenuated VSV-EBOV vaccine, we immunized mice intramuscularly with $3x10^5$ PFU of VSV-EBOV (Figure 22). Control mice induced a strongly enhanced VSV-EBOV specific antibody response, whereas *CD169*-Cre$^{+/ki}$ x *Usp18*$^{fl/fl}$ mice showed only low levels of VSV-EBOV specific antibodies (Figure 22a).

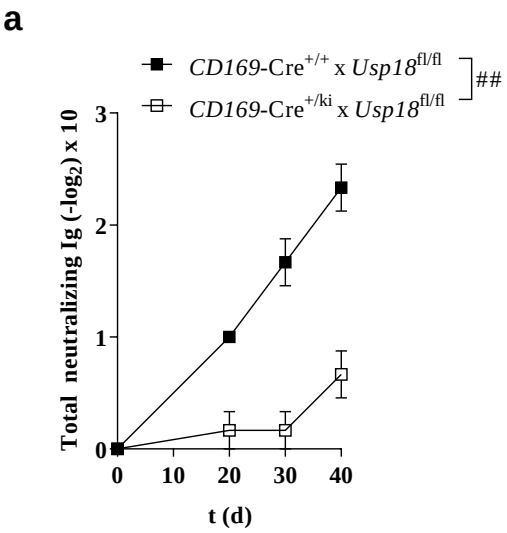

Figure 22: Enforced VSV-EBOV replication is essential for vaccination success

a VSV-EBOV neutralizing total Ig titers in serum of *CD169*-Cre$^{+/+}$ x *Usp18*$^{fl/fl}$ (black squares) and *CD169*-Cre$^{+/ki}$ x *Usp18*$^{fl/fl}$ (white squares) mice i.m. infected with $3x10^5$ PFU of VSV-EBOV on indicated time points after infection. ## $P < 0.0001$ (Two-way-Anova, **a**). Data are representative of two (**a**) experiments (mean ± S.E.M (**a**)).

To conclude, we proved that enforced replication of the attenuated Ebola virus vaccine VSV-EBOV mediated by USP18 expression in CD169$^+$ MΦs of injection site draining lymph nodes is essential to induce a protective vaccination status control in mice.

4.2. Chapter 2: Mechanism of immune system specific IAV replication

Immune cell specific virus replication is essential to activate immunity. We showed that spleen resident $CD169^+$ macrophages and DCs play a major role in capturing various viruses and influencing the outcome of the immune response. Here, we want to analyze the impact of SLO specific IAV replication on the induction of innate and adaptive immunity. As the spleen displays the biggest SLO, which is essential for capturing blood borne pathogens, we performed our experiments by systemic application of IAV.

4.2.1. Influenza replicates in spleen

Due to the natural route of infection via inhalation and its tropism IAV majorly replicates in lung epithelial cells. To identify if IAV replicates SLOs, we intravenously infected control mice (C57BL/6) with $2x10^7$ PFU of IAV H1N1 strain PR8 and analyzed virus replication in indicated organs (Figure 23). The highest amount of IAV particles was detectable in spleen, followed by lung after 24 hours of infection. Liver, inguinal lymph nodes, brain and kidney did not show presence of IAV particles (Figure 23a). To distinguish if the measured IAV particles were primary inoculated or actively replicating virus particles, we injected $2x10^7$ PFU of UV-inactivated or live IAV intravenously in control mice. IAV RNA expression in spleens was significantly decreased in mice infected with UV-inactivated IAV, compared to live IAV infected mice (Figure 23b). Immunohistochemical analysis of spleen sections of mice infected with UV-inactivated IAV did not show staining for IAV HA (red). In contrast, spleen sections of live IAV infected mice showed expression for IAV. IAV HA (red) colocalizing with $CD169^+$ macrophages (green) as well as $CD11c^+$ cells (blue) (Figure 23c).

We concluded, that intravenously injected IAV is captured in the spleen of mice and replicates in immune cells.

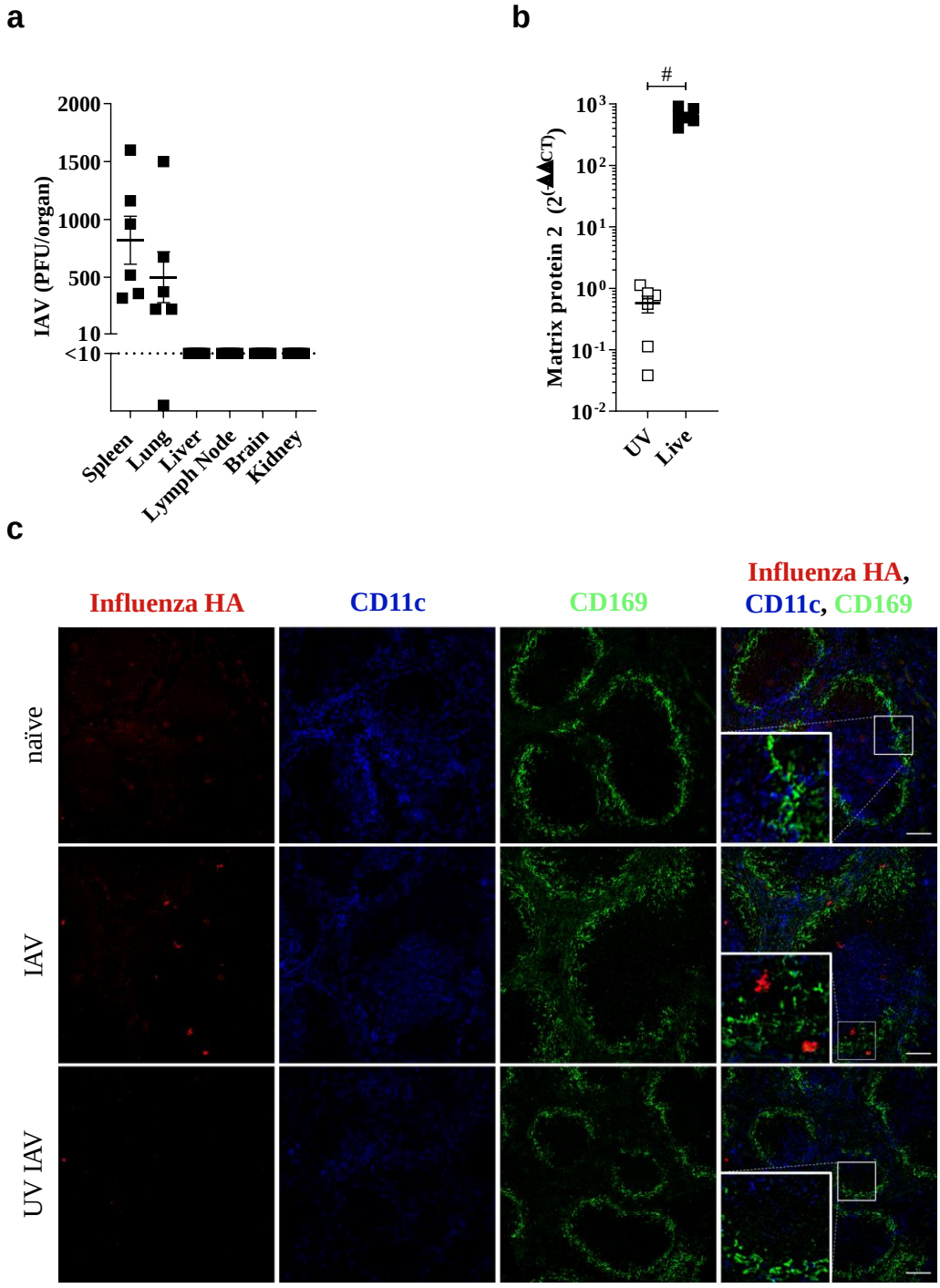

Figure 23: IAV replication is detectable in spleen after systemic infection

a Viral titers of indicated organs in C57BL/6 mice i.v infected with $2x10^7$ PFU of IAV 24 h p.i.. Dotted line represents assay detection limit. **b** Quantitative analysis of Matrix protein 2 expression via qRT-PCR of C57BL/6 mice intravenously infected with $2x10^7$ PFU of live IAV (black squares) or C57BL/6 mice infected with $2x10^7$ PFU of UV-inactivated IAV (white squares) normalized to naïve spleen values. Mice were sacrificed 24 h after infection. **c** Immunohistochemistry of spleen sections of mice infected as described in **b** stained for CD169 (green), CD11c (blue) and IAV HA (red). Scale bar 100 µm. One representative picture of each group from two experiments (n=3) shown. # $P < 0.0001$ Data are representative of two (**a**,**b**) experiments (mean ± S.E.M. (**a**,**b**)).

4.2.2. α2,3-linked sialic acid residues on spleen immune cells

It is known, that α2,3-linked sialic acid residues (α2,3-SA) on host cells serve as entry receptor for IAV H1N1 strain PR8 (Arias et al. 2009; Chen et al. 2018). To examine if spleen resident immune cells express the IAV entry receptor, we analyzed the expression of α2,3-SA via Flow cytometry (Figure 24a). $F4/80^+$ and $CD169^+$ cells showed expression of α2,3-SA, whereas $CD11c^+CD4^-CD8^-$ cells displayed only moderate levels of α2,3-SA expression. Interestingly, high expression of α2,3-SA was observed on $CD11c^+CD4^+$ and $CD11c^+CD8^+$ cells (Figure 24a). As DC subsets displayed high expression of α2,3-SA and we observed IAV colocalization in $CD11c^+$ cells upon immunohistochemical analysis of infected mice (Figure 24c), we wanted to analyze the presence of IAV proteins in DCs after systemic infection of mice. Western blot analysis of pan DCs from naïve or $2x10^7$ PFU of IAV infected mice showed presence of IAV Matrix protein in DCs of infected mice (Figure 24b).

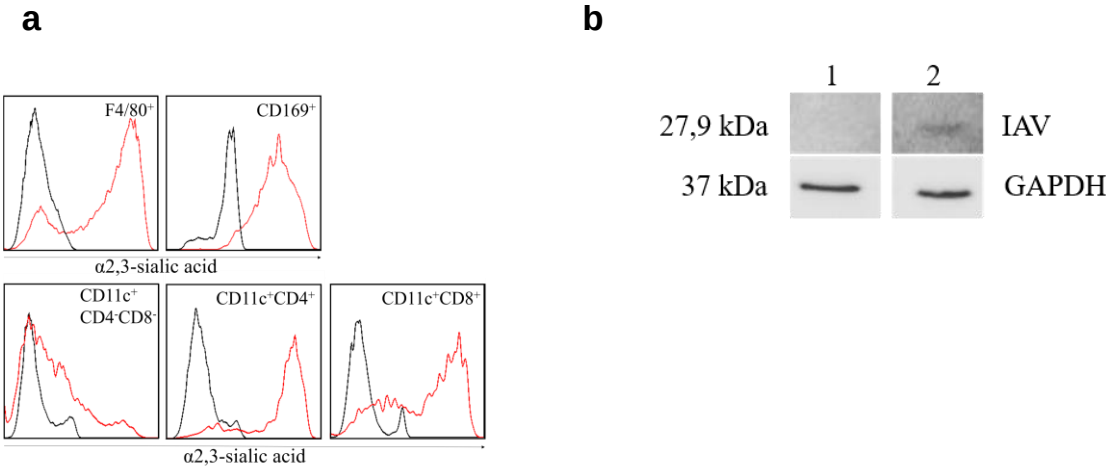

Figure 24: α2,3-linked SA are detectable on various immune cells

a Representative histograms of cell populations binding to secondary antibody control (black line) or MAL II lectin (α2,3-SA, red line). One mouse of two independent experiments (n=3 mice per experiment) shown. **b** Western blot analysis of MACS isolated pan DCs of naïve mice (lane 1) or mice i.v. infected with $2x10^7$ of IAV 24 h p.i. (lane 2). Staining with GAPDH antibody serves as loading control. Quantitative staining for IAV Matrix protein (IAV). Data are representative of two (**a**,**b**) experiments (n=3 per group).

We concluded, that α2,3-SA residues are present on various spleen resident immune cells with the greatest extent to DC subsets in which IAV is captured after systemic inoculation of mice.

4.2.3. Sialidase treatment reduces IAV replication in spleen

We further analyzed if the expression of SA residues on spleen resident immune cells is essential for IAV uptake. Therefore, mice were either treated with Sialidase to remove SA residues and infected $2x10^7$ PFU of IAV, solely infected with $2x10^7$ PFU of IAV or left untreated and sacrificed after 24 hours (Figure 25).

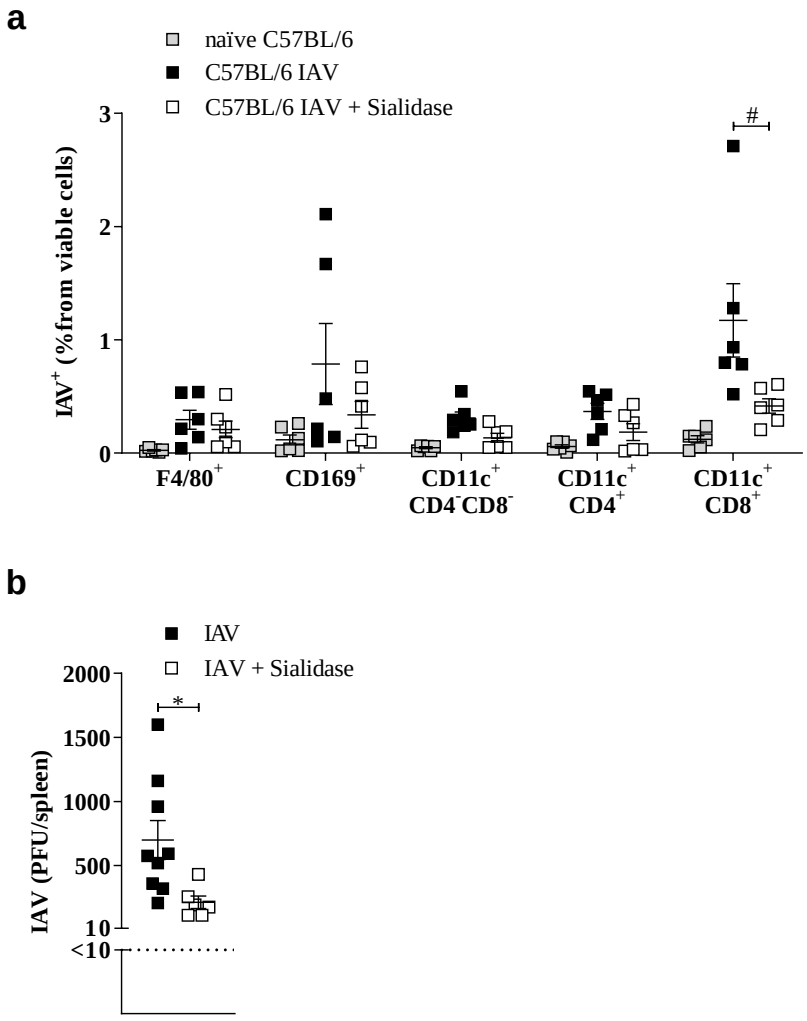

Figure 25: Sialidase treatment reduces IAV replication

a Intracellular IAV staining of indicated cells from naïve C57BL/6 mice (grey squares), mice i.v. infected with $2x10^7$ PFU of IAV (black squares) or mice pretreated with Sialidase and i.v. infected with $2x10^7$ PFU of IAV 24 h p.i. (white squares). **b** IAV titers of spleen samples from mice infected as described in **a.** Dotted line represents assay detection limit. * $P < 0.05$, and # $P < 0.001$, (Two-way-Anova, **a**) (Student's t-test, **b**). Data are representative of two (**a**) or three independent (**b**) experiments (n=3 per group) (mean ± S.E.M. (**a**,**b**)).

FACS analysis of spleen samples revealed slightly reduced levels of IAV^+ cells of $F4/80^+$, $CD169^+$, $CD11c^+CD4^-CD8^-$ and $CD11c^+CD4^+$ cells in infected, Sialidase-pretreated mice compared to infected, untreated mice. The strongest reduction of IAV expression was detectable for $CD11c^+CD8^+$ cells (Figure 25a). Next, we wanted to analyze if reduced IAV expression in spleen of Sialidase treated mice results in IAV titer reduction. Analysis of IAV titers in spleen samples 24 h after i.v. infection with $2x10^7$ PFU of IAV revealed a significant virus titer reduction in mice treated with Sialidase compared to untreated controls (Figure 25b).

We concluded, that Sialidase treatment reduced viral burden of mice spleen with the highest extent to $CD11c^+CD8^+$ cells most likely by removal of the IAV entry receptor.

4.2.4. Sialidase treatment reduces innate immune response after IAV infection

Sialidase treatment of mice strongly reduced the presence of viral antigen as well as viral replication in spleen of IAV infected mice. The anti-viral immune response is strongly dependent not only from the presence but also from the magnitude of viral antigen presence. Therefore, we analyzed the influence of sialidase treatment dependent IAV reduction on the activation of innate immunity (Figure 26). Indeed, analysis of IFNα serum titers as a marker for innate immune activation were reduced in mice infected with $2x10^7$ PFU of IAV and pretreated with Sialidase compared to untreated, infected controls (Figure 26a). In accordance, 24 h p.i. the relative expression of *Ifna2*, *Ifna4*, *Ifna5* as well as *Ifnb1* was significantly reduced in spleens of mice infected intravenously with IAV and treated with Sialidase compared to infected, untreated controls (Figure 26b).

Taken together, we show, that Sialidase treatment of mice resulted in decreased IAV presence in spleen of mice after systemic IAV infection. Further, reduced viral presence in immune cells decreased the induction of innate immunity in Sialidase treated mice, compared to untreated control mice.

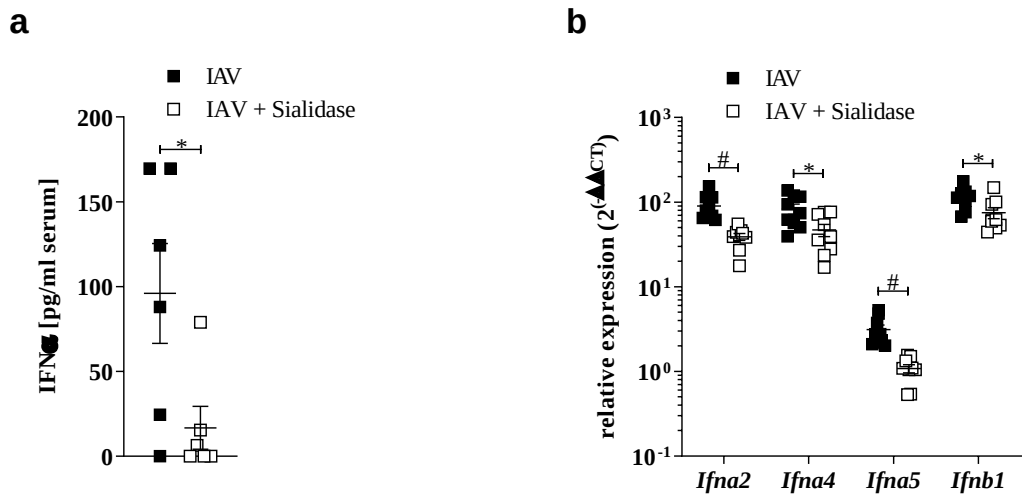

Figure 26: Sialidase treatment reduces innate immune response

a IFNα serum levels of C57BL/6 mice i.v. infected with $2x10^7$ PFU of IAV (black squares) or C57BL/6 mice pretreated with Sialidase and i.v. infected with $2x10^7$ PFU of IAV 24 h p.i. (white squares). **b** Relative expression of *Ifna2, Ifna4, Ifna5* and *Ifnb1* of mice treated as described in **a.** * $P < 0.05$, # $P < 0.001$, (Student's t-test, **a**, **b**). Data are representative of two (**a**) or three independent (**b**) experiments (n=3 per group) (mean ± S.E.M. (**a**,**b**)).

4.2.5. Oseltamivir treatment reduces IAV burden in spleen

Oseltamivir is a broadly used drug, which prevents IAV budding from cells by inhibiting neuraminidase activity (Kim et al. 1997). Therefore, Oseltamivir treatment inhibits IAV from spreading from cell to cell, whereas intracellular replication in of primary infected cells in not affected (Kamal et al. 2015). To analyze the spread of IAV particles within in the spleen, we infected mice pretreated with Oseltamivir with $2x10^7$ PFU of IAV i.v. and compared the presence of IAV particles to infected control mice 24 hours after infection (Figure 27). Mice treated with Oseltamivir and infected with IAV displayed a strong reduction of IAV infected $CD169^+$ macrophages and $CD11c^+CD8^+$ cells compared to untreated controls. The percentage of IAV expressing cells was comparable for $F4/80^+$, $CD11c^+CD4^-CD8^-$ and $CD11c^+CD4^+$ cells in Oseltamivir treated mice and untreated controls (Figure 27a). In line, overall reduction of IAV titers 24 h after i.v. infection was observed in spleen samples of mice treated with Oseltamivir, compared to untreated controls (Figure 27b).

We concluded that $F4/80^+$, $CD11c^+CD4^-CD8^-$ and $CD11c^+CD4^+$ cells are primarily infected after systemic IAV infection, whereas $CD169^+$ macrophages and $CD11c^+CD8^+$ cells are more likely to be infected with *de novo* synthesized IAV particles of the before mentioned cell types.

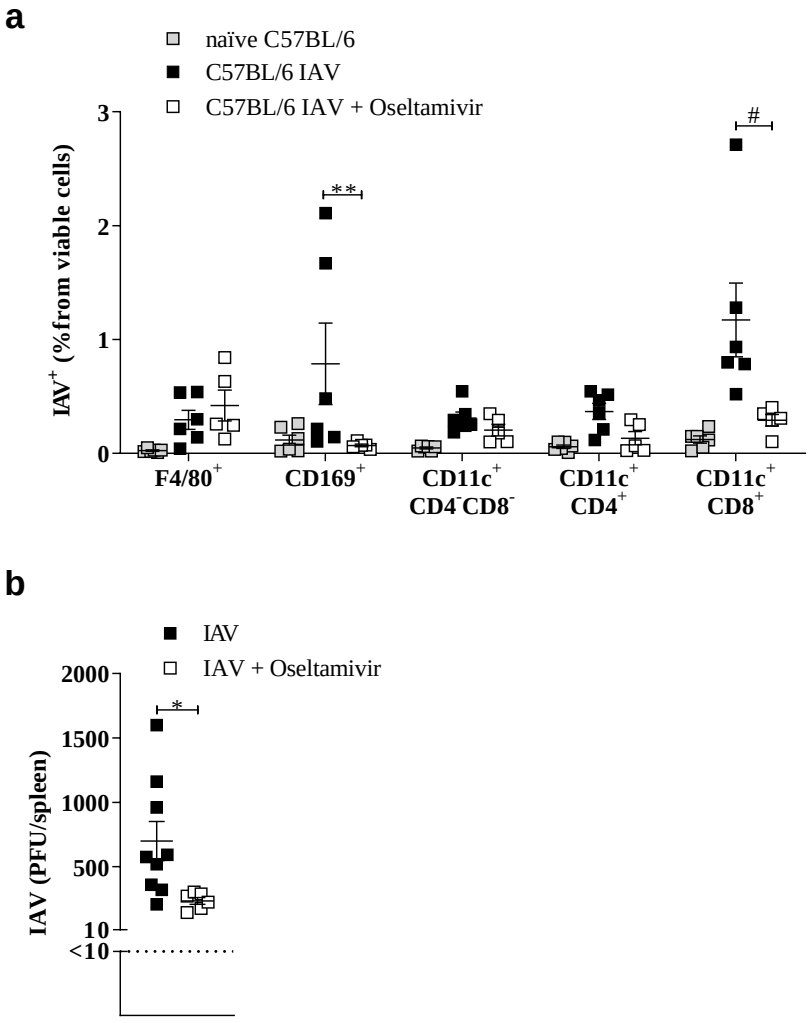

Figure 27: Oseltamivir treatment reduced IAV infection

a Intracellular IAV staining of indicated cells from naïve C57BL/6 mice (gray squares), C57BL/6 mice i.v. infected with $2x10^7$ PFU of IAV (black squares) or C57BL/6 mice pretreated with Oseltamivir and i.v. infected with $2x10^7$ PFU of IAV 24 h p.i. (white squares). **b** IAV titers of spleen samples obtained in **a**. Dotted line represents assay detection limit. * $P < 0.05$, ** $P < 0.01$ and # $P < 0.001$, (Two-way-Anova, **a**) (Student's t-test, **b**). Data are representative of two (**a**) or three independent (**b**) experiments (n=3 per group) (mean ± S.E.M. (**a**,**b**)).

4.2.6. Oseltamivir treatment reduces innate immunity after IAV infection

We demonstrated that Oseltamivir treatment suppressed IAV spread from specific immune cells of the spleen but not the magnitude of IAV antigen expression for some immune cells, therefore we wanted to investigate the influence of the altered IAV load on the activation of the innate immune response in mice. We analyzed if Oseltamivir treatment of mice influenced the activation of the innate immunity (Figure 28). Investigation of type I interferons induction as marker of an innate immune activation revealed slightly reduced IFNα serum levels in mice pretreated with Oseltamivir and infected with $2x10^7$ PFU of IAV compared to untreated, infected controls 24 hours after intravenous inoculation (Figure 28a). In line, expression of *Ifna2* and *Ifna5* was reduced in mice treated with Oseltamivir compared to untreated controls 24 h p.i.. The expression of *Ifna4* and *Ifnb1* was similar in Oseltamivir pre-treated and untreated controls (Figure 28b).

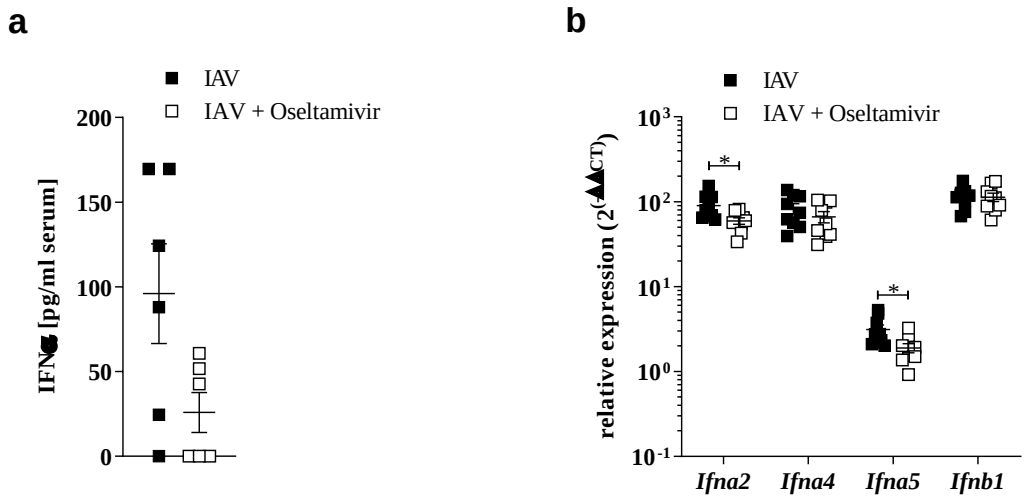

Figure 28: Oseltamivir treatment influences innate immune response

a IFNα serum levels of C57BL/6 mice i.v. infected with $2x10^7$ PFU of IAV (black squares) or C57BL/6 mice pretreated with Oseltamivir and i.v. infected with $2x10^7$ PFU of IAV 24 h p.i. (white squares). **b** Relative expression of *Ifna2*, *Ifna4*, *Ifna5* and *Ifnb1* of mice treated as described in **a**. * $P < 0.05$ (Student's t-test, **a**, **b**). Data are representative of two (**a**) or three independent (**b**) experiments (n=3 per group) (mean ± S.E.M. (**a**,**b**)).

We concluded that the reduced the viral burden in splenic immune cells of Oseltamivir pretreated and IAV infected mice repressed the innate immune response only partially.

4.2.7. IAV replication is essential to activate immunity

We demonstrated that intracellular presence of IAV particles and replication induced a strong activation of the innate immune response. As splenic tissue is usually not a target of IAV tropism, we wanted to evaluate if IAV replication is in SLO is essential to boost adaptive immunity. To analyze if IAV replication in immune cells of SLOs is essential to induce a strong immune response, we infected mice with $2x10^7$ PFU of live IAV or $2x10^7$ PFU of UV-inactivated IAV intravenously (Figure 29). Indeed, we showed that live IAV infection results in strong upregulation of interferon type I genes *Ifna4* and *Ifnb1* in spleen samples, compared to spleen samples of UV-inactivated IAV infected mice 24 h post infection (Figure 29a). To further investigate if IAV replication activation mediated innate immune response is essential to enhance the adaptive immune response to IAV, we analyzed the anti-IAV $CD8^+$ T cell response after intravenous infection of mice with $2x10^7$ PFU of live IAV or $2x10^7$ PFU UV-inactivated of IAV. Twelve days post infection IFNγ production of $CD8^+$ cells stimulated with IAV peptide was highly increased in live IAV immunized mice compared to UV-inactivated IAV infected mice (Figure 29b).

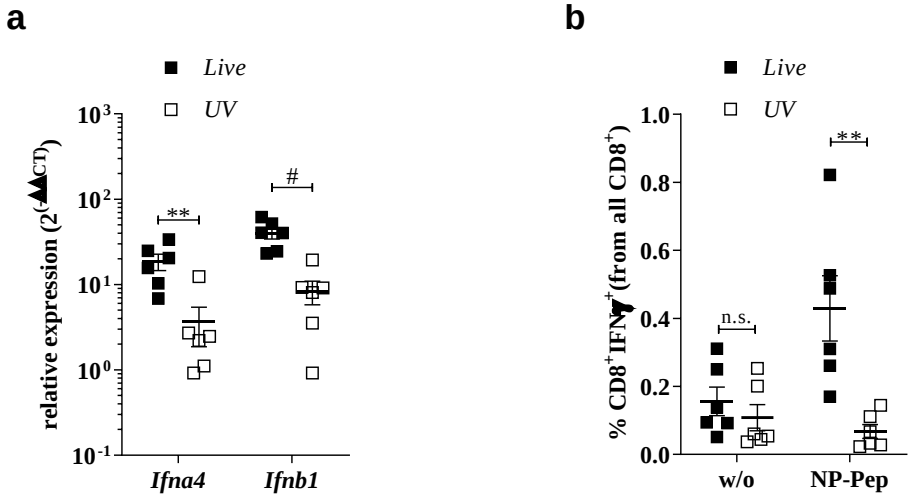

Figure 29: Systemic IAV replication drives immunity

a Relative expression of *Ifna2* and *Ifnb1* of spleen samples from C57BL/6 mice i.v. infected with $2x10^7$ PFU of IAV (black squares) or $2x10^7$ PFU of UV-inactivated IAV (white squares) 24 h p.i.. **b** Intracellular IFNγ staining of $CD8^+$ cells of C57BL/6 mice infected as described in **a** sacrificed after 12 days of infection. Spleen samples were not stimulated (w/o) or stimulated with IAV NP peptide (NP-Pep). ** $P < 0.01$ and # $P < 0.001$, (Student's t-test, **a,b**). Data are representative of two (**a**,**b**) experiments (n=3-4 per group) (mean ± S.E.M. (**a**,**b**)).

We concluded that active replication of IAV in SLOs is essential to enhance innate as well as adaptive immunity.

4.2.8. Role of IFN type I signaling in intravenous IAV infection

The induction of type I interferons is essential to suppress viral replication. To analyze the influence of type I interferons on IAV replication in SLOs, we injected control mice (C57BL/6) and *Ifnar*$^{-/-}$ mice intravenously with 2x10^{7} PFU of IAV and sacrificed both groups after 24 h (Figure 30). Evaluation of immunohistochemical staining of spleen sections revealed differences in IAV HA staining (red) between control and *Ifnar*$^{-/-}$ mice. In control mice, colocalization of IAV HA (red) and CD169^{+} (green) as well as CD11c^{+} (blue) cells was detectable. *Ifnar*$^{-/-}$ mice showed an increased appearance of IAV HA expressing cells, which either colocalized with CD169^{+} (green) as well as CD11c^{+} (blue) cells or did not colocalize with any of these cells (Figure 30a). We further analyzed spleen samples of infected mice via Flow cytometry to evaluate which cells were infected by IAV. Investigation of spleen samples showed an increase of IAV^{+} cells in both infected mice groups compared to naïve mice. *Ifnar*$^{-/-}$ mice showed slightly increased amount of IAV^{+} cells for CD169^{+}, CD11c^{+}CD4^{-}CD8^{-}, CD11c^{+}CD4^{+} and CD11c^{+}CD8^{+} cells compared to control mice. F4/80^{+} cells showed IAV^{+} staining at comparable levels for *Ifnar*$^{-/-}$ and control mice (Figure 30b).

We concluded that in the presence of interferon signaling, IAV replication in SLO is restricted to specialized immune cells. Absence of interferon signaling enhanced the abundance if IAV replication slightly in immune cells and but more strikingly in other cells in the spleen.

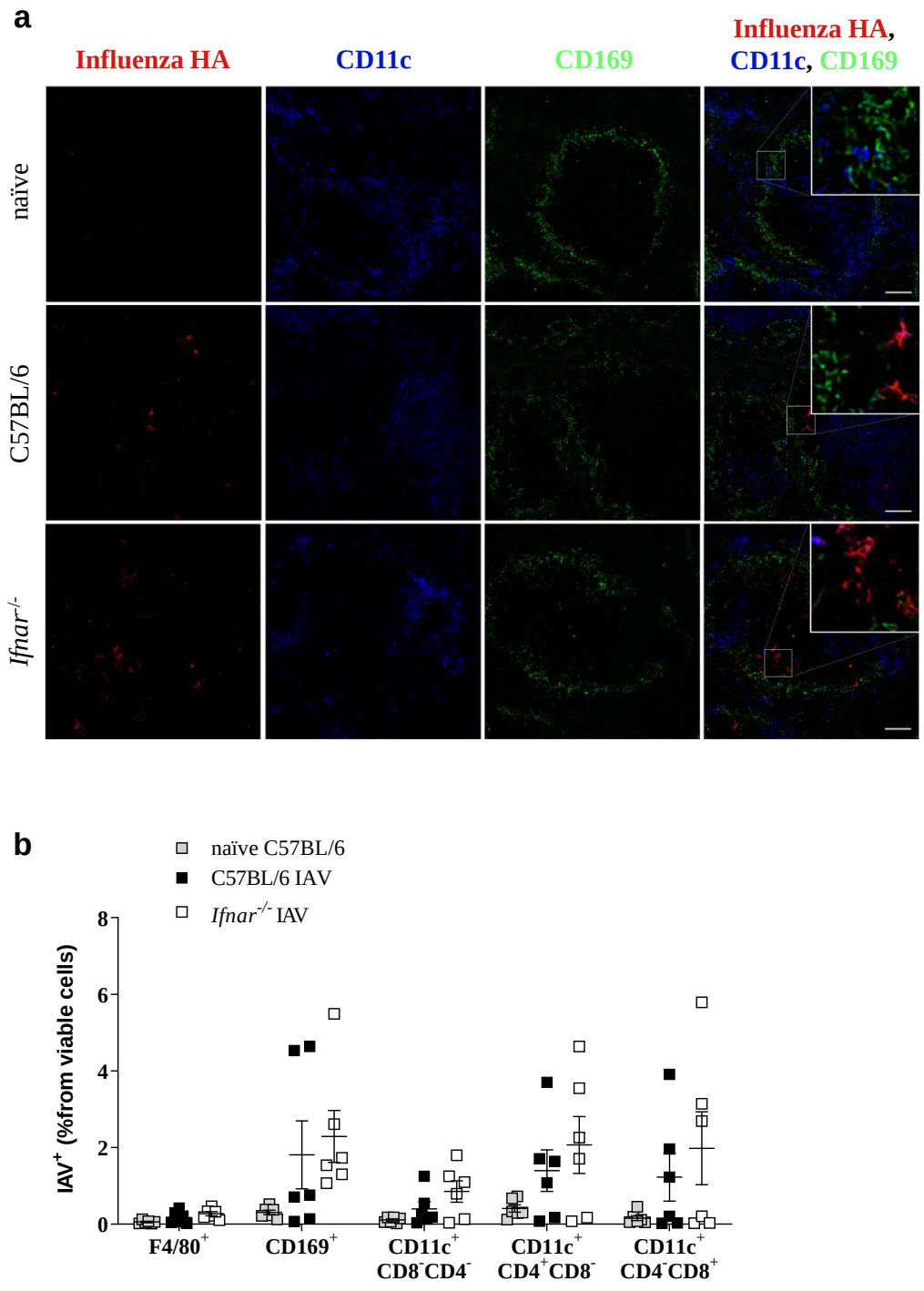

Figure 30: Interferon is essential to suppress IAV replication in spleen

a Immunohistochemistry of spleen sections of C57BL/6 or *Ifnar*$^{-/-}$ mice infected intravenously with 2x10^{7} PFU of IAV or naïve control mice stained for CD169 (green), CD11c (blue) and IAV HA (red) 24 h p.i.. Scale bar 100 µm. One representative picture of each group from two experiments (n=3) shown. **b** Intracellular staining for IAV presence from spleen samples of naïve (gray squares), C57BL/6 (black squares) or *Ifnar*$^{-/-}$ mice (white squares) of mice infected as described in **a**. Data are representative of two (**a**,**b)** experiments (n=3 per group) (mean ± S.E.M. (**b**)).

4.2.9. USP18 drives enforced replication in spleen of IAV infected mice

It is known, that USP18 is an essential blocker of IFN type I signaling. Especially in CD169$^+$ macrophages and dendritic cells, a constitutive high expression of USP18 was shown to be essential to enforce virus replication, which was in terms necessary to induce a strong immune response and ensure anti-viral protection in case of a VSV or LCMV infection (Honke et al. 2011; Honke et al. 2013). As we could show that in the presence of interferon signaling, IAV replication is predominately restricted to CD169$^+$ macrophages and DCs, we analyzed if USP18 mediated enforced IAV replication is essential to enhance antigen production. The CAG$^+$*Usp18*$^{fl/fl}$ mouse model allowed ubiquitous Tamoxifen inducible gene knockout of *Usp18* in cells including CD169$^+$ macrophages and DCs without side effect on cell development and function as seen in constitutive *Usp18* gene knockout mouse models. We infected CAG$^-$ *Usp18*$^{fl/fl}$ (control mice) or CAG$^+$*Usp18*$^{fl/fl}$ mice intravenously with 2x10^7 PFU of IAV and analyzed viral titers in spleen samples 24 h p.i. (Figure 31). Spleen samples of control mice showed highly increased IAV replication compared to CAG$^+$*Usp18*$^{fl/fl}$ mice (Figure 31a).

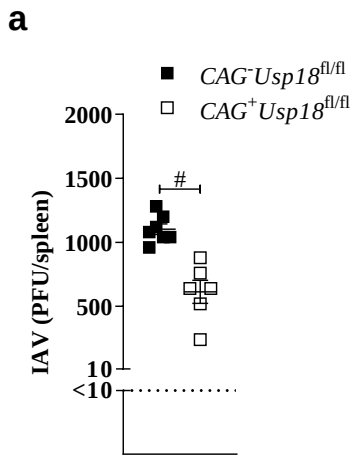

Figure 31: USP18 is essential for IAV replication in spleen

a IAV titers of spleen samples obtained from CAG$^-$*Usp18*$^{fl/fl}$ (black squares) or CAG$^+$*Usp18*$^{fl/fl}$ (white squares) mice treated with Tamoxifen and intravenously infected with 2x10^7 PFU of IAV 24 h p.i.. Dotted line represents assay detection limit. # P < 0.001, (Student's t-test, **a**). Data are representative of two (**a**) experiments (mean ± S.E.M. (**a**)).

We concluded that USP18 expression is essential enforce IAV replication and thereby enhanced the presence of IAV antigen in the spleen.

4.2.10. Influence of enforced replication on IAV immune response

Presence of viral antigen is essential to trigger innate immunity via for example activation of TLR signaling. We showed that CAG^{-}*Usp18*$^{fl/fl}$ mice displayed enhanced IAV replication compared to CAG^{-}*Usp18*$^{fl/fl}$, therefore we analyzed the impact of EVR of the induction of anti-IAV immunity (Figure 32). Analysis of serum IFNα levels as a marker for innate immune induction displayed strongly elevated IFNα levels in control mice compared to CAG^{+}*Usp18*$^{fl/fl}$ (Figure 32a). In line, gene expression of *Ifnα4* and *Ifnb1* was significantly upregulated in control mice compared to CAG^{+}*Usp18*$^{fl/fl}$ mice (Figure 32b). To analyze the effect of USP18 mediated enforced IAV replication on the adaptive immune response, we injected mice intravenously with $2x10^{7}$ PFU of IAV and analyzed the T cell response twelve days after infection (Figure 32c). *Ex vivo* stimulation of IAV specific CD8^{+} T cells with IAV NP peptide revealed significantly increased IFNγ production by CD8^{+} T cells of control mice compared to CAG^{+}*Usp18*$^{fl/fl}$.

In conclusion, we showed that immune cell specific enforced IAV replication mediated by USP18 in SLOs is essential to activate innate and adaptive immune response.

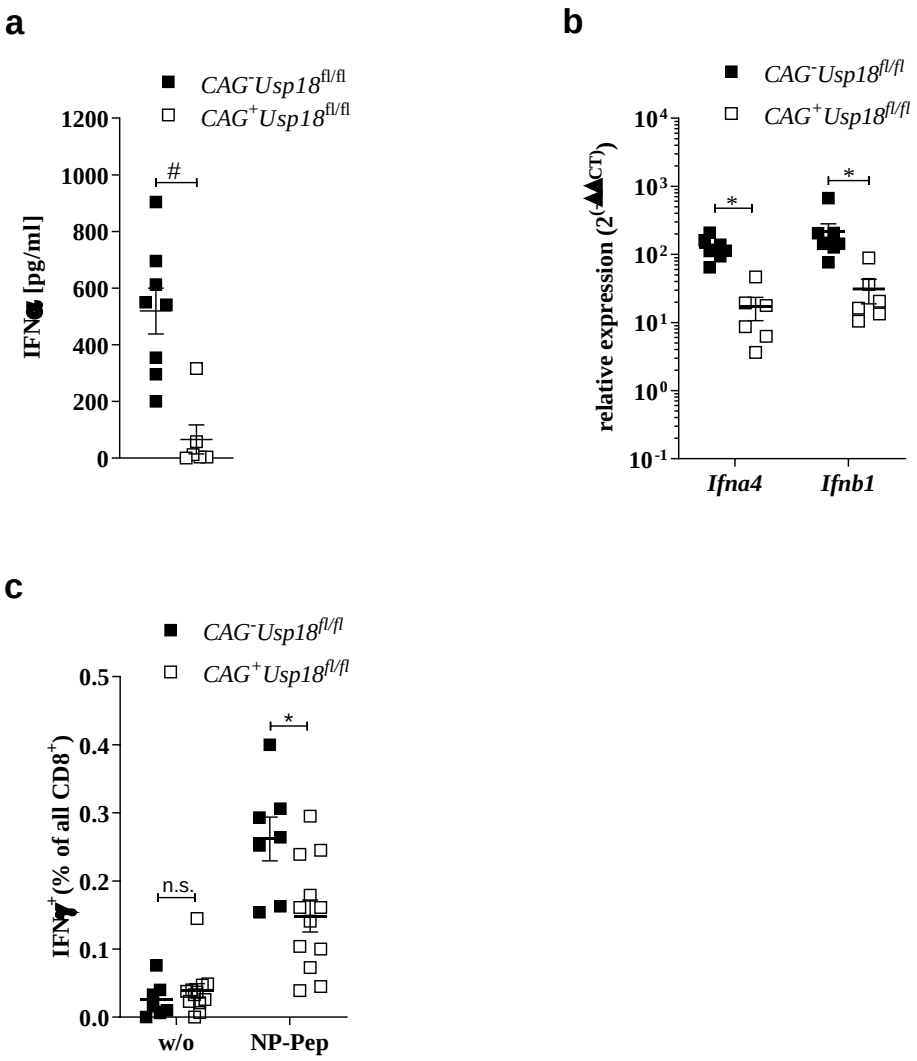

Figure 32: Enforced IAV replication boosts immunity

a IFNα serum levels of CAG-*Usp18*$^{fl/fl}$ (white squares) or CAG+*Usp18*$^{fl/fl}$ (back squares) mice treated with Tamoxifen and infected intravenously with 2x10^7 PFU of IAV 24 h p.i.**b** Relative expression of *Ifna4* and *Ifnb1* of mice treated as described in **a**. Intracellular IFNγ staining of spleen resident CD8$^+$ cells of mice infected as described in **a** 12 days after infection. Spleen samples were not stimulated (w/o) or stimulated with IAV NP peptide (NP-Pep). * P < 0.05, # P < 0,001 (Student's t-test, **a-c**). Data are representative of two (**a-c**) experiments (mean ± S.E.M. (**a-c**)).

4.2.11. IAV replicates in lung draining lymph nodes

We demonstrated that IAV replication is detectable in spleen and relies on the expression of USP18. We wanted to further clarify, if IAV replicates in lung draining lymph nodes after virus transmission via the natural route of infection. Therefore, we infected mice with $2x10^6$ PFU of IAV intranasally and sacrificed mice 24 hours later (Figure 33). Immunohistochemical analysis of lung draining lymph nodes revealed colocalization of IAV particles (red) with $CD11c^+$ cells 24h p.i. (Figure 33a).

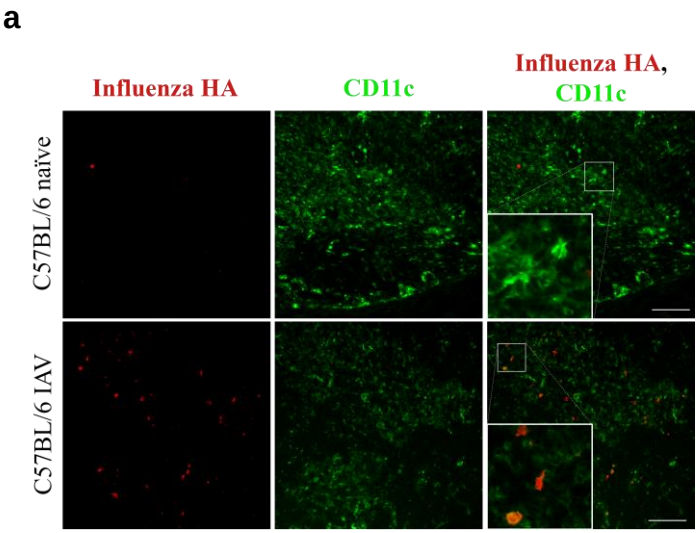

Figure 33: IAV replicates in lung draining LNs

a Immunohistochemistry of lung draining lymph node sections of C57BL/6 mice infected intranasally with $2x10^6$ PFU of IAV or naïve stained for CD11c (green) and IAV HA (red) 24 h p.i.. Scale bar 100 µm. One representative picture of each group from two experiments (n=3) shown**.** Data are representative of two **(a)** experiments (n=3 per group)

To conclude, we could show, that indeed IAV particle are present in DCs of lung draining LNs 24 h after intranasal infection.

5. Discussion

Virus replication can be a double-edged sword if it is not tightly controlled. On the one hand uncontrolled replication can lead to an overwhelming infection and to fast death of the host. On the other hand, low or no virus replication fails to induce an anti-viral response in the host. The immune system evolved in a way, which allows simultaneously boosted replication in specialized immune cells, as well as fast induction of an anti-viral status. Especially the tight organization of the splenic architecture has been regarded as essential for viral replication since decades (Muller et al. 2002). Different cell types influence hereby the outcome of virus replication. In particular, specialized macrophages and dendritic cells influence the progression of a viral infection.

In this work, we highlighted these mechanisms and the relevance of enforced virus replication for replication competent, recombinant vaccines, such as VSV-EBOV (Chapter 1), as well as natural infection with IAV (Chapter 2).

5.1. Chapter 1

The immune response after live virus infection has to be strictly controlled to prevent excessive or poor immune activation. Excessive activation of the immune system might lead to harmful inflammatory processes such as neurodegenerative diseases or autoimmunity (Baccala, Kono, and Theofilopoulos 2005; Cembrzynska-Nowak et al. 2005; Jung et al. 2005). On the other side, negligible immune activation might fail to induce protection against the invading pathogen, which leads to enhanced susceptibility to a fatal outcome on an infection (Zhou et al. 2007). Multiplication of live virus particles and the according immune response have to be tightly equated. It is known that for VSV these early events of the immune response play a critical role in virus control. Especially the interferon response plays a major role in the control of cytopathic VSV (Lang et al. 2007).

5.1.1. USP18 in CD169$^+$ MΦs is essential to enforce systemic VSV replication

CD169$^+$ MΦs build the first line of defense against viruses invading the spleen and lymph nodes via the bloodstream. With their localization at the end of blood conduits, they display crucial gatekeepers of the immune system (Eloranta and Alm 1999; Junt et al. 2007; Iannacone et al. 2010; Chavez-Galan et al. 2015). One of the most important mechanisms which strengthens the

immune function of CD169^{+} MΦs is enforced virus replication, which was previously primary described by Honke et. al (Honke et al. 2011). USP18 (also known as UBP43) is the major multifunctional molecule involved in this process. Despite its protease activity, which affects transcriptional activation and cell metabolism, it is essential for the development of several cell types (Honke et al. 2016). It has been described that development of Th17 cells and CD11b cells highly relies on the presence of USP18 (Cong et al. 2012; Liu et al. 2013). Due to this multifunctionality of USP18, it was not possible in the past to evaluate if VSV enforced virus replication is solely relying on the presence of this protein in CD169^{+} MΦs. Former mouse models used for the investigation of enforced virus replication only displayed an ubiquitous knockout of *Usp18* (Honke et al. 2011; Honke et al. 2013). To investigate the function of USP18 in CD169^{+} MΦs in more detail, we established a mouse model with a CD169^{+} cell specific knockout of *Usp18* (*CD169*-Cre$^{+/ki}$ x *Usp18*$^{fl/fl}$) and compared key findings to control mice (*CD169*-Cre$^{+/+}$ x *Usp18*$^{fl/fl}$).

In the presence of USP18, VSV replication was strongly restricted to CD169^{+} MΦs of the marginal zone of the spleen. Absence of USP18 CD169^{+} MΦs was associated with absence of VSV particles in histological analysis of spleen sections (Figure 11c). In line with this observation, VSV titers in inguinal lymph nodes, as well as the presence of the virus protein VSV-NP in lymph nodes and spleens, were found to be increased in an USP18 dependent manner (Figure 11a+b). Previous work pointed to a strong, early innate immune response to be essential to efficiently control VSV infection. It was shown that VSV replication is highly sensitive to the anti-viral effects of type I interferons. The induction of interferon stimulated genes, such as *Mx1* interferes with viral RNA synthesis and suppresses *de novo* formation of virus particles already at low levels (Meier et al. 1990; Staeheli and Pavlovic 1991). In the presence of type I interferon signaling in mice, VSV replication is limited to CD169^{+} MΦs of the marginal zone by the constitutive expression of the INFAR signaling inhibitor USP18 (Honke et al. 2011) (Figure 11c). Loss of USP18 dependent type I interferon signaling inhibition in CD169^{+} MΦs of *CD169*-Cre$^{+/ki}$ x *Usp18*$^{fl/fl}$ was indeed accompanied by reduced VSV replication (Figure 11a+b), but concomitantly type I interferon induction was strongly inhibited as a consequence of reduced antigen presence compared to control mice (Figure 12). As it was shown that a strong interferon induction to be essential to prevent a fatal outcome of a VSV infection (Muller et al. 1994), we analyzed the susceptibility of *CD169*-Cre$^{+/ki}$ x *Usp18*$^{fl/fl}$ to a challenging dose of VSV (Figure 13). Indeed, enhanced the deprived interferon induction in *CD169*-Cre$^{+/ki}$ x *Usp18*$^{fl/fl}$ the mortality rate after VSV infection. Enhanced susceptibility to the fatal neurovirulence of VSV in *CD169*-Cre$^{+/ki}$ x *Usp18*$^{fl/fl}$ was further

associated with decelerated VSV neutralizing antibody induction (Figure 13a+b). VSV neutralizing antibodies are essential to prevent a lethal outcome of the infection. Even in the absence of type I interferon signaling, adoptive transfer of VSV neutralizing antibodies sufficed to protect against lethal neurovirulence of VSV (Steinhoff et al. 1995). Our data indicated, that USP18 driven EVR is not only essential to boost anti-VSV innate but also generates a protective neutralizing antibody response.

Interestingly, in contrast to Honke et al., we did not observe an impact of USP18 mediated EVR in $CD169^{+}$ macrophages on the induction of an VSV specific T cell response. Our data show comparable IFNγ production by VSV specific CD8 T cell after stimulation with a VSV specific peptide for *CD169*-$Cre^{+/ki}$ x *Usp18*$^{fl/fl}$ and control mice (Figure 13d), whereas Honke et al., described significantly decreased IFNγ production after stimulation of anti-viral T cells of VSV infected *Usp18*$^{-/-}$ mice (Honke et al. 2011). It has been described that constitutive gene knockout of *Usp18* leads to developmental alteration of conventional dendritic cells (Cong et al. 2012). As dendritic cells are essential to activate T cells, functional modification of these cells in constitutive knockout *Usp18*$^{-/-}$ might influence the induction of anti-viral T cells. The role of *Usp18* in DCs on the induction of VSV specific T cells must be further evaluated.

5.1.2. Local VSV immunization builds the cornerstone for effective vaccination

$CD169^{+}$ MΦs do not only play a unique role during blood-borne infections. Iannacone et al. showed that lymph node-resident $CD169^{+}$ MΦs are crucial for preventing VSV from CNS invasion during subcutaneous infection in a type I interferon-dependent fashion [16]. In detail, it was demonstrated that $CD169^{+}$ subcapsular sinus macrophages capture virus particles and present them to B cells to initiate a humoral immune response. Based on these findings, we were able to demonstrate that USP18 expression in CD169 MΦs is essential for driving VSV replication in injection site draining LN (Figure 14). Hence, solely in the presence of VSV replication a strong IFN type I induction was detectable (Figure 15). In addition, the neutralizing antibody response of WT mice was drastically increased when compared to *CD169*-$Cre^{+/ki}$ x *Usp18*$^{fl/fl}$ mice after intramuscular immunization of mice with VSV. This is especially important as previous findings showed that solely replication competent VSV and vectors thereof are able to induce a neutralizing antibody response (Roberts et al. 1999). Furthermore, we could show that EVR is also essential after intramuscular injection of VSV (Figure 16) which corroborates previous studies using a Rabies virus model showing a transient infection of draining lymph nodes after intramuscular application being critical for virus control [31]. Together, these

results build the foundation for our working hypothesis that EVR is essential for the successful immunization using VSV-vector based vaccines.

5.1.3. VSV and VSV-EBOV show comparable features upon systemic administration

Because of its desirable features, VSV is commonly used as a backbone of recombinant live vaccines (Clarke et al. 2016). One of the recently developed VSV vaccines is VSV-EBOV, which was lately released under the name "Ervebo". For this vaccine, the VSV glycoprotein (VSV-G) was exchanged by the Ebola virus glycoprotein which influences viral tropism and results in attenuation and reduced replication of the virus. To evaluate if VSV-EBOV and its wildtype equivalent VSV show comparable features, we analyzed the viral replication after systemic application (Figure 17). Indeed, we observed a strong USP18 dependent replication which was limited to $CD169^{+}$ macrophages for VSV and VSV-EBOV (Figure 11c, Figure 17c). In line with previous findings for VSV, VSV-EBOV replication was decreased in lymph nodes, and expression of VSV-NP virus protein was decreased in spleen and lymph nodes of *CD169*-$Cre^{+/ki}$ x *Usp18*$^{fl/fl}$ mice (Figure 17a+b). Interestingly, VSV-EBOV titers in lymph nodes of control animals were more than 10-fold reduced (Figure 17a) compared to VSV infected control animals (Figure 11a) at comparable infectious titer of $3x10^6$ (VSV-EBOV) and $2x10^6$ (VSV) PFU/mouse. This result impressively demonstrates the attenuation of VSV-EBOV as a result of the glycoprotein exchange. We therefore hypothesized that for replication competent vaccines with low replication capacity (e.g., as a result of attenuation) EVR in C169 MΦs driven by USP18 is especially of high relevance. Indeed, by analyzing the innate immune response after systemic administration of VSV-EBOV, we observed only diminished induction of type I IFNs in the absence of USP18 in $CD169^{+}$ MΦs (Figure 18). Since long term protection upon vaccination is a result of the induction of virus neutralizing antibodies, we subsequently analyzed the neutralizing antibody response of systemically infected animals by VSV-EBOV. In conformity with our previous findings, EVR is also inevitable to induce a strong neutralizing antibody response. USP18 dependent enforced replication of VSV-EBOV was essential to induce a strong neutralizing antibody response when compared to mice lacking *Usp18* in $CD169^{+}$ MΦs (Figure 19).

5.1.4. Enforced VSV-EBOV replication in dLN is inevitable for success of vaccination

To further confirm the necessity of EVR for the induction of a protective vaccination response, we administered the vaccine subcutaneously to analyze VSV-EBOV replication and localization in the injection site dLN (Figure 20). Despite its attenuated characteristics, we were able to detect an increased viral load of VSV-EBOV particles in control animals compared to *CD169*-Cre$^{+/ki}$ x *Usp18*$^{fl/fl}$ mice (Figure 20a+b). Furthermore, the visualization of Ebola virus GP expressing cells in the dLN showed a corresponding picture with increased numbers of GP expressing cells upon VSV-EBOV inoculation. Even more important, solely in the presence of USP18 Ebola virus GP presence in CD169^{+} macrophages was enhanced (Figure 20c). In contrast to systemic application, the difference of the replication capacity between the attenuated Ebola virus vaccine and the WT VSV virus was more pronounced. Not only the VSV-EBOV titers in the dLN were tenfold reduced in control mice, but the expression of viral proteins was also more abundant in mice treated with WT VSV despite the 100 times higher infectious dose of VSV-EBOV used to infect mice (Figure 14, Figure 20). These findings are in accordance with and confirm above data, that exchange of viral glycoproteins between two viruses represents an essential factor to attenuate the virus of origin (Garbutt et al. 2004).

Interestingly enough, we did not observe an alteration of the cellular tropism in secondary lymphoid organs whereas VSV-EBOV lost its neurotropism in contrast to VSV. The distribution of viral particles of VSV or VSV-EBOV was comparable in spleen as well as inguinal lymph nodes. Even more important, we did not observe the described neurovirulent effects of VSV in infected animals (Figure 13c) upon administration of VSV-EBOV via the different routes of application (data not shown). These data emphasize the previously described benign safety profile of this attenuated vaccine, and suggests such attenuated viruses being safe compared to their WT counterpart due to their reduced replication capacity.

To further analyze the effect of EVR on the outcome of VSV-EBOV vaccination, we investigated the induction of type I interferons in dLN after subcutaneous infection (Figure 21). The induction of *Ifna4* in control mice was strongly elevated compared to *CD169*-Cre$^{+/ki}$ x *Usp18*$^{fl/fl}$ mice (Figure 21). In line with our data from systemic VSV-EBOV administration (see above), we further strengthen our hypothesis that EVR is essential to boost anti-viral immunity. Similar findings were yet only reported upon VSV-EBOV vaccination in non-human primate (NHP) experiments (Menicucci et al. 2019).

To finally verify the essential role of EVR for an efficient vaccination, we analyzed the presence of protective Ebola virus glycoprotein antibodies subsequent to intramuscular immunization. We indeed showed that the presence of USP18 in $CD169^{+}$ MΦs was essential to induce the generation of VSV-EBOV protecting antibodies faster and stronger (Figure 22).

5.1.5. Enforced replication in the context of live virus vaccines

The presented data clearly underline the beneficial effect of USP18 driven EVR for the outcome of an effective vaccination response. VSV represents the ideal vector for the generation of recombinant vaccines for a variety of virus infections. Due to its features, it is easy modifiable, safe to use in humans and easy to produce. In animal models, VSV-based vaccines were able to induce protection against a variety of pathogens. Recent data showed the efficiency of this vector using Marburg virus, HIV or Influenza virus envelope proteins or glycoproteins (Rose et al. 2001; Schwartz et al. 2010; Geisbert and Feldmann 2011; Bresk et al. 2019). Due to the latest developments in the global COVID-19 (Coronavirus Disease 2019) pandemic, it is not surprising that the recombinant VSV platform was also employed to develop a SARS-CoV-2 (severe acute respiratory syndrome coronavirus type 2) vaccine (Case et al. 2020; Yahalom-Ronen et al. 2020). The VSV-ΔG-spike vaccine, expressing the Coronavirus spike surface glycoprotein, was shown to induce a protective state in Syrian hamsters. VSV-ΔG-spike vaccinated hamsters showed decreased weight loss and decreased viral titers after SARS-CoV-2 infection compared to unvaccinated controls. Using a mouse model elevated SARS-CoV-2 antibody titers upon VSV-ΔG-spike vaccination were demonstrated (Yahalom-Ronen et al. 2020). These data suggest that also for this SARS-CoV-2 vaccine approach, EVR plays a crucial role in the induction of a vaccination status against SARS-CoV-2, which should be evaluated in more detail, and further underlines the importance of the presented work.

5.2. Chapter 2

We could show in Chapter 1 that USP18 dependent EVR plays a major role for the activation of innate and adaptive immunity upon VSV and VSV-EBOV infection. As recent attempts for the design of an Influenza virus (IAV) vaccine also uses the recombinant VSV platform, we also analyzed if EVR is an essential mechanism to induce an anti-viral IAV response during natural infections. By using the IAV strain PR8 as a model virus in CAG^{+}*Usp18*$^{fl/fl}$ mice, we were able to analyze the role of specialized immune cells in secondary lymphoid tissue upon Influenza virus infection.

5.2.1. IAV entry in leukocytes

Specialized immune cells play a major role in the control of viral infections. Especially macrophages and dendritic cells have been shown to represent crucial players to induce an efficient anti-viral state after the infection with IAV (Iwasaki and Pillai 2014). During natural infection, IAV first invades the epithelial layer of the respiratory tract, to potentially spread further to immune and non-immune cells (Perrone et al. 2008; Manicassamy et al. 2010). It is already known that IAV antigen must be presented in SLO in order to induce a strong immune response (Chiu et al. 2015). Gonzalez et al. showed that an UV-inactivated IAV strain PR8 is captured in DCs of lung draining lymph nodes after subcutaneous inoculation (Gonzalez et al. 2010). Moreover, it has also been already demonstrated that UV-inactivated IAV PR8 is internalized into CD169^{+} macrophages (Chatziandreou et al. 2017). Since these experiments were carried out with UV-inactivated IAV, we first wanted to investigate if IAV can not only be internalized into lymphoid tissue resident immune cells (which happens upon using an UV-inactivated and not replication competent IAV) but can actively replicate. Via systemic application of replicating IAV we were able to target and analyze the immune processes in the largest of the secondary lymphoid organs, the spleen. Indeed, we showed that immune cells of the spleen home replicating IAV (Figure 23). Furthermore, and in accordance with previous findings, we identified dendritic cells and macrophages as a major site of IAV replication in spleen (Figure 24b, Figure 25a). IAV tropism is determined by its preferred binding to α2,3-linked Sialic acid residues mainly on the cell surface of lung epithelial cells. The results of Chatziandreou et al. hinted towards a sialic acid receptor dependent internalization of IAV particles into CD169^{+} macrophages (Chatziandreou et al. 2017). We could extend this finding by demonstrating that spleen resident macrophages and dendritic cells express α2,3-SA residues (Figure 24a). To prove that SA residues indeed are majorly essential for IAV entry, we

enzymatically removed SA residues *in vivo*. Treatment of mice with the SA removing enzyme Sialidase and subsequent infection resulted in a decreased presence of IAV in cells including $CD169^+$ MΦs, as well as a decreased overall viral load in the spleen (Figure 25a+b). The observed incomplete reduction of viral load in spleens after Sialidase treatment might be explained by either alternative cell entry, such as via micropinocytosis, or by binding to alternative receptors. SIGN-R1 (CD209b) has already been described as alternative IAV receptor on dendritic cells (Gonzalez et al. 2010). Interestingly, Freigang et al. described the capability of DCs to replicate pathogens even in the absence of their adequate receptors (Freigang et al. 2003). For example, they were able to show Polio virus (PV) accumulation in murine DCs in the absence of the PV receptor. Together, these published and presented data suggest two potential mechanisms for the critical engagement of DCs in the anti-viral response: on the one hand, DCs may represent specialized immune cells which are able to internalize pathogens without requiring the presence of an adequate receptor, and on the other hand, IAV entry into DCs might be performed via more yet undescribed receptors. The dependency on specific receptor expression for IAV entry into DCs will have to be further evaluated.

5.2.2. IAV spread within the spleen

Marginal zone macrophages in the spleen are the first line of defense and the first cell type being infected upon pathogen encounter via the bloodstream (Seiler et al. 1997; Gupta et al. 2016). To analyze the spread of IAV particles within lymphoid organs after such infection, we treated mice with Oseltamivir. The drug Oseltamivir, also known as Tamiflu, is a broadly used IAV therapeutic. Mechanistically, Oseltamivir inhibits the enzymatic activity of the IAV NA proteins of newly formed IAV particles. Usually during virus replication, after HA and NA association with lipid rafts on the cell membrane and packaging of the viral components, the virus is released by the enzymatic activity of the protein NA. IAV NA cleaves sialic acids from the host cell and glycoproteins on the virus particles to allow virus release from the cell membrane. In the presence of Oseltamivir, the NA dependent cleavage is suppressed and IAV particles are not released from the cell membrane (Gubareva, Kaiser, and Hayden 2000). We showed that Oseltamivir treatment lowers the presence of IAV particles to some extent in macrophages and dendritic cells in the spleen of mice (Figure 27a). The highest decrease was observed for $CD169^+$ macrophages and $CD11c^+CD8^+$ DCs and was associated with significantly decreased IAV load (Figure 27b). Further infection of neighboring $CD169^+$ macrophages as well as subsequent infection of $CD11c^+CD8^+$ DCs is thereof prevented in the

presence of Oseltamivir because newly formed IAV particles are not released from cells. $CD11c^+CD8^-CD4^-$ and $CD11c^+CD4^+$ DCs did not show high numbers of IAV particles after infection (Figure 25a, Figure 27a), which was also not altered after Oseltamivir treatment. In summary, the primary inoculum of virus particles is indeed taken up by $CD169^+$ macrophages, confirming the critical role of these cells to encounter virus early upon infection. The reduction of IAV infected $CD169^+$ MΦs and $CD11c^+CD8^+$ DCs subsequent Oseltamivir treatment indicates that *de novo* synthesized and released IAV particles in these cell types might infect neighboring $CD169^+$ MΦs and $CD11c^+CD8^+$ DCs.

5.2.3. Impact of IAV uptake and replication in secondary lymphoid tissue on innate immune response

We observed a SA-dependent IAV uptake into dendritic cells and macrophages of the spleen upon infection, and further evaluated the consequences of infection of these cells in SLO on the initiation of an anti-viral innate immune response. Contingent to the decreased viral load in the spleen after Sialidase treatment, we observed a strongly reduced innate immune activation (Figure 26). It was previously demonstrated that IAV is sensed via intracellular PRRs such as TLR3 and TLR7 (Iwasaki and Pillai 2014). Absence of viral particles should not result in activating these receptors which are expressed in intracellular compartments and might therefore impede the subsequent induction of type I IFNs (Figure 26). However, the reduction of the overall viral load by Oseltamivir treatment did not severely alter the innate immune response (Figure 28a+b). Oseltamivir does not repress entry into the cell or viral replication, whereby early activation of PRRs is not altered. Therefore, in Oseltamivir treated animals, the expression of the type I interferons *Ifna4* and *Ifnb1* was comparable to non-treated animals. It is known that these interferon subtypes are very early induced upon infection via the IRF3/IRF7 signaling pathway in non-DC cell types (Hata et al. 2001; Civas et al. 2002; Tailor et al. 2007). Further, IFNα levels in serum of Oseltamivir treated IAV infected mice was not reduced which can be explained by an IAV mediated induction of the secretion of type I IFNs and subsequent paracrine signaling, which enhances IFN response subsequent to viral infection (Patil et al. 2015). We conclude that the initial IAV infection in the spleen initiates the induction of early interferons, whereas acceleration of viral load and subsequent enhancement of the interferon response is absent at this time point.

Furthermore, we also observed that the intracellular replication and sensing of IAV particles in primary infected cells impacts the strength of the consecutive innate immune repose. Mice

infected with UV-inactivated IAV showed a significant reduction in the expression of *Ifna4* and *Ifnb1* (Figure 29a). This extends our previous observation and demonstrates that in addition to $CD169^+$ macrophages and DCs also replication of IAV in primary infected cells is essential to drive innate immunity.

5.2.4. Enforced virus replication is essential for IAV immunity

We demonstrated that active IAV replication in the spleen is essential to induce a strong anti-viral innate immune response. IFN type I induction is crucial to limit and control IAV replication and to regulate viral tissue tropism (Londrigan et al. 2020; Ida-Hosonuma et al. 2005). Indeed, infection of $Ifnar^{-/-}$ mice, not capable to mount an anti-viral type I interferon response, with IAV showed a widespread virus distribution in the spleen (Figure 30a). However, in the absence of IFNAR signaling, presence of IAV particles was not strongly increased in $CD169^+$ macrophages and dendritic cells (Figure 30b). This indicates that already under wildtype conditions $CD169^+$ macrophages and DCs may have specialized mechanisms to suppress type I interferon signaling and thereof decrease the anti-viral effects of type I interferon on IAV replication. It is known that $CD169^+$ macrophages and DCs express high constitutive levels of the type I IFN signaling regulator USP18 which promotes replication of viruses in these cells (Honke et al. 2011; Honke et al. 2013; Friedrich et al. 2020). Indeed, expression of USP18 is essential in the spleen to enforce IAV replication after systemic application (Figure 31). We further demonstrated that the presence of USP18 highly enhances the type IFN response after systemic IAV application (Figure 32a+b), representing an explanation for the relative insensitivity of $CD169^+$ macrophages and DCs towards the absence of IFNAR.

DCs play a critical role at the interface of innate and anti-viral T cell responses, and we further analyzed if active IAV replication is not only essential to induce innate immunity, but also to initiate an anti-viral T cell response (Sallusto and Lanzavecchia 2002). Indeed, our findings demonstrate that EVR in $CD169^+$ macrophages and DCs in the spleen is of critical importance to induce an efficient anti-IAV T cell response (Figure 32c). T cells are known to play a major role in IAV control in mice (Bender et al. 1992). In line, we demonstrated that enforced IAV replication in spleen is essential to enhance anti-viral CD8 T cell response against IAV (Figure 32c). We therefore hypothesize that antigen presentation from DCs to T cells is more efficient in control compared to $CAG^+Usp18^{fl/fl}$ mice due to the increased presence of IAV antigens which combines with an enhanced release of cytokines, such as type I IFNs. Therefore, EVR is essential not only to boost innate but also adaptive immunity.

To further verify that EVR is also a mechanism to boost immunity in natural IAV infection, we infected control mice intranasally with IAV and imaged the presence of viral particles via histological analysis (Figure 33). Indeed, we detected IAV particles in DCs of lung draining lymph nodes. It is known that these lymph nodes are essential to induce anti-viral IAV T cell mediated responses (del Rio et al. 2007; Dolfi et al. 2011). In summary, we demonstrate here that USP18 mediated EVR of IAV particles in specialized DCs and macrophages of secondary lymphoid tissues is essential to strengthen innate immunity and provide sufficient amounts of antigen to present to T cells to induce an efficient adaptive immune response.

5.3. EVR as central mechanism in host defense

Over the last decades, Ebola virus as well as Influenza virus outbreaks represented a great risk to public health. Many viral infections can be cleared with the help of the body's own immune system, but some epidemic and pandemic outbreaks show the urgent need for effective vaccines. The immune response to live attenuated, replicating viruses and replication competent viral vaccines must be strictly regulated to counterbalance adverse and beneficial aspects. After infection of control mice with VSV or VSV-EBOV and IAV virus replication was restricted to specialized immune cells, in particular DCs and $CD169^{+}$ macrophages. Viral entry into these cells was influenced by their natural tropism to the viral entry receptor or dependent of cell specific mechanisms. Suppression of the interferon signaling in these cells by constitutive expression of high levels of USP18 enhanced viral replication. Consequently, USP18 mediated EVR boosted innate and adaptive immunity after viral infection.

In summary, using VSV-EBOV as model vaccine for replication competent vector vaccines (Chapter 1) and IAV as model for natural infections (Chapter 2), we were able to conclusively show that EVR is a central mechanism in immune regulation upon virus infection, and USP18 plays a critical role in this mechanism of virus control (Figure 34).

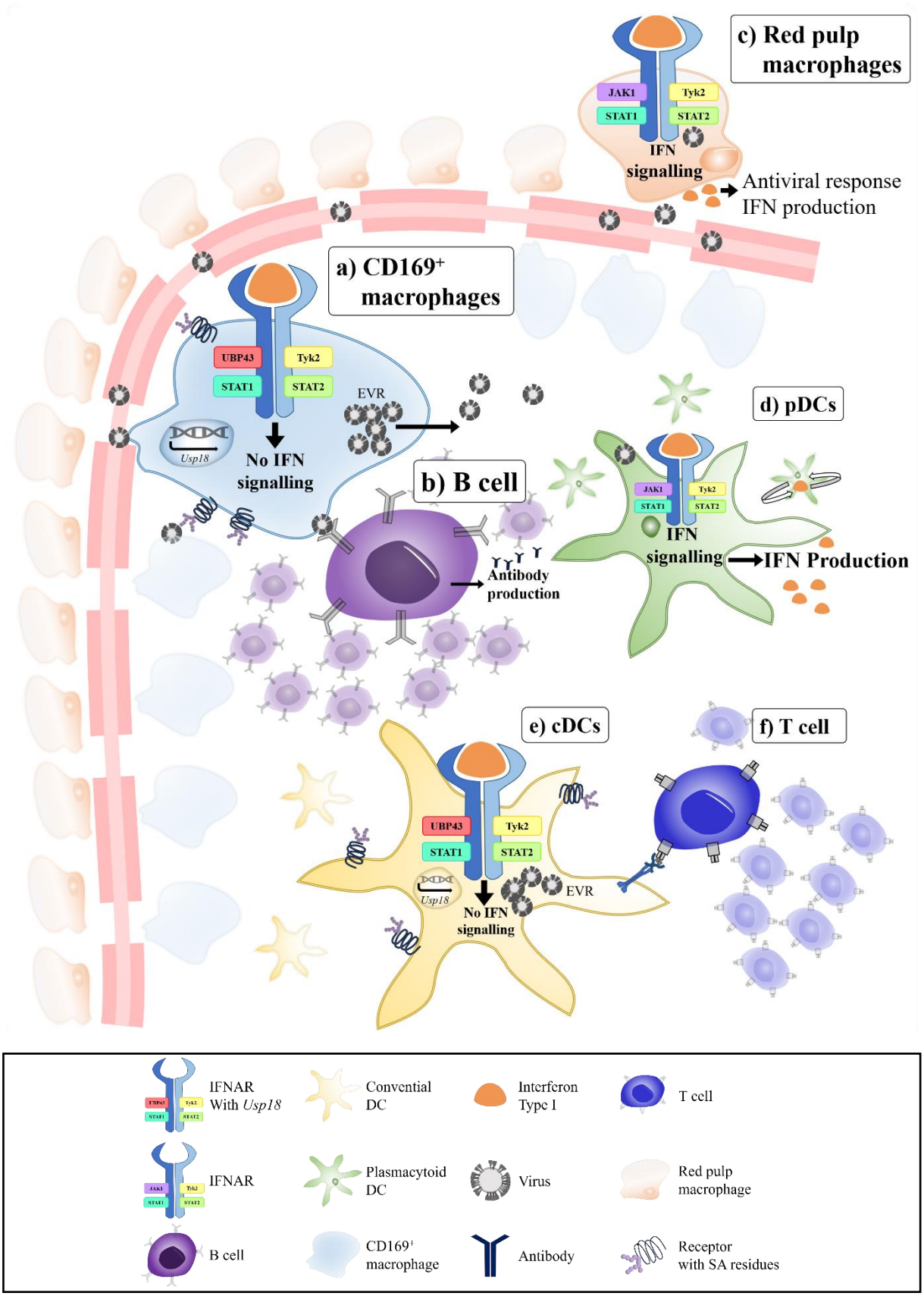

Figure 34: Lymphatic system specific virus replication

Virus replication in secondary lymphatic organs is essential for the initiation of an anti-viral immune response. Virus reaches secondary lymphatic organs via blood vessels. CD169^{+} macrophages **a)** display crucial gatekeepers and are strategically placed at the end of small blood conduits. They take up viruses such as VSV, VSV-EBOV

and IAV via unspecific entry mechanisms or receptor binding. Due to their high constitutive expression of USP18 interferon signaling via IFNAR is prevented, and virus can replicate without limitation. This process known as enforced virus replication (EVR) ensures appropriate antigen production even for viruses with low replication capacity. Viral antigens are subsequently presented to B cells **b)**, which initiate anti-viral antibody production. In addition, red pulp macrophages **c** are infected with virus, but unlike $CD169^{+}$ macrophages, they do not constitutively express high levels of USP18. Upon activation of innate immune signaling, e.g. via TLRs, red pulp macrophages induce interferon production and an anti-viral status within the cell. The other major cell type which is involved in interferon production upon virus infection are plasmacytoid DCs **d)**. pDCs produce massive amounts of IFN type I via the INFAR activation. **e)** Another subset of DCs, conventional DCs are similar to $CD169^{+}$ macrophages characterized by their high constitutive expression of USP18. cDCs take up and replicate virus to finally present antigens to T cells. They also play a major role in the induction of type I IFNs.

6. Summary

Cells of the immune system build the first line of defense against invading pathogens such as viruses. Virus replication in various cells initiates the induction of an interferon dependent, anti-viral immune response e.g., by activating pattern recognition receptors (PRRs) such as Toll-like receptors. The anti-viral status in these cells usually represses viral replication and prevents viral spread and a fatal outcome of the infection. Strikingly, under normal conditions, specialized cells of secondary lymphoid organs (SLOs) display enhanced virus replication. These cells, mainly marginal zone CD169^{+} macrophages and dendritic cells (DCs), express high constitutive levels of the interferon signaling repressor USP18. USP18 substitutes for JAK1 at the interferon-α/β receptor (IFNAR) and thereby decelerates the anti-viral interferon signaling and promotes virus replication. This mechanism known as enforced virus replication (EVR) was shown to be essential in the control of VSV infection by the production of sufficient amounts of virus antigen to enhance activation of innate and adaptive immunity. The influence of USP18 mediated EVR on the outcome of immunization with a live attenuated virus vaccine or other natural virus infections remained yet to be unknown.

Ebola viruses are endemic to Africa, and mainly spread in humans through direct exchange of body fluids. Ebola virus infection is often fatal before the virus has had a chance to broadly spread. The first Ebola virus vaccine (Ervebo, VSV-EBOV) was approved by the U.S. Food and Drug Administration (FDA) in 2019 and has been found to be safe and protective against Zaire Ebola virus, which has caused the largest and most deadly Ebola virus outbreaks to date. In the first part of this work, we investigated the influence of EVR on the outcome of immunization with the live attenuated Ebola virus vaccine VSV-EBOV. We established a mouse model carrying a CD169^{+} cell specific gene knockout of *Usp18* (*CD169*-Cre$^{+/ki}$ x *Usp18*$^{fl/fl}$), which circumvents the disadvantageous effects of conventional USP18 knockouts on the development of distinct cell subsets. VSV infection in control mice demonstrated an increase of viral antigen in CD169^{+} macrophages upon systemic and local virus infection dependent on USP18 expression. USP18 deletion in CD169^{+} macrophages of *CD169*-Cre$^{+/ki}$ x *Usp18*$^{fl/fl}$ mice decreased type I interferon production and enhanced susceptibility to neurovirulence and lethality of VSV infection, which was strongly associated with poor induction of protective VSV neutralizing antibodies. Using the clinically available attenuated VSV-EBOV vaccine (Ervebo) we demonstrated that USP18 driven EVR is essential to amplify VSV-EBOV virus antigen in CD169^{+} macrophages. Such an enforced VSV-EBOV replication in control mice induced a significantly increased type I interferon dependent innate immune response compared to *CD169*-Cre$^{+/ki}$ x *Usp18*$^{fl/fl}$ mice, which finally was necessary to introduce

a protective immune status by the induction of a strong Ebola virus glycoprotein neutralizing antibody response.

EVR was yet shown to be essential for the control of a VSV infection, but it is unclear if EVR also plays a role in virus infections relevant for humans. Therefore, in the second part, we investigated the mechanism and impact of immune cell specific Influenza A virus (IAV) replication in SLOs on the activation of anti-viral immunity. Upon systemic IAV infection, we demonstrated receptor mediated IAV uptake into dendritic cells (DCs) and $CD169^{+}$ macrophages of the spleen. Repression of viral progression by UV inactivation of IAV, receptor removal and viral spread inhibition all significantly impaired the induction of anti-IAV innate and adaptive immunity. Expression of the interferon signaling inhibitor USP18 was essential to drive IAV replication in $CD169^{+}$ macrophages and DCs. We also demonstrated that USP18 dependent EVR of IAV in secondary lymphoid organs contributed considerably to the activation of an innate type I interferon driven and adaptive anti-viral T cell immune response.

Taken together, we demonstrated for the first time that USP18 mediated virus replication in specialized immune cells of SLOs is an essential mechanism to induce protective immune status after the immunization with live attenuated VSV-EBOV vaccine and natural IAV infection.

7. Zusammenfassung

Die Zellen des Immunsystems die erste Barriere gegen in den Körper eindringende Pathogene wie Viren. Die Virusreplikation in unterschiedlichen Zellen initiiert die Induktion einer Interferon-abhängigen, angeborenen Immunantwort beispielsweise durch die Aktivierung von Pattern Recognition Rezeptoren (PRRs) wie Toll-like Rezeptoren. Der anti-virale Status dieser Zellen unterdrückt für gewöhnlich die Virusreplikation und verhindert so die Ausbreitung des Virus sowie einen letalen Ausgang der Infektion. Interessanter Weise zeigen spezialisierte Zellen in sekundären lymphoiden Organen (SLO) unter normalen Konditionen verstärkte Virusreplikation. Diese Zellen, hauptsächlich $CD169^{+}$ Marginalzonenmakrophagen und Dendritische Zellen, exprimieren konstitutiv hohe Level des Interferon-Signalweg Inhibitors USP18. USP18 ersetzt JAK1 am Interferon-α/β Rezeptor (IFNAR), verlangsamt so den Interferon-Signalweg und begünstigt die Virusreplikation. Es wurde gezeigt, dass dieser Mechanismus, bekannt als forcierte Virusreplikation (FVR), essenziell für die Kontrolle einer VSV Infektion, durch die Generierung ausreichender Virusantigenmengen für die Verstärkung der angeborenen und adaptiven Immunantwort, ist. Der Einfluss der USP18 -abhängigen FVR auf das Ergebnis der Immunisierung mit einem lebend-attenuierten Virus-Vakzin oder natürlich vorkommenden Virusinfektionen war bisher nicht erforscht.

Ebolaviren sind in Afrika endemisch und verbreiten sich hauptsächlich im Menschen durch direkten Austausch von Körperflüssigkeiten. Ebolavirus Infektionen sind häufig fatal, bevor das Virus sich verbreiten kann. Der erste Ebolavirus Impfstoff (Ervebo, VSV-EBOV), wurde durch die U.S. Food and Drug Administration (FDA) 2019 zugelassen und zeigte sich als sicher und protektiv gegen das Zaire Ebolavirus, welches den bisher größten und fatalsten Ebolavirus Ausbruch verursacht hat. Im ersten Teil dieser Arbeit wurde der Einfluss FVR auf das Ergebnis der Immunisierung mit dem lebend-attenuierten Ebolavirus Impfstoff VSV-EBOV untersucht. Es wurde ein Maus-Model mit einem $CD169^{+}$ zellspezifischen *Usp18*-Gen-Knockout etabliert (*CD169*-$Cre^{+/ki}$ x *Usp18*$^{fl/fl}$), durch welches sich die nachteiligen Effekte eines konventionellen *Usp18*-Gen-Knockout auf die Zellentwicklung spezifischer Immunzellen umgehen lassen konnten. Systemische und lokale VSV Infektionen führten in diesem Maus-Model zu einer USP18-abhängigen Erhöhung von viralen Antigenen in $CD169^{+}$ Makrophagen. Die Deletion von USP18 in $CD169^{+}$ Makrophagen der *CD169*-$Cre^{+/ki}$ x *Usp18*$^{fl/fl}$ Mäuse verringerte die Typ I Interferon Produktion und erhöhte die Suszeptibilität gegenüber der Neurovirulenz und Letalität einer VSV Infektion, was darüber hinaus mit einer schwachen Induktion von VSV neutralisierenden Antikörpern assoziiert war. Durch die Verwendung des in klinischer Anwendung befindlichen Ebolavirus Vakzins VSV-EBOV (Ervebo) wurde gezeigt, dass

USP18-mediierte FVR essenziell für die Amplifikation von VSV-EBOV in CD169^{+} Makrophagen ist. Diese forcierte VSV-EBOV Replikation induzierte in Kontrollmäusen eine signifikant erhöhte Typ I Interferon-abhängige, angeborene Immunantwort im Vergleich zu *CD169*-Cre$^{+/ki}$ x *Usp18*$^{fl/fl}$ Mäusen, was schlussendlich unabdingbar für die Ausbildung eines protektiven Immunstatus, durch die Induktion einer starken Ebolavirus Glykoprotein neutralisierenden Antikörperantwort, war.

Die FVR wurde als essenziell für die Kontrolle einer VSV Infektion gezeigt, jedoch ist der Einfluss der FVR auf Infektionen mit relevanten Humanpathogenen unklar. Aufgrund dessen, wurde im zweiten Teil dieser Arbeit der Mechanismen und Einfluss von Immunzell-spezifischer Influenza A Virus (IAV) Replikation in SLO auf die Aktivierung der anti-viralen Immunantwort untersucht. Durch eine systemische IAV Infektion wurde die Rezeptor-mediierte Aufnahme von IAV in Dendritische Zellen (DZ) und CD169^{+} Makrophagen der Milz gezeigt. Durch die Repression der viralen Progression durch UV-Inaktivierung des IAV, sowie das Entfernen des viralen Eintritt-Rezeptors und die Inhibition der viralen Ausbreitung wurde die Induktion einer gegen IAV gerichteten angeborenen und adaptiven Immunantwort stark beeinflusst. Die Expression des Interferon-Signalweg Inhibitors USP18 war essenziell, um die IAV Replikation CD169^{+} Makrophagen und DZ zu begünstigen. Weiterhin wurde gezeigt, dass USP18-mediierte FVR von IAV in sekundären lymphoiden Organen maßgeblich zur Aktivierung einer angeborenen Typ I Interferon abhängigen und adaptiven anti-virale T Zell Immunantwort beiträgt.

Zusammenfassend wurde zum ersten Mal gezeigt, dass eine USP18-abhängige Virusreplikation in spezialisierten Immunzellen sekundärer lymphoider Organe ein essenzieller Mechanismus zur Induktion eines protektiven Immunstatus nach einer Immunisierung mit der lebend-attenuierten Vakzine VSV-EBOV, sowie für natürliche Influenza Infektionen ist.

8. Outlook

Over the last decades replication competent, virus-based drugs have risen for different therapeutic fields. Especially for the therapy of malignant diseases, replication competent oncolytic viruses (OV) showed to have a high treatment potential. On the one hand, OVs destruct infected tumor cells by their lytic replication cycle, on the other hand OV therapy triggers the induction of anti-viral and antitumoral T cells. Anti-viral T cells eradicate OV infected tumor cells by direct lysis. Expansion of anti-tumoral T cells is favored by the expression of tumor specific epitopes by the OV (e.g., HVP epitope E7E6 expression). Especially OV approaches using replication competent VSV or LCMV viruses as backbones, like VSV-GP or TT1-E7E6 displayed great antitumoral activity in *in vivo* mouse models. Unlike their wildtype virus counterparts, these chimeric OVs are highly attenuated (Muik et al. 2011; Schmidt et al. 2020). Therefore, EVR of OVs in SLOs might play an essential role in mediating and enhancing replication, and therefore driving anti-viral and anti-tumoral T cell responses.

$CD169^+$ macrophages, which are essential to promote EVR by their constitutive high expression of USP18, have been shown to directly influence tumor progression. Deletion of $CD169^+$ macrophages in tumor-draining LNs enhances tumor progression and metastasis formation in a breast cancer model in a B cell dependent fashion (Tacconi et al. 2021). Therefore, it is tempting to speculate from our data that USP18 is also a critical factor in the induction of an efficient anti-tumoral immune response by OVs, and it is of high interest to evaluate the role of USP18 mediated EVR in $CD169^+$ macrophages and DCs in the induction of antitumoral effects upon OV therapy.

Besides virus-based tumor therapy approaches, the latest developments in the global SARS-CoV-2 pandemic, but also the yearly recurring Influenza virus epidemics, clearly show the urge for the development of novel vaccination approaches. The replication competent VSV-based SARS-CoV-2 vaccine VSV-ΔG-spike is one of the latest inventions in the field of SARS-CoV-2 vaccines (Yahalom-Ronen et al. 2020). We here underlined the necessity of USP18 driven EVR in the induction of a protective vaccination status after virus immunization, and our findings may further contribute to a better understanding and manipulation of the host immune response to a live attenuated vaccine such as VSV-ΔG-spike.

Interestingly, natural virus infections were associated with a favorable progression of malignant disease in some cases. For example, a rare case of complete tumor remission was observed in a patient with a follicular lymphoma infected with SARS-CoV-2 (Sollini et al. 2021). Also, Influenza virus infections showed beneficial effects on tumor progression in patients as well as

in mouse models (Ono et al. 1955; Lindenmann and Klein 1967; Kasloff et al. 2014). As the wildtype variants of such viruses usually induce strong side effects, attenuated viruses are currently in preclinical development. Therefore, it may be interesting to investigate if the use of other attenuated virus variants, such as the VSV-ΔG-spike vaccine, display comparable antitumoral efficacy. Moreover, such models could be used to more universally demonstrate that in virus mediated tumor therapy therapeutic success is dependent on EVR.

Overall, we demonstrated that USP18 mediated EVR represents a significant component in the induction of immunity to replication competent virus vaccines and natural virus infections. Our work shed light on the potential to further investigate the contribution of EVR to the efficacy of viral antitumoral and vaccine therapeutics, for a better understanding of the mechanisms driving efficient anti-viral and anti-tumoral immune responses in the treatment of cancer patients or populations especially vulnerable to specific virus infections.

9. List of abbreviations

µ	micron
µl	microliter
AID	activation-induced cytidine deaminase
APC	antigen presenting cell
APC	ammonium persulfate
BCL2	B-cell lymphoma 2
BCR	B cell receptor
BHK	baby hamster kidney
Bim	B cell lymphoma 2–interacting mediator
BMDC	bone marrow derived dendritic cell
BMSC	bone marrow stromal cell
bp	base pair
BSA	bovine serum albumin
CARD	caspase activation and recruitment domain
CCR7	C-C chemokine receptor type 7
CD	cluster of differentiation
cDC	Conventional dendritic cell
cDNA	complementary DNA
CLR	C-type lectin receptors
CMI	cell-mediated immunity
CNS	central nervous system
COVID-19	Coronavirus Disease 2019
Cxcl11	C-X-C motif chemokine 11
DAMP	danger associated molecular pattern
DC	dendritic cell
DEPC	diethylpyrocarbonate
dLN	draining lymph node
DMEM	Dulbecco's Modified Eagle's Medium
DN	double negative
DNA	deoxyribonucleic acid
dNTPs	deoxyribonucleoside triphosphate
DP	double positive

dsRNA	double-stranded RNA
EBF	early B cell factor 1
EDTA	ethylenediaminetetraacetate
ELISA	enzyme-linked Immunosorbent Assay
EVR	enforced virus replication
FACS	fluorescence-activated cell sorting
FCS	fetal calf serum
FDA	U.S. Food and Drug Administration
Flt3-L	Fms-like tyrosine kinase 3 ligand
G	glycoprotein
GAPDH	glyceraldehyde 3-phosphate dehydrogenase
GAS	gamma-activated sequences
GM-CSF	granulocyte-macrophage colony-stimulating factor
GTP	guanosine triphosphate
HA	hemagglutinin
HSC	hematopoietic stem cell
i.m.	intramuscular
i.v.	intravenous
IAV	influenza A virus
ICAM1	intercellular adhesion molecule 1
iDC	immature dendritic cell
IFN	interferon
IFNAR	interferon-α/β receptor
IKROS	IKAROS family zinc finger 1
IL	interleukin
IMDM	Iscove's Modified Dulbecco Media
IPS-1	IFN-β-promoter stimulator 1
IRAK	IL-1R-associated kinase
IRF	interferon regulatory factor
ISG	interferon stimulated gene
ISRE	interferon-sensitive response element
JAK1	Janus kinase 1
LAV	live attenuated vaccine

LCMV	lymphocytic choriomeningitis virus
LFA-1	lymphocyte function-associated antigen 1
LGP2	laboratory of genetics and physiology 2
log	logarithm
LP	large protein
LPS	lipopolysaccharide
LT	lymphotoxin
M	Matrix protein
MACS	Magnetic Activated Cell Sorting
MAPK	mitogen-activated protein kinase
MDA5	melanoma differentiation-associated gene 5
MDCK II	Madin-Darby canine kidney II cells
MFI	Median fluorescence intensity
mg	milligram
MHC	major histocompatibility complex
ml	milliliter
MOI	multiplicity of infection
Mx1	MX Dynamin Like GTPase 1
MyD88	myeloid differentiation primary response gene 88
MZ	marginal zone
MΦ	macrophage
n.s.	not significant
NA	neuraminidase
NF-κB	nuclear factor 'kappa-light-chain-enhancer' of activated B-cells
ng	nanogram
NK	natural killer
NLR	nucleotide-binding oligomerization domain-like receptors
NOD	nucleotide-binding oligomerization domain
NP	nucleoprotein
O.C.T.	optimal cutting temperature
OAS1	2´-5´-oligoadenylate synthase1
p	p value
p.i.	post infection

PAMP	pathogen associated molecular pattern
PBS	phosphate buffered saline
PCR	polymerase chain reaction
pDC	plasmacytoid DC
PFU	plaque forming unit
PR8	Influenza A H1N1 (A/Puerto Rico/8/34)
PRR	pattern recognition receptor
PSG	L-Glutamine-Penicillin-Streptomycin
PV	Polio virus
qRT-PCR	quantitative reverse transcriptase polymerase chain reaction
RAG	recombination activating gene
RIG-1	retinoic acid inducible gene I
RLR	retinoic acid-inducible gene 1 (RIG-1) like receptor
RNA	ribonucleic acid
RNP	ribonucleoprotein
rpm	rotation per minute
RSS	recombination signal sequence
s.c.	subcutaneous
S.E.M.	standard error of the mean
SA	Sialidase
SARS-CoV-2	severe acute respiratory syndrome coronavirus type 2
SCF	stem cell factor
SDS-PAGE	sodium dodecyl sulfate polyacrylamide gel electrophoresis
SLO	secondary lymphoid organ
SP	single positive
ssRNA	single-stranded RNA
STAT	signal transducer and activator of transcription
TCR	T cell receptor
TD	T cell dependent
TdT	terminal deoxynucleotidyl transferase
TEMED	Tetramethylethylenediamine
TI	T cell independent

TLR	Toll-like receptor
TNFα	tumor necrosis factor alpha
TORCH	(T)oxoplasmosis, (O)ther Agents, (R)ubella, (C)ytomegalovirus, and (H)erpes Simplex
TRIF	TIR-domain-containing adapter-inducing interferon-β
Tyk2	tyrosine kinase 2
USP18	ubiquitin specific peptidase 18
VCAM1	Vascular cell adhesion protein 1
VLA4	very late antigen-4
VLP	virus like particle
vRNP	viral ribonucleoprotein
VSV	vesicular stomatitis virus
VSV-EBOV	vesicular stomatitis virus vaccine expressing the Ebola virus glycoprotein
VSV-G	VSV glycoprotein
XRCC1	X-ray repair cross-complementing protein 1

10. List of Figures and Tables

10.1. List of Figures

10.2. List of Tables

11. Literature

Ahmed, M., T. R. Marino, S. Puckett, N. D. Kock, and D. S. Lyles. 2008. 'Immune response in the absence of neurovirulence in mice infected with m protein mutant vesicular stomatitis virus', *Journal of virology*, 82: 9273-7.

Akira, S., S. Uematsu, and O. Takeuchi. 2006. 'Pathogen recognition and innate immunity', *Cell*, 124: 783-801.

Arias, C. F., M. Escalera-Zamudio, L. Soto-Del Rio Mde, A. G. Cobian-Guemes, P. Isa, and S. Lopez. 2009. 'Molecular anatomy of 2009 influenza virus A (H1N1)', *Arch Med Res*, 40: 643-54.

B., Alberts, Johnson A., and Lewis J. 2002. 'B Cells and Antibodies.' in, *Molecular Biology of the Cell* (Garland Science).

Baccala, R., D. H. Kono, and A. N. Theofilopoulos. 2005. 'Interferons as pathogenic effectors in autoimmunity', *Immunol Rev*, 204: 9-26.

Bachmann, M. F., B. Odermatt, H. Hengartner, and R. M. Zinkernagel. 1996. 'Induction of long-lived germinal centers associated with persisting antigen after viral infection', *The Journal of experimental medicine*, 183: 2259-69.

Basters, A., K. P. Knobeloch, and G. Fritz. 2018. 'How USP18 deals with ISG15-modified proteins: structural basis for the specificity of the protease', *FEBS J*, 285: 1024-29.

Bender, B. S., T. Croghan, L. Zhang, and P. A. Small, Jr. 1992. 'Transgenic mice lacking class I major histocompatibility complex-restricted T cells have delayed viral clearance and increased mortality after influenza virus challenge', *The Journal of experimental medicine*, 175: 1143-5.

Bird, N. L., M. R. Olson, A. C. Hurt, C. M. Oshansky, D. Y. Oh, P. C. Reading, B. Y. Chua, Y. Sun, L. Tang, A. Handel, D. C. Jackson, S. J. Turner, P. G. Thomas, and K. Kedzierska. 2015. 'Oseltamivir Prophylaxis Reduces Inflammation and Facilitates Establishment of Cross-Strain Protective T Cell Memory to Influenza Viruses', *PLoS One*, 10: e0129768.

Bresk, C. A., T. Hofer, S. Wilmschen, M. Krismer, A. Beierfuss, G. Effantin, W. Weissenhorn, M. J. Hogan, A. P. O. Jordan, R. S. Gelman, D. C. Montefiori, H. X. Liao, J. E. Schmitz, B. F. Haynes, D. von Laer, and J. Kimpel. 2019. 'Induction of Tier 1 HIV Neutralizing Antibodies by Envelope Trimers Incorporated into a Replication Competent Vesicular Stomatitis Virus Vector', *Viruses*, 11.

Case, J. B., P. W. Rothlauf, R. E. Chen, N. M. Kafai, J. M. Fox, B. K. Smith, S. Shrihari, B. T. McCune, I. B. Harvey, S. P. Keeler, L. M. Bloyet, H. Zhao, M. Ma, L. J. Adams, E. S.

Winkler, M. J. Holtzman, D. H. Fremont, S. P. J. Whelan, and M. S. Diamond. 2020. 'Replication-Competent Vesicular Stomatitis Virus Vaccine Vector Protects against SARS-CoV-2-Mediated Pathogenesis in Mice', *Cell Host Microbe*, 28: 465-74 e4.

Cembrzynska-Nowak, M., J. Liebhart, M. Bienkowska-Haba, E. Liebhart, A. Kulczak, I. Siemieniec, R. Dobek, A. Dor, W. Barg, and B. Panaszek. 2005. 'The overproduction of nitric oxide associated with neutrophilic predominance is relevant to airway mycotic infections in asthmatics undergoing prolonged glucocorticoid treatment', *Cell Mol Biol Lett*, 10: 677-87.

Chatziandreou, N., Y. Farsakoglu, M. Palomino-Segura, R. D'Antuono, D. U. Pizzagalli, F. Sallusto, V. Lukacs-Kornek, M. Uguccioni, D. Corti, S. J. Turley, A. Lanzavecchia, M. C. Carroll, and S. F. Gonzalez. 2017. 'Macrophage Death following Influenza Vaccination Initiates the Inflammatory Response that Promotes Dendritic Cell Function in the Draining Lymph Node', *Cell Rep*, 18: 2427-40.

Chavez-Galan, L., M. L. Olleros, D. Vesin, and I. Garcia. 2015. 'Much More than M1 and M2 Macrophages, There are also CD169(+) and TCR(+) Macrophages', *Frontiers in immunology*, 6: 263.

Chen, X., S. Liu, M. U. Goraya, M. Maarouf, S. Huang, and J. L. Chen. 2018. 'Host Immune Response to Influenza A Virus Infection', *Frontiers in immunology*, 9: 320.

Chiu, C., A. H. Ellebedy, J. Wrammert, and R. Ahmed. 2015. 'B cell responses to influenza infection and vaccination', *Curr Top Microbiol Immunol*, 386: 381-98.

Chutinimitkul, S., D. van Riel, V. J. Munster, J. M. van den Brand, G. F. Rimmelzwaan, T. Kuiken, A. D. Osterhaus, R. A. Fouchier, and E. de Wit. 2010. 'In vitro assessment of attachment pattern and replication efficiency of H5N1 influenza A viruses with altered receptor specificity', *Journal of virology*, 84: 6825-33.

Civas, A., M. L. Island, P. Genin, P. Morin, and S. Navarro. 2002. 'Regulation of virus-induced interferon-A genes', *Biochimie*, 84: 643-54.

Clarke, D. K., R. M. Hendry, V. Singh, J. K. Rose, S. J. Seligman, B. Klug, S. Kochhar, L. M. Mac, B. Carbery, R. T. Chen, and Group Brighton Collaboration Viral Vector Vaccines Safety Working. 2016. 'Live virus vaccines based on a vesicular stomatitis virus (VSV) backbone: Standardized template with key considerations for a risk/benefit assessment', *Vaccine*, 34: 6597-609.

Cong, X. L., M. C. Lo, B. A. Reuter, M. Yan, J. B. Fan, and D. E. Zhang. 2012. 'Usp18 promotes conventional CD11b+ dendritic cell development', *J Immunol*, 188: 4776-81.

Crocker, P. R., and S. Gordon. 1986. 'Properties and distribution of a lectin-like hemagglutinin differentially expressed by murine stromal tissue macrophages', *The Journal of experimental medicine*, 164: 1862-75.

Curry, J. D., J. K. Geier, and M. S. Schlissel. 2005. 'Single-strand recombination signal sequence nicks in vivo: evidence for a capture model of synapsis', *Nat Immunol*, 6: 1272-9.

Dagenais-Lussier, X., H. Loucif, H. Cadorel, J. Blumberger, S. Isnard, M. G. Bego, E. A. Cohen, J. P. Routy, J. van Grevenynghe, and Group Montreal Primary Infection Study. 2019. 'USP18 is a significant driver of memory CD4 T-cell reduced viability caused by type I IFN signaling during primary HIV-1 infection', *PLoS Pathog*, 15: e1008060.

del Rio, M. L., J. I. Rodriguez-Barbosa, E. Kremmer, and R. Forster. 2007. 'CD103- and CD103+ bronchial lymph node dendritic cells are specialized in presenting and cross-presenting innocuous antigen to CD4+ and CD8+ T cells', *J Immunol*, 178: 6861-6.

den Haan, J. M., S. M. Lehar, and M. J. Bevan. 2000. 'CD8(+) but not CD8(-) dendritic cells cross-prime cytotoxic T cells in vivo', *The Journal of experimental medicine*, 192: 1685-96.

den Haan, J. M., and L. Martinez-Pomares. 2013. 'Macrophage heterogeneity in lymphoid tissues', *Semin Immunopathol*, 35: 541-52.

Der, S. D., A. Zhou, B. R. Williams, and R. H. Silverman. 1998. 'Identification of genes differentially regulated by interferon alpha, beta, or gamma using oligonucleotide arrays', *Proc Natl Acad Sci U S A*, 95: 15623-8.

Diebold, S. S., T. Kaisho, H. Hemmi, S. Akira, and C. Reis e Sousa. 2004. 'Innate antiviral responses by means of TLR7-mediated recognition of single-stranded RNA', *Science*, 303: 1529-31.

Dolfi, D. V., P. A. Duttagupta, A. C. Boesteanu, Y. M. Mueller, C. H. Oliai, A. B. Borowski, and P. D. Katsikis. 2011. 'Dendritic cells and CD28 costimulation are required to sustain virus-specific CD8+ T cell responses during the effector phase in vivo', *J Immunol*, 186: 4599-608.

Eloranta, M. L., and G. V. Alm. 1999. 'Splenic marginal metallophilic macrophages and marginal zone macrophages are the major interferon-alpha/beta producers in mice upon intravenous challenge with herpes simplex virus', *Scand J Immunol*, 49: 391-4.

Fink, K., K. S. Lang, N. Manjarrez-Orduno, T. Junt, B. M. Senn, M. Holdener, S. Akira, R. M. Zinkernagel, and H. Hengartner. 2006. 'Early type I interferon-mediated signals on B cells specifically enhance antiviral humoral responses', *Eur J Immunol*, 36: 2094-105.

Freigang, S., D. Egger, K. Bienz, H. Hengartner, and R. M. Zinkernagel. 2003. 'Endogenous neosynthesis vs. cross-presentation of viral antigens for cytotoxic T cell priming', *Proc Natl Acad Sci U S A*, 100: 13477-82.

Friedrich, S. K., R. Schmitz, M. Bergerhausen, J. Lang, L. B. Cham, V. Duhan, D. Haussinger, C. Hardt, M. Addo, M. Prinz, K. Asano, P. A. Lang, and K. S. Lang. 2020. 'Usp18 Expression in CD169(+) Macrophages is Important for Strong Immune Response after Vaccination with VSV-EBOV', *Vaccines (Basel)*, 8.

Fugmann, S. D., A. I. Lee, P. E. Shockett, I. J. Villey, and D. G. Schatz. 2000. 'The RAG proteins and V(D)J recombination: complexes, ends, and transposition', *Annu Rev Immunol*, 18: 495-527.

Garbutt, M., R. Liebscher, V. Wahl-Jensen, S. Jones, P. Moller, R. Wagner, V. Volchkov, H. D. Klenk, H. Feldmann, and U. Stroher. 2004. 'Properties of replication-competent vesicular stomatitis virus vectors expressing glycoproteins of filoviruses and arenaviruses', *Journal of virology*, 78: 5458-65.

Gautier, E. L., T. Shay, J. Miller, M. Greter, C. Jakubzick, S. Ivanov, J. Helft, A. Chow, K. G. Elpek, S. Gordonov, A. R. Mazloom, A. Ma'ayan, W. J. Chua, T. H. Hansen, S. J. Turley, M. Merad, G. J. Randolph, and Consortium Immunological Genome. 2012. 'Gene-expression profiles and transcriptional regulatory pathways that underlie the identity and diversity of mouse tissue macrophages', *Nat Immunol*, 13: 1118-28.

Geijtenbeek, T. B., and S. I. Gringhuis. 2009. 'Signalling through C-type lectin receptors: shaping immune responses', *Nat Rev Immunol*, 9: 465-79.

Geisbert, T. W., and H. Feldmann. 2011. 'Recombinant vesicular stomatitis virus-based vaccines against Ebola and Marburg virus infections', *The Journal of infectious diseases*, 204 Suppl 3: S1075-81.

Geissmann, F., M. G. Manz, S. Jung, M. H. Sieweke, M. Merad, and K. Ley. 2010. 'Development of monocytes, macrophages, and dendritic cells', *Science*, 327: 656-61.

Germain, R. N. 2002. 'T-cell development and the CD4-CD8 lineage decision', *Nat Rev Immunol*, 2: 309-22.

Glaser, L., J. Stevens, D. Zamarin, I. A. Wilson, A. Garcia-Sastre, T. M. Tumpey, C. F. Basler, J. K. Taubenberger, and P. Palese. 2005. 'A single amino acid substitution in 1918 influenza virus hemagglutinin changes receptor binding specificity', *Journal of virology*, 79: 11533-6.

Goldmann, T., N. Zeller, J. Raasch, K. Kierdorf, K. Frenzel, L. Ketscher, A. Basters, O. Staszewski, S. M. Brendecke, A. Spiess, T. L. Tay, C. Kreutz, J. Timmer, G. M. Mancini, T. Blank, G. Fritz, K. Biber, R. Lang, D. Malo, D. Merkler, M. Heikenwalder,

K. P. Knobeloch, and M. Prinz. 2015. 'USP18 lack in microglia causes destructive interferonopathy of the mouse brain', *The EMBO journal*, 34: 1612-29.

Gonzalez, S. F., V. Lukacs-Kornek, M. P. Kuligowski, L. A. Pitcher, S. E. Degn, Y. A. Kim, M. J. Cloninger, L. Martinez-Pomares, S. Gordon, S. J. Turley, and M. C. Carroll. 2010. 'Capture of influenza by medullary dendritic cells via SIGN-R1 is essential for humoral immunity in draining lymph nodes', *Nat Immunol*, 11: 427-34.

Gubareva, L. V., L. Kaiser, and F. G. Hayden. 2000. 'Influenza virus neuraminidase inhibitors', *Lancet*, 355: 827-35.

Guillot, L., R. Le Goffic, S. Bloch, N. Escriou, S. Akira, M. Chignard, and M. Si-Tahar. 2005. 'Involvement of toll-like receptor 3 in the immune response of lung epithelial cells to double-stranded RNA and influenza A virus', *J Biol Chem*, 280: 5571-80.

Gummuluru, S., N. G. Pina Ramirez, and H. Akiyama. 2014. 'CD169-dependent cell-associated HIV-1 transmission: a driver of virus dissemination', *The Journal of infectious diseases*, 210 Suppl 3: S641-7.

Gupta, P., S. M. Lai, J. Sheng, P. Tetlak, A. Balachander, C. Claser, L. Renia, K. Karjalainen, and C. Ruedl. 2016. 'Tissue-Resident CD169(+) Macrophages Form a Crucial Front Line against Plasmodium Infection', *Cell Rep*, 16: 1749-61.

Hand, T. W., and S. M. Kaech. 2009. 'Intrinsic and extrinsic control of effector T cell survival and memory T cell development', *Immunol Res*, 45: 46-61.

Hata, N., M. Sato, A. Takaoka, M. Asagiri, N. Tanaka, and T. Taniguchi. 2001. 'Constitutive IFN-alpha/beta signal for efficient IFN-alpha/beta gene induction by virus', *Biochem Biophys Res Commun*, 285: 518-25.

Hochrein, H., K. Shortman, D. Vremec, B. Scott, P. Hertzog, and M. O'Keeffe. 2001. 'Differential production of IL-12, IFN-alpha, and IFN-gamma by mouse dendritic cell subsets', *J Immunol*, 166: 5448-55.

Honke, N., N. Shaabani, G. Cadeddu, U. R. Sorg, D. E. Zhang, M. Trilling, K. Klingel, M. Sauter, R. Kandolf, N. Gailus, N. van Rooijen, C. Burkart, S. E. Baldus, M. Grusdat, M. Lohning, H. Hengel, K. Pfeffer, M. Tanaka, D. Haussinger, M. Recher, P. A. Lang, and K. S. Lang. 2011. 'Enforced viral replication activates adaptive immunity and is essential for the control of a cytopathic virus', *Nat Immunol*, 13: 51-7.

Honke, N., N. Shaabani, D. E. Zhang, C. Hardt, and K. S. Lang. 2016. 'Multiple functions of USP18', *Cell death & disease*, 7: e2444.

Honke, N., N. Shaabani, D. E. Zhang, G. Iliakis, H. C. Xu, D. Haussinger, M. Recher, M. Lohning, P. A. Lang, and K. S. Lang. 2013. 'Usp18 driven enforced viral replication in

dendritic cells contributes to break of immunological tolerance in autoimmune diabetes', *PLoS Pathog*, 9: e1003650.

Horimoto, T., and Y. Kawaoka. 1994. 'Reverse genetics provides direct evidence for a correlation of hemagglutinin cleavability and virulence of an avian influenza A virus', *Journal of virology*, 68: 3120-8.

Hu, X., C. Herrero, W. P. Li, T. T. Antoniv, E. Falck-Pedersen, A. E. Koch, J. M. Woods, G. K. Haines, and L. B. Ivashkiv. 2002. 'Sensitization of IFN-gamma Jak-STAT signaling during macrophage activation', *Nat Immunol*, 3: 859-66.

Hu, X., K. H. Park-Min, H. H. Ho, and L. B. Ivashkiv. 2005. 'IFN-gamma-primed macrophages exhibit increased CCR2-dependent migration and altered IFN-gamma responses mediated by Stat1', *J Immunol*, 175: 3637-47.

Iannacone, M., E. A. Moseman, E. Tonti, L. Bosurgi, T. Junt, S. E. Henrickson, S. P. Whelan, L. G. Guidotti, and U. H. von Andrian. 2010. 'Subcapsular sinus macrophages prevent CNS invasion on peripheral infection with a neurotropic virus', *Nature*, 465: 1079-83.

Ida-Hosonuma, M., T. Iwasaki, T. Yoshikawa, N. Nagata, Y. Sato, T. Sata, M. Yoneyama, T. Fujita, C. Taya, H. Yonekawa, and S. Koike. 2005. 'The alpha/beta interferon response controls tissue tropism and pathogenicity of poliovirus', *Journal of virology*, 79: 4460-9.

Imai, M., and Y. Kawaoka. 2012. 'The role of receptor binding specificity in interspecies transmission of influenza viruses', *Current opinion in virology*, 2: 160-7.

Ingulli, E., D. R. Ulman, M. M. Lucido, and M. K. Jenkins. 2002. 'In situ analysis reveals physical interactions between CD11b+ dendritic cells and antigen-specific CD4 T cells after subcutaneous injection of antigen', *J Immunol*, 169: 2247-52.

Inohara, Chamaillard, C. McDonald, and G. Nunez. 2005. 'NOD-LRR proteins: role in host-microbial interactions and inflammatory disease', *Annu Rev Biochem*, 74: 355-83.

Ivashkiv, L. B., and L. T. Donlin. 2014. 'Regulation of type I interferon responses', *Nat Rev Immunol*, 14: 36-49.

Iwasaki, A., and P. S. Pillai. 2014. 'Innate immunity to influenza virus infection', *Nat Rev Immunol*, 14: 315-28.

Jin, M. S., S. E. Kim, J. Y. Heo, M. E. Lee, H. M. Kim, S. G. Paik, H. Lee, and J. O. Lee. 2007. 'Crystal structure of the TLR1-TLR2 heterodimer induced by binding of a tri-acylated lipopeptide', *Cell*, 130: 1071-82.

Jung, D. Y., H. Lee, B. Y. Jung, J. Ock, M. S. Lee, W. H. Lee, and K. Suk. 2005. 'TLR4, but not TLR2, signals autoregulatory apoptosis of cultured microglia: a critical role of IFN-beta as a decision maker', *J Immunol*, 174: 6467-76.

Junt, T., E. A. Moseman, M. Iannacone, S. Massberg, P. A. Lang, M. Boes, K. Fink, S. E. Henrickson, D. M. Shayakhmetov, N. C. Di Paolo, N. van Rooijen, T. R. Mempel, S. P. Whelan, and U. H. von Andrian. 2007. 'Subcapsular sinus macrophages in lymph nodes clear lymph-borne viruses and present them to antiviral B cells', *Nature*, 450: 110-4.

Junt, T., A. V. Tumanov, N. Harris, M. Heikenwalder, N. Zeller, D. V. Kuprash, A. Aguzzi, B. Ludewig, S. A. Nedospasov, and R. M. Zinkernagel. 2006. 'Expression of lymphotoxin beta governs immunity at two distinct levels', *Eur J Immunol*, 36: 2061-75.

Kaech, S. M., E. J. Wherry, and R. Ahmed. 2002. 'Effector and memory T-cell differentiation: implications for vaccine development', *Nat Rev Immunol*, 2: 251-62.

Kamal, M. A., R. Gieschke, A. Lemenuel-Diot, C. A. Beauchemin, P. F. Smith, and C. R. Rayner. 2015. 'A drug-disease model describing the effect of oseltamivir neuraminidase inhibition on influenza virus progression', *Antimicrobial agents and chemotherapy*, 59: 5388-95.

Kasloff, S. B., M. S. Pizzuto, M. Silic-Benussi, S. Pavone, V. Ciminale, and I. Capua. 2014. 'Oncolytic activity of avian influenza virus in human pancreatic ductal adenocarcinoma cell lines', *Journal of virology*, 88: 9321-34.

Kato, H., O. Takeuchi, S. Sato, M. Yoneyama, M. Yamamoto, K. Matsui, S. Uematsu, A. Jung, T. Kawai, K. J. Ishii, O. Yamaguchi, K. Otsu, T. Tsujimura, C. S. Koh, C. Reis e Sousa, Y. Matsuura, T. Fujita, and S. Akira. 2006. 'Differential roles of MDA5 and RIG-I helicases in the recognition of RNA viruses', *Nature*, 441: 101-5.

Kawagoe, T., S. Sato, K. Matsushita, H. Kato, K. Matsui, Y. Kumagai, T. Saitoh, T. Kawai, O. Takeuchi, and S. Akira. 2008. 'Sequential control of Toll-like receptor-dependent responses by IRAK1 and IRAK2', *Nat Immunol*, 9: 684-91.

Kawai, T., and S. Akira. 2006. 'Innate immune recognition of viral infection', *Nat Immunol*, 7: 131-7.

Khairnar, V., V. Duhan, S. K. Maney, N. Honke, N. Shaabani, A. A. Pandyra, M. Seifert, V. Pozdeev, H. C. Xu, P. Sharma, F. Baldin, F. Marquardsen, K. Merches, E. Lang, C. Kirschning, A. M. Westendorf, D. Haussinger, F. Lang, U. Dittmer, R. Kuppers, M. Recher, C. Hardt, I. Scheffrahn, N. Beauchemin, J. R. Gothert, B. B. Singer, P. A. Lang, and K. S. Lang. 2015. 'CEACAM1 induces B-cell survival and is essential for protective antiviral antibody production', *Nature communications*, 6: 6217.

Kim, C. U., W. Lew, M. A. Williams, H. Liu, L. Zhang, S. Swaminathan, N. Bischofberger, M. S. Chen, D. B. Mendel, C. Y. Tai, W. G. Laver, and R. C. Stevens. 1997. 'Influenza neuraminidase inhibitors possessing a novel hydrophobic interaction in the enzyme

active site: design, synthesis, and structural analysis of carbocyclic sialic acid analogues with potent anti-influenza activity', *J Am Chem Soc*, 119: 681-90.

Kitamura, D., A. Kudo, S. Schaal, W. Muller, F. Melchers, and K. Rajewsky. 1992. 'A critical role of lambda 5 protein in B cell development', *Cell*, 69: 823-31.

Koroleva, E. P., Y. X. Fu, and A. V. Tumanov. 2018. 'Lymphotoxin in physiology of lymphoid tissues - Implication for antiviral defense', *Cytokine*, 101: 39-47.

Lakadamyali, M., M. J. Rust, and X. Zhuang. 2004. 'Endocytosis of influenza viruses', *Microbes Infect*, 6: 929-36.

Lang, K. S., A. A. Navarini, M. Recher, P. A. Lang, M. Heikenwalder, B. Stecher, A. Bergthaler, B. Odermatt, S. Akira, K. Honda, H. Hengartner, and R. M. Zinkernagel. 2007. 'MyD88 protects from lethal encephalitis during infection with vesicular stomatitis virus', *Eur J Immunol*, 37: 2434-40.

Levin, M. J., M. N. Oxman, J. H. Zhang, G. R. Johnson, H. Stanley, A. R. Hayward, M. J. Caulfield, M. R. Irwin, J. G. Smith, J. Clair, I. S. Chan, H. Williams, R. Harbecke, R. Marchese, S. E. Straus, A. Gershon, A. Weinberg, and Investigators Veterans Affairs Cooperative Studies Program Shingles Prevention Study. 2008. 'Varicella-zoster virus-specific immune responses in elderly recipients of a herpes zoster vaccine', *The Journal of infectious diseases*, 197: 825-35.

Levy, D. E., and J. E. Darnell, Jr. 2002. 'Stats: transcriptional control and biological impact', *Nat Rev Mol Cell Biol*, 3: 651-62.

Lichty, B. D., A. T. Power, D. F. Stojdl, and J. C. Bell. 2004. 'Vesicular stomatitis virus: re-inventing the bullet', *Trends Mol Med*, 10: 210-6.

Lieber, M. R. 2008. 'The mechanism of human nonhomologous DNA end joining', *J Biol Chem*, 283: 1-5.

Lindenmann, J., and P. A. Klein. 1967. 'Viral oncolysis: increased immunogenicity of host cell antigen associated with influenza virus', *The Journal of experimental medicine*, 126: 93-108.

Liu, X., H. Li, B. Zhong, M. Blonska, S. Gorjestani, M. Yan, Q. Tian, D. E. Zhang, X. Lin, and C. Dong. 2013. 'USP18 inhibits NF-kappaB and NFAT activation during Th17 differentiation by deubiquitinating the TAK1-TAB1 complex', *The Journal of experimental medicine*, 210: 1575-90.

Londrigan, S. L., L. M. Wakim, J. Smith, A. J. Haverkate, A. G. Brooks, and P. C. Reading. 2020. 'IFITM3 and type I interferons are important for the control of influenza A virus replication in murine macrophages', *Virology*, 540: 17-22.

Lund, J. M., L. Alexopoulou, A. Sato, M. Karow, N. C. Adams, N. W. Gale, A. Iwasaki, and R. A. Flavell. 2004. 'Recognition of single-stranded RNA viruses by Toll-like receptor 7', *Proc Natl Acad Sci U S A*, 101: 5598-603.

Ma, Y., U. Pannicke, K. Schwarz, and M. R. Lieber. 2002. 'Hairpin opening and overhang processing by an Artemis/DNA-dependent protein kinase complex in nonhomologous end joining and V(D)J recombination', *Cell*, 108: 781-94.

Macauley, M. S., P. R. Crocker, and J. C. Paulson. 2014. 'Siglec-mediated regulation of immune cell function in disease', *Nat Rev Immunol*, 14: 653-66.

Malakhova, O. A., K. I. Kim, J. K. Luo, W. Zou, K. G. Kumar, S. Y. Fuchs, K. Shuai, and D. E. Zhang. 2006. 'UBP43 is a novel regulator of interferon signaling independent of its ISG15 isopeptidase activity', *The EMBO journal*, 25: 2358-67.

Manicassamy, B., S. Manicassamy, A. Belicha-Villanueva, G. Pisanelli, B. Pulendran, and A. Garcia-Sastre. 2010. 'Analysis of in vivo dynamics of influenza virus infection in mice using a GFP reporter virus', *Proc Natl Acad Sci U S A*, 107: 11531-6.

Marciani, D. J. 2003. 'Vaccine adjuvants: role and mechanisms of action in vaccine immunogenicity', *Drug Discov Today*, 8: 934-43.

Matlin, K. S., H. Reggio, A. Helenius, and K. Simons. 1981. 'Infectious entry pathway of influenza virus in a canine kidney cell line', *J Cell Biol*, 91: 601-13.

Matsuoka, Y., H. Matsumae, M. Katoh, A. J. Eisfeld, G. Neumann, T. Hase, S. Ghosh, J. E. Shoemaker, T. J. Lopes, T. Watanabe, S. Watanabe, S. Fukuyama, H. Kitano, and Y. Kawaoka. 2013. 'A comprehensive map of the influenza A virus replication cycle', *BMC Syst Biol*, 7: 97.

McAuley, J. L., B. P. Gilbertson, S. Trifkovic, L. E. Brown, and J. L. McKimm-Breschkin. 2019. 'Influenza Virus Neuraminidase Structure and Functions', *Front Microbiol*, 10: 39.

McGill, J., J. W. Heusel, and K. L. Legge. 2009. 'Innate immune control and regulation of influenza virus infections', *Journal of leukocyte biology*, 86: 803-12.

McGill, J., and K. L. Legge. 2009. 'Cutting edge: contribution of lung-resident T cell proliferation to the overall magnitude of the antigen-specific CD8 T cell response in the lungs following murine influenza virus infection', *J Immunol*, 183: 4177-81.

Medzhitov, R., and C. A. Janeway, Jr. 1997. 'Innate immunity: impact on the adaptive immune response', *Curr Opin Immunol*, 9: 4-9.

Medzhitov, R., P. Preston-Hurlburt, and C. A. Janeway, Jr. 1997. 'A human homologue of the Drosophila Toll protein signals activation of adaptive immunity', *Nature*, 388: 394-7.

Meier, E., G. Kunz, O. Haller, and H. Arnheiter. 1990. 'Activity of rat Mx proteins against a rhabdovirus', *Journal of virology*, 64: 6263-9.

Melchers, F. 2015. 'Checkpoints that control B cell development', *J Clin Invest*, 125: 2203-10.

Menicucci, A. R., A. Jankeel, H. Feldmann, A. Marzi, and I. Messaoudi. 2019. 'Antiviral Innate Responses Induced by VSV-EBOV Vaccination Contribute to Rapid Protection', *mBio*, 10: e00597-19.

Meuwissen, M. E., R. Schot, S. Buta, G. Oudesluijs, S. Tinschert, S. D. Speer, Z. Li, L. van Unen, D. Heijsman, T. Goldmann, M. H. Lequin, J. M. Kros, W. Stam, M. Hermann, R. Willemsen, R. W. Brouwer, IJcken W. F. Van, M. Martin-Fernandez, I. de Coo, J. Dudink, F. A. de Vries, A. Bertoli Avella, M. Prinz, Y. J. Crow, F. W. Verheijen, S. Pellegrini, D. Bogunovic, and G. M. Mancini. 2016. 'Human USP18 deficiency underlies type 1 interferonopathy leading to severe pseudo-TORCH syndrome', *The Journal of experimental medicine*, 213: 1163-74.

Mond, J. J., A. Lees, and C. M. Snapper. 1995. 'T cell-independent antigens type 2', *Annu Rev Immunol*, 13: 655-92.

Moseman, E. A., M. Iannacone, L. Bosurgi, E. Tonti, N. Chevrier, A. Tumanov, Y. X. Fu, N. Hacohen, and U. H. von Andrian. 2012. 'B cell maintenance of subcapsular sinus macrophages protects against a fatal viral infection independent of adaptive immunity', *Immunity*, 36: 415-26.

Muik, A., I. Kneiske, M. Werbizki, D. Wilflingseder, T. Giroglou, O. Ebert, A. Kraft, U. Dietrich, G. Zimmer, S. Momma, and D. von Laer. 2011. 'Pseudotyping vesicular stomatitis virus with lymphocytic choriomeningitis virus glycoproteins enhances infectivity for glioma cells and minimizes neurotropism', *Journal of virology*, 85: 5679-84.

Muller, S., L. Hunziker, S. Enzler, M. Buhler-Jungo, J. P. Di Santo, R. M. Zinkernagel, and C. Mueller. 2002. 'Role of an intact splenic microarchitecture in early lymphocytic choriomeningitis virus production', *Journal of virology*, 76: 2375-83.

Muller, U., U. Steinhoff, L. F. Reis, S. Hemmi, J. Pavlovic, R. M. Zinkernagel, and M. Aguet. 1994. 'Functional role of type I and type II interferons in antiviral defense', *Science*, 264: 1918-21.

Mundy, C. L., N. Patenge, A. G. Matthews, and M. A. Oettinger. 2002. 'Assembly of the RAG1/RAG2 synaptic complex', *Mol Cell Biol*, 22: 69-77.

Obukhanych, T. V., and M. C. Nussenzweig. 2006. 'T-independent type II immune responses generate memory B cells', *The Journal of experimental medicine*, 203: 305-10.

Ono, S., O. Hattori, Y. Nagai, and I. Nagata. 1955. '[Oncolytic effect of influenza virus upon Ehrlich carcinoma and Yoshida ascites hepatoma]', *Gan*, 46: 512-4.

Palese, P., K. Tobita, M. Ueda, and R. W. Compans. 1974. 'Characterization of temperature sensitive influenza virus mutants defective in neuraminidase', *Virology*, 61: 397-410.

Patil, S., M. Fribourg, Y. Ge, M. Batish, S. Tyagi, F. Hayot, and S. C. Sealfon. 2015. 'Single-cell analysis shows that paracrine signaling by first responder cells shapes the interferon-beta response to viral infection', *Sci Signal*, 8: ra16.

Perez-Zsolt, D., I. Erkizia, M. Pino, M. Garcia-Gallo, M. T. Martin, S. Benet, J. Chojnacki, M. T. Fernandez-Figueras, D. Guerrero, V. Urrea, X. Muniz-Trabudua, L. Kremer, J. Martinez-Picado, and N. Izquierdo-Useros. 2019. 'Anti-Siglec-1 antibodies block Ebola viral uptake and decrease cytoplasmic viral entry', *Nat Microbiol*, 4: 1558-70.

Perrone, L. A., J. K. Plowden, A. Garcia-Sastre, J. M. Katz, and T. M. Tumpey. 2008. 'H5N1 and 1918 pandemic influenza virus infection results in early and excessive infiltration of macrophages and neutrophils in the lungs of mice', *PLoS Pathog*, 4: e1000115.

Plotkin, S. A. 2008. 'Vaccines: correlates of vaccine-induced immunity', *Clin Infect Dis*, 47: 401-9.

Poolman, J., and R. Borrow. 2011. 'Hyporesponsiveness and its clinical implications after vaccination with polysaccharide or glycoconjugate vaccines', *Expert Rev Vaccines*, 10: 307-22.

Pulendran, B., and R. Ahmed. 2011. 'Immunological mechanisms of vaccination', *Nat Immunol*, 12: 509-17.

Pulle, G., M. Vidric, and T. H. Watts. 2006. 'IL-15-dependent induction of 4-1BB promotes antigen-independent CD8 memory T cell survival', *J Immunol*, 176: 2739-48.

Querec, T., S. Bennouna, S. Alkan, Y. Laouar, K. Gorden, R. Flavell, S. Akira, R. Ahmed, and B. Pulendran. 2006. 'Yellow fever vaccine YF-17D activates multiple dendritic cell subsets via TLR2, 7, 8, and 9 to stimulate polyvalent immunity', *The Journal of experimental medicine*, 203: 413-24.

Ramsden, D. A., K. Baetz, and G. E. Wu. 1994. 'Conservation of sequence in recombination signal sequence spacers', *Nucleic Acids Res*, 22: 1785-96.

Rauch, S., E. Jasny, K. E. Schmidt, and B. Petsch. 2018. 'New Vaccine Technologies to Combat Outbreak Situations', *Frontiers in immunology*, 9: 1963.

Roberts, A., L. Buonocore, R. Price, J. Forman, and J. K. Rose. 1999. 'Attenuated vesicular stomatitis viruses as vaccine vectors', *Journal of virology*, 73: 3723-32.

Robey, E., and B. J. Fowlkes. 1994. 'Selective events in T cell development', *Annu Rev Immunol*, 12: 675-705.

Rose, N. F., P. A. Marx, A. Luckay, D. F. Nixon, W. J. Moretto, S. M. Donahoe, D. Montefiori, A. Roberts, L. Buonocore, and J. K. Rose. 2001. 'An effective AIDS vaccine based on live attenuated vesicular stomatitis virus recombinants', *Cell*, 106: 539-49.

Rothenfusser, S., N. Goutagny, G. DiPerna, M. Gong, B. G. Monks, A. Schoenemeyer, M. Yamamoto, S. Akira, and K. A. Fitzgerald. 2005. 'The RNA helicase Lgp2 inhibits TLR-independent sensing of viral replication by retinoic acid-inducible gene-I', *J Immunol*, 175: 5260-8.

Saito, T., R. Hirai, Y. M. Loo, D. Owen, C. L. Johnson, S. C. Sinha, S. Akira, T. Fujita, and M. Gale, Jr. 2007. 'Regulation of innate antiviral defenses through a shared repressor domain in RIG-I and LGP2', *Proc Natl Acad Sci U S A*, 104: 582-7.

Sallusto, F., and A. Lanzavecchia. 2002. 'The instructive role of dendritic cells on T-cell responses', *Arthritis Res*, 4 Suppl 3: S127-32.

Santin, I., F. Moore, F. A. Grieco, P. Marchetti, C. Brancolini, and D. L. Eizirik. 2012. 'USP18 is a key regulator of the interferon-driven gene network modulating pancreatic beta cell inflammation and apoptosis', *Cell death & disease*, 3: e419.

Sato, K., and S. Fujita. 2007. 'Dendritic cells: nature and classification', *Allergol Int*, 56: 183-91.

Saunderson, S. C., A. C. Dunn, P. R. Crocker, and A. D. McLellan. 2014. 'CD169 mediates the capture of exosomes in spleen and lymph node', *Blood*, 123: 208-16.

Schatz, D. G., and P. C. Swanson. 2011. 'V(D)J recombination: mechanisms of initiation', *Annu Rev Genet*, 45: 167-202.

Schmidt, S., W. V. Bonilla, A. Reiter, F. Stemeseder, T. Kleissner, D. Oeler, U. Berka, A. El-Gazzar, B. Kiefmann, S. C. Schulha, J. Raguz, M. Habbeddine, M. Scheinost, X. Qing, H. Lauterbach, I. Matushansky, D. D. Pinschewer, and K. K. Orlinger. 2020. 'Live-attenuated lymphocytic choriomeningitis virus-based vaccines for active immunotherapy of HPV16-positive cancer', *Oncoimmunology*, 9: 1809960.

Schneider, J. S., T. N. Seyfried, H. S. Choi, and S. K. Kidd. 2015. 'Intraventricular Sialidase Administration Enhances GM1 Ganglioside Expression and Is Partially Neuroprotective in a Mouse Model of Parkinson's Disease', *PLoS One*, 10: e0143351.

Schwabenland, M., O. Mossad, A. G. Peres, F. Kessler, F. J. M. Maron, L. A. Harsan, T. Bienert, D. von Elverfeldt, K. P. Knobeloch, O. Staszewski, F. L. Heppner, M. E. C. Meuwissen, G. M. S. Mancini, M. Prinz, and T. Blank. 2019. 'Loss of USP18 in microglia induces white matter pathology', *Acta Neuropathol Commun*, 7: 106.

Schwartz, J. A., L. Buonocore, A. L. Suguitan, Jr., A. Silaghi, D. Kobasa, G. Kobinger, H. Feldmann, K. Subbarao, and J. K. Rose. 2010. 'Potent vesicular stomatitis virus-based

avian influenza vaccines provide long-term sterilizing immunity against heterologous challenge', *Journal of virology*, 84: 4611-8.

Seiler, P., P. Aichele, B. Odermatt, H. Hengartner, R. M. Zinkernagel, and R. A. Schwendener. 1997. 'Crucial role of marginal zone macrophages and marginal zone metallophils in the clearance of lymphocytic choriomeningitis virus infection', *Eur J Immunol*, 27: 2626-33.

Sewald, X., M. S. Ladinsky, P. D. Uchil, J. Beloor, R. Pi, C. Herrmann, N. Motamedi, T. T. Murooka, M. A. Brehm, D. L. Greiner, L. D. Shultz, T. R. Mempel, P. J. Bjorkman, P. Kumar, and W. Mothes. 2015. 'Retroviruses use CD169-mediated trans-infection of permissive lymphocytes to establish infection', *Science*, 350: 563-67.

Shortman, K., and W. R. Heath. 2010. 'The CD8+ dendritic cell subset', *Immunol Rev*, 234: 18-31.

Sollini, M., F. Gelardi, C. Carlo-Stella, and A. Chiti. 2021. 'Complete remission of follicular lymphoma after SARS-CoV-2 infection: from the "flare phenomenon" to the "abscopal effect"', *European journal of nuclear medicine and molecular imaging*: 1-3.

Solmaz, G., F. Puttur, M. Francozo, M. Lindenberg, M. Guderian, M. Swallow, V. Duhan, V. Khairnar, U. Kalinke, B. Ludewig, B. E. Clausen, H. Wagner, K. S. Lang, and T. D. Sparwasser. 2019. 'TLR7 Controls VSV Replication in CD169(+) SCS Macrophages and Associated Viral Neuroinvasion', *Frontiers in immunology*, 10: 466.

Staeheli, P., and J. Pavlovic. 1991. 'Inhibition of vesicular stomatitis virus mRNA synthesis by human MxA protein', *Journal of virology*, 65: 4498-501.

Stark, G. R., and J. E. Darnell, Jr. 2012. 'The JAK-STAT pathway at twenty', *Immunity*, 36: 503-14.

Stavnezer, J., J. E. Guikema, and C. E. Schrader. 2008. 'Mechanism and regulation of class switch recombination', *Annu Rev Immunol*, 26: 261-92.

Steinhoff, U., U. Muller, A. Schertler, H. Hengartner, M. Aguet, and R. M. Zinkernagel. 1995. 'Antiviral protection by vesicular stomatitis virus-specific antibodies in alpha/beta interferon receptor-deficient mice', *Journal of virology*, 69: 2153-8.

Swiecki, M., and M. Colonna. 2015. 'The multifaceted biology of plasmacytoid dendritic cells', *Nat Rev Immunol*, 15: 471-85.

Tacconi, C., C. D. Commerford, L. C. Dieterich, S. Schwager, Y. He, K. Ikenberg, E. Friebel, B. Becher, S. Tugues, and M. Detmar. 2021. 'CD169(+) lymph node macrophages have protective functions in mouse breast cancer metastasis', *Cell Rep*, 35: 108993.

Tailor, P., T. Tamura, H. J. Kong, T. Kubota, M. Kubota, P. Borghi, L. Gabriele, and K. Ozato. 2007. 'The feedback phase of type I interferon induction in dendritic cells requires interferon regulatory factor 8', *Immunity*, 27: 228-39.

Takeuchi, O., and S. Akira. 2009. 'Innate immunity to virus infection', *Immunol Rev*, 227: 75-86.

Tassiulas, I., X. Hu, H. Ho, Y. Kashyap, P. Paik, Y. Hu, C. A. Lowell, and L. B. Ivashkiv. 2004. 'Amplification of IFN-alpha-induced STAT1 activation and inflammatory function by Syk and ITAM-containing adaptors', *Nat Immunol*, 5: 1181-9.

Tobon, G. J., J. H. Izquierdo, and C. A. Canas. 2013. 'B lymphocytes: development, tolerance, and their role in autoimmunity-focus on systemic lupus erythematosus', *Autoimmune diseases*, 2013: 827254.

Tsuji, S., M. Matsumoto, O. Takeuchi, S. Akira, I. Azuma, A. Hayashi, K. Toyoshima, and T. Seya. 2000. 'Maturation of human dendritic cells by cell wall skeleton of Mycobacterium bovis bacillus Calmette-Guerin: involvement of toll-like receptors', *Infection and immunity*, 68: 6883-90.

'The Vaccination History of Small-Pox Cases'. 1902. *British medical journal*, 2: 67-8.

van Boxel-Dezaire, A. H., M. R. Rani, and G. R. Stark. 2006. 'Complex modulation of cell type-specific signaling in response to type I interferons', *Immunity*, 25: 361-72.

van Dinther, D., H. Veninga, S. Iborra, E. G. F. Borg, L. Hoogterp, K. Olesek, M. R. Beijer, S. T. T. Schetters, H. Kalay, J. J. Garcia-Vallejo, K. L. Franken, L. B. Cham, K. S. Lang, Y. van Kooyk, D. Sancho, P. R. Crocker, and J. M. M. den Haan. 2018. 'Functional CD169 on Macrophages Mediates Interaction with Dendritic Cells for CD8(+) T Cell Cross-Priming', *Cell Rep*, 22: 1484-95.

van Riel, D., and E. de Wit. 2020. 'Next-generation vaccine platforms for COVID-19', *Nat Mater*, 19: 810-12.

Venkatesh, D., T. Ernandez, F. Rosetti, I. Batal, X. Cullere, F. W. Luscinskas, Y. Zhang, G. Stavrakis, G. Garcia-Cardena, B. H. Horwitz, and T. N. Mayadas. 2013. 'Endothelial TNF receptor 2 induces IRF1 transcription factor-dependent interferon-beta autocrine signaling to promote monocyte recruitment', *Immunity*, 38: 1025-37.

von Boehmer, H., and H. J. Fehling. 1997. 'Structure and function of the pre-T cell receptor', *Annu Rev Immunol*, 15: 433-52.

Vremec, D., J. Pooley, H. Hochrein, L. Wu, and K. Shortman. 2000. 'CD4 and CD8 expression by dendritic cell subtypes in mouse thymus and spleen', *J Immunol*, 164: 2978-86.

Vuillier, F., Z. Li, P. H. Commere, L. T. Dynesen, and S. Pellegrini. 2019. 'USP18 and ISG15 coordinately impact on SKP2 and cell cycle progression', *Sci Rep*, 9: 4066.

Wang, J. Q., Y. S. Jeelall, L. L. Ferguson, and K. Horikawa. 2014. 'Toll-Like Receptors and Cancer: MYD88 Mutation and Inflammation', *Frontiers in immunology*, 5: 367.

Wang, X., S. Huang, and J. L. Chen. 2017. 'Understanding of leukemic stem cells and their clinical implications', *Molecular cancer*, 16: 2.

Whelan, S. P. J. 2008. 'Vesicular Stomatitis Virus.' in Brian W. J. Mahy and Marc H. V. Van Regenmortel (eds.), *Encyclopedia of Virology* (Academic Press: Oxford).

Wynn, T. A., A. Chawla, and J. W. Pollard. 2013. 'Macrophage biology in development, homeostasis and disease', *Nature*, 496: 445-55.

Xu, H. C., J. Huang, V. Khairnar, V. Duhan, A. A. Pandyra, M. Grusdat, P. Shinde, D. R. McIlwain, S. K. Maney, J. Gommerman, M. Lohning, P. S. Ohashi, T. W. Mak, K. Pieper, H. Sic, M. Speletas, H. Eibel, C. F. Ware, A. V. Tumanov, A. A. Kruglov, S. A. Nedospasov, D. Haussinger, M. Recher, K. S. Lang, and P. A. Lang. 2015. 'Deficiency of the B cell-activating factor receptor results in limited CD169+ macrophage function during viral infection', *Journal of virology*, 89: 4748-59.

Yahalom-Ronen, Y., H. Tamir, S. Melamed, B. Politi, O. Shifman, H. Achdout, E. B. Vitner, O. Israeli, E. Milrot, D. Stein, I. Cohen-Gihon, S. Lazar, H. Gutman, I. Glinert, L. Cherry, Y. Vagima, S. Lazar, S. Weiss, A. Ben-Shmuel, R. Avraham, R. Puni, E. Lupu, E. Bar-David, A. Sittner, N. Erez, R. Zichel, E. Mamroud, O. Mazor, H. Levy, O. Laskar, S. Yitzhaki, S. C. Shapira, A. Zvi, A. Beth-Din, N. Paran, and T. Israely. 2020. 'A single dose of recombinant VSV-G-spike vaccine provides protection against SARS-CoV-2 challenge', *Nature communications*, 11: 6402.

Yoneyama, M., M. Kikuchi, T. Natsukawa, N. Shinobu, T. Imaizumi, M. Miyagishi, K. Taira, S. Akira, and T. Fujita. 2004. 'The RNA helicase RIG-I has an essential function in double-stranded RNA-induced innate antiviral responses', *Nat Immunol*, 5: 730-7.

Zhao, C., H. Sridharan, R. Chen, D. P. Baker, S. Wang, and R. M. Krug. 2016. 'Influenza B virus non-structural protein 1 counteracts ISG15 antiviral activity by sequestering ISGylated viral proteins', *Nature communications*, 7: 12754.

Zhou, S., E. A. Kurt-Jones, K. A. Fitzgerald, J. P. Wang, A. M. Cerny, M. Chan, and R. W. Finberg. 2007. 'Role of MyD88 in route-dependent susceptibility to vesicular stomatitis virus infection', *J Immunol*, 178: 5173-81.

Zinkernagel, R. M. 1997. 'Felix Hoppe-Seyler Lecture 1997. Protective antibody responses against viruses', *Biol Chem*, 378: 725-9.

Zou, W., J. H. Kim, A. Handidu, X. Li, K. I. Kim, M. Yan, J. Li, and D. E. Zhang. 2007. 'Microarray analysis reveals that Type I interferon strongly increases the expression of

immune-response related genes in Ubp43 (Usp18) deficient macrophages', *Biochem Biophys Res Commun*, 356: 193-9.

12. Lebenslauf

Der Lebenslauf ist in der Online-Version aus Gründen des Datenschutzes nicht enthalten.

13. Erklärungen

Erklärung:

Hiermit erkläre ich, gem. § 6 Abs. (2) g) der Promotionsordnung der Fakultät für Biologie zur Erlangung der Dr. rer. nat., dass ich das Arbeitsgebiet, dem das Thema *„**Mechansims and systemic relevance of immune cell specific virus replication“*** zuzuordnen ist, in Forschung und Lehre vertrete und den Antrag von ***Sarah-Kim Friedrich-Becker*** befürworte und die Betreuung auch im Falle eines Weggangs, wenn nicht wichtige Gründe dem entgegenstehen, weiterführen werde.

Essen, den _____ _____ _____

Name des Betreuers an der Universität Duisburg-Essen

Unterschrift

Erklärung:

Hiermit erkläre ich, gem. § 7 Abs. (2) d) + f) der Promotionsordnung der Fakultät für Biologie zur Erlangung des Dr. rer. nat., dass ich die vorliegende Dissertation selbständig verfasst und mich keiner anderen als der angegebenen Hilfsmittel bedient, bei der Abfassung der Dissertation nur die angegeben Hilfsmittel benutzt und alle wörtlich oder inhaltlich übernommenen Stellen als solche gekennzeichnet habe.

Essen, den _____ _____

Unterschrift des/r Doktoranden/in

Erklärung:

Hiermit erkläre ich, gem. § 7 Abs. (2) e) + g) der Promotionsordnung der Fakultät für Biologie zur Erlangung des Dr. rer. nat., dass ich keine anderen Promotionen bzw. Promotionsversuche in der Vergangenheit durchgeführt habe und dass diese Arbeit von keiner anderen Fakultät/Fachbereich abgelehnt worden ist.

Essen, den _____ _____

Unterschrift des/r Doktoranden/in